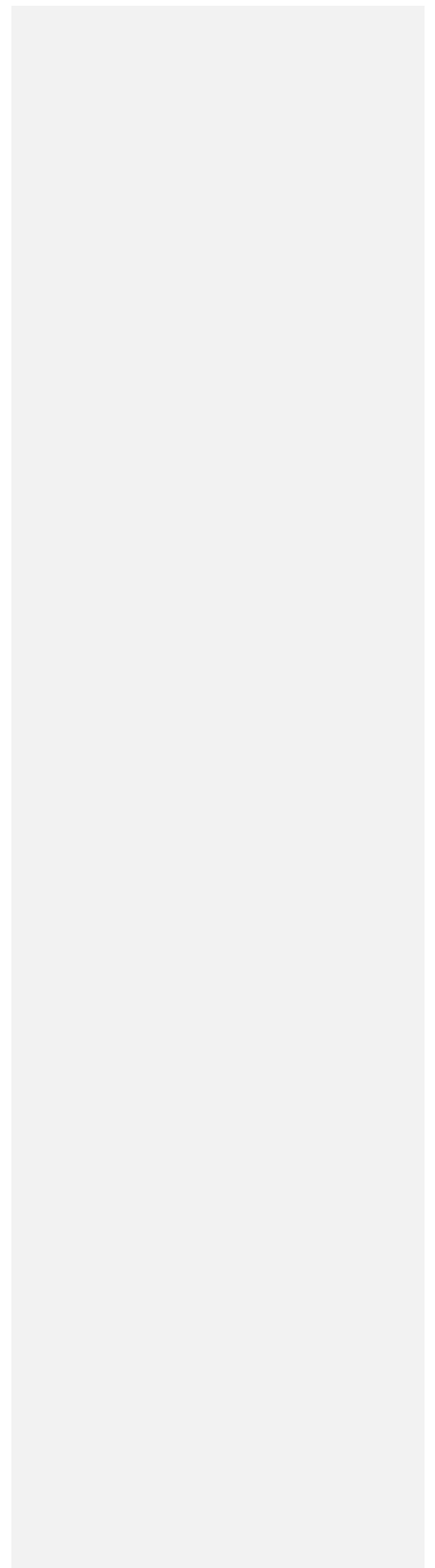


CIRS RINGS
Target NOTEBOOK



Foreword

The purpose of the target notebook is to provide the end user with a “one stop shop” for information about the target from a CIRS perspective – from the planning of each observation and its science intent to collection of the data and its quality. The goal of this effort is to enable better use of the CIRS dataset archived at the Planetary Data System.

The notebook contains the following sections: Introduction, Planning, Data Collection, Database Contents, and Publications/Science Research generated by the dataset. The Introduction section discusses the science objectives, descriptions of the observation types and their intent. The Planning section contains a time ordered listing of all the observations planned with a suite of supporting files that provide plots, pointing, and instrument commanding for each observation. The Data Collection section provides the user with information about the data that was collected with a comparison to what was planned and a commentary on any lost data. The Database contents section provides a discussion of the data in the database at PDS at a high level – what was calibrated, what was not, and why as well as a brief commentary the challenges in calibrating the data. The final section – Publications/Science Research provides the user with a list of publications for the target, a high level description of the science analysis undertaken with contact information for those CIRS team members involved.

Table of Contents

1. Summary: Observing Saturn's Rings with CIRS

a. Philosophy

2. CIRS Rings Objectives and Traceability Matrix

- a. Key science objectives for the rings
- b. Tracing Ring Science Objectives

3. Description of Observation Types

a. Overview

b. PRIME MISSION

- i. *thermal inertia and spin campaign*
- ii. *radial structure campaign*
- iii. *spectral features campaign*

c. EXTENDED (Equinox) MISSION

- i. *Azimuthal campaign*
- ii. *Phase/lat AND particle properties*
- iii. *Vertical structure campaign*
- iv. *Equinox planning*

d. SOLSTICE MISSION

- i. *Phase-Latitude Scans*
- ii. *Thermal Difference Campaign*
- iii. *Shadow Region Mapping*
- iv. *Composition Sit & Stares*

e. F-RING/PROXIMAL ORBITS

- i. RSCAN
- ii. HALO
- iii. CASDIV
- iv. UNSHAD
- v. AZSHADSCN
- vi. PLAT
- vii. ANSASTARE

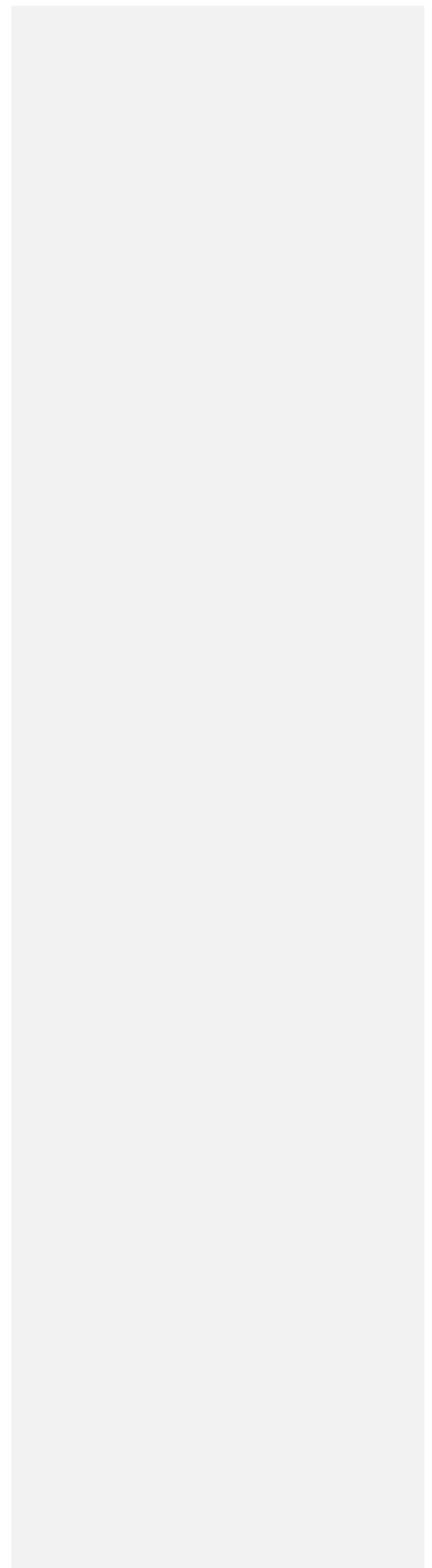
f. ODDS & ENDS

- i. Polarization Integrations
- ii. Stellar Occultations
- iii. On-Saturn Observations
- iv. *Saturn Reflection*

4. Observation Lists

- v.

4. Rider Observations
5. Support Imaging Observations
6. Data Volume Strategies (or Why Not Collect Data 24-7?)



1. Summary: Observing Saturn's Rings with CIRS

a. Philosophy

2. CIRS Rings Objectives and Traceability Matrix

a. Key science objectives for the rings:

CIRS has provided major advances over previous spacecraft infrared observations of Saturn's rings in three respects: the extension of the spectral range to sub-millimeter wavelengths; the higher spatial resolution on the rings as result of closer proximity during the Cassini tour, as well as of a linear detector array with much finer spatial resolution in the mid-infrared; and the temporal extent of the mission, which provided greatly improved sampling in illumination and viewing geometries. With its enhanced capabilities, CIRS addressed many of the rings science objectives of the Cassini mission, particularly those pertaining to radial thermal structure, ring optical depth in the mid-IR, ring particle thermal properties and rotation states, ring-scale properties including vertical structure, and thermal roll-off in the sub-millimeter. The key CIRS ring science objectives are listed below and each one is discussed in the Science Results section.

i. **Ring Thermal Structure:** Determine Saturn's ring thermal structure and how the ring temperatures vary with ring optical depth, solar elevation, phase angle, azimuth angle and distance to the planet. What is the source of the temperature variations? Determine the azimuthal asymmetries in the rings, apart from the diurnal cooling/heating cycle. What is their origin?

ii. **Ring optical depth at mid-IR wavelengths:** Determine the variation of ring optical depths at mid-IR wavelengths and compare to UV and near-IR optical depths.

iii. **Particle-scale Properties:** Determine key particle properties such as Bond albedo, thermal inertia and particle spin. On what factors do they depend? Determine the distribution of particle spins of the ring particles. What does this distribution tell us about local dynamics? Compare the diurnal and seasonal thermal inertia and any differences between them.

iv. **Ring-scale Properties:** Determine the volume filling factors for the rings. Search for an opposition surge in the thermal infrared. Is it driven by mutual shadowing alone? Determine vertical temperature gradient between lit and unlit sides of the rings. What does this tell us about the ring vertical structure and dynamics? Determine the ring thermal inertia and compare it to the particle thermal inertia. Does it change with seasons?

v. **Regolith Properties deduced from CIRS Emissivity Roll-off:** Determine the wavelength of the roll-off in ring emissivity. What do we learn from this roll-off about particle structure and composition?

b. Tracing Ring Science Objectives

The original Announcement of Opportunity (AO) and the Cassini Traceability Matrix (TM) were developed for the Equinox and Solstice missions. Each CIRS ring science objective (above) can be paired with either an AO or TM science objective (Table 1). Assessment of these objectives are shown in Table 2.

Table 1: AO and TM Science Objectives
--

Ring Structure and Dynamics (R_AO1) - Study configuration of the rings and dynamical processes (gravitational, viscous, erosional, and electromagnetic) responsible for ring structure.
Changing Rings (RC1a) - Determine the production mechanisms of spokes, and the microscale properties of ring structure, by observing at the seasonally maximum opening angle of the rings near Solstice.
Ring Temporal Variability (RC1b) - Understand the time-variability of ring phenomena on decadal timescales (Encke gap, D ring, ring edges, etc) by substantially increasing the time baseline of observations.
F Ring (RC2a) - Focus on F Ring structure, and distribution of associated moonlets or clumps, as sparse observations show clumps, arcs, and possibly transient objects appearing and disappearing.

Table 2. CIRS Ring Science Assessment: AO and TM Objectives are paired with CIRS Science objectives. Green = fully/mostly accomplished; Yellow = partially accomplished.

CIRS Ring Science Objectives	AO and TM Science Objectives	CIRS Ring Science Assessment	Comments if yellow (partially fulfilled)
Ring Thermal Structure			
--- Radius and Ring Optical Depth	R_AO1, RC1a		
--- Solar elevation	R_AO1, RC1a		
--- Phase angle	R_AO1, RC1a		
--- Ring Equinox temperatures	R_AO1, RC1a		
--- Azimuthal dependence	R_AO1, RC1a		
Ring optical depth at mid-IR wavelengths	R_AO1, RC1a		
Particle-scale Properties			
--- Bolometric Bond Albedo	R_AO1, RC1a		
--- Particle Spin	R_AO1, RC1a		

--- Diurnal Thermal Inertia	R_AO1, RC1a		
--- Seasonal Thermal Inertia and Particle Size	R_AO1, RC1a		
--- Average Thermal Emissivity	R_AO1, RC1a		
Ring-scale Properties			
--- Volume Filling Factors of A and B rings	R_AO1, RC1a		
--- Opposition Surge	R_AO1, RC1a		
--- Energy budget and heat transfer in B ring	R_AO1, RC1a		
--- Thermal Properties, Thickness and Surface Mass Density of B ring	R_AO1, RC1a		
--- Self-gravity wakes in the A ring	R_AO1, RC1a		
Regolith Properties deduced from CIRS Emissivity Roll-off			
--- Thermal Emissivity Roll-off at Submillimeter wavelengths	R_AO1, RC1a		
F ring Clumps	RC2a		

3. Description of Observation Types

a. Overview:

Most CIRS observations of the rings were taken with the FP1 focal plane at a resolution of 15.5 cm⁻¹. Shortly after SOI we found that most mid/far-IR spectra of the rings could be very well characterized by a temperature and scalar emissivity factor, and this influenced the choice of resolution thereafter.

Early in PM we determined that there were not many spectral features in the rings in FP1, and that FP3 didn't generally have good enough S/N to see them. Focus in the ring team

shifted nearly completely into obtaining information on ring emission after characterizing it by the Planck function fit.

Observation campaigns and objectives changed during the mission, as data were acquired and analyzed, and as our picture of the rings changed. Design campaigns were re-organized between the several major segments of the mission which we broadly label as the Prime Mission (00A-073), XM (074-109), Equinox (109-139), Solstice (124-243), and FProx (244-292). Note that, according to project documentation, our category of "Equinox" fits into the end of the extended mission, and our category of "F-Prox" fits into the end of the Solstice mission.

Broad constraints applied throughout the mission. At low sub-spacecraft latitudes (considered to be 10 degrees in main mission, but later relaxed as the team grew more adventurous), it is not possible to observe far from the Ansa. Radial scans at the Ansa maximize the signal. Observations at high sub-spacecraft latitudes have been harder to obtain time for, and are planned accordingly. A brief history of this evolution is presented below.

b. PRIME MISSION:

Originally, prime mission observations were planned using the model of the rings as consisting of independent little orbiting moonlets, each of which had a spin and could be analysed in the same manner that had worked for icy moons. The observations for prime mission were divided up according to what they would reveal about particle properties under this paradigm. There were broadly three categories of observation:

- i. *thermal inertia and spin campaign*: SHAD and VERT observations were designed as scans near the shadow and radial scans that would allow one to fit cooling curves to particles.

1. Observation Type: SHADU*, SHADL*, SHADA*, SHADC*, SHAD*CAS*

Prime Instrument: CIRS

Usual Riders:

Number of Observations

18 SHADL

6 SHADU

4 SHAD*CAS

3 SHADA,SHADC*

These were all main mission campaigns intended to investigate heating and cooling of particles at representative radii in the main rings as they went through the shadow region. These were originally designed for purposes of fitting cooling curves under the assumption that CIRS was seeing emission from rotating particle models. The intention was to constrain particle thermal inertia and size distribution.

The naming convention for most of these observations has a 'U' (or sometimes 'UL') for unlit or 'L' for lit following the 'SHAD' predicate. During the prime mission 'U' is always the North side of the rings and 'L' the South side. Following that is a rough classification of whether the data were at low, medium, or high phase angle ('LP', 'MP', or 'HP').

In the early revs, before naming convention was established and observation design templates elaborated, there were several observations labeled as 'SHADA', 'SHADC', and 'SHADCOUT'. These were all unlit side observations containing a large number of footprints aimed at finding radial variation near shadow ingress, in order to see whether temperature effects could be seen in the unlit A and C rings.

There are additionally several 'SHADCAS' observations that were placed when Cassini was at close enough range that the FP1 footprint fit entirely within the Cassini division.

Pointing: These were FP1 to rings, and were mostly azimuthal scans at fixed radius.

Instrument Parameters: These were all specifically designed for FP1, and mostly taken at 15cm⁻¹ resolution.

List of observations:

Observation	Start Time	Duration
CIRS_00ARC_SHADA001_PRIME	2004-302T09:00:00	000T03:00:00
CIRS_00ARC_SHADCIN001_PRIME	2004-302T07:15:00	000T01:45:00
CIRS_00ARC_SHADCOUT001_PRIME	2004-302T12:00:00	000T02:00:00
CIRS_000RI_SHADLMP001_PRIME	2004-184T22:00:00	000T02:45:00
CIRS_007RB_SHADLLP001_PRIME	2005-122T14:35:00	000T02:00:00
CIRS_011RC_SHADLLP001_PRIME	2005-194T00:00:00	000T04:00:00
CIRS_011RA_SHADLLP001_PRIME	2005-194T04:00:00	000T04:00:00
CIRS_031RC_SHADLMP001_PRIME	2006-300T00:30:00	000T08:30:00
CIRS_037RC_SHADLLP001_PRIME	2007-016T09:30:00	000T04:00:00
CIRS_037RB_SHADLLP001_PRIME	2007-016T13:30:00	000T05:00:00
CIRS_037RA_SHADLLP001_PRIME	2007-016T18:30:00	000T04:00:00
CIRS_039RI_SHADLMP004_PRIME	2007-048T15:50:00	000T08:25:00
CIRS_039RI_SHADLMP005_PRIME	2007-049T15:55:00	000T01:35:00
CIRS_039RI_SHADLMP006_PRIME	2007-049T21:20:00	000T03:45:00
CIRS_041RI_SHADLMP001_PRIME	2007-082T01:20:00	000T10:20:00
CIRS_041RI_SHADLMP002_PRIME	2007-082T14:40:00	000T01:40:00
CIRS_062RB_SHADLLP001_PRIME	2008-083T18:20:00	000T05:30:00
CIRS_063RB_SHADLLP001_PRIME	2008-093T09:05:00	000T06:30:00
CIRS_074RI_SHADLMP001_PRIME	2008-182T20:00:00	000T04:00:00
CIRS_077RI_SHADLMP001_PRIME	2008-204T02:50:00	000T04:00:00
CIRS_098RI_SHADLMP001_PRIME	2008-362T09:09:00	000T21:11:00

CIRS_010RC_SHADULHP001_PRIME	2005-178T00:44:00	000T02:52:00
CIRS_010RA_SHADULHP001_PRIME	2005-178T03:36:00	000T04:00:00
CIRS_031RC_SHADULMP001_PRIME	2006-301T22:00:00	000T02:00:00
CIRS_033RB_SHADULHP001_PRIME	2006-326T22:00:00	000T03:00:00
CIRS_034RC_SHADULMP001_PRIME	2006-337T17:00:00	000T04:00:00
CIRS_064RI_SHADULMP001_PRIME	2008-101T16:00:00	000T02:45:00
CIRS_042RI_SHADLCAS001_PRIME	2007-098T17:10:00	000T00:55:00
CIRS_042RI_SHADLCAS002_PRIME	2007-098T19:40:00	000T02:05:00
CIRS_044RI_SHADLCAS001_PRIME	2007-130T08:44:00	000T04:26:00
CIRS_066RI_SHADLCAS001_PRIME	2008-120T23:30:00	000T09:40:00

1. Observation Type: VERTL, VERTU , VERTULCAS, VCAS, VENC

Prime Instrument: CIRS

Usual Riders:

Number of Observations

16 VERTL PM

24 VERTU PM

2 VERTULCAS PM

3 VCAS XM

3 VENC XM

These observations were designed as a campaign to observe the heating and cooling properties of the rings farther from the shadow region than the SHAD observations, with the idea that vertical structure of the rings might be contributing to previously observed anomalous brightnesses on the afternoon Ansa as heat dissipated through the ring from the lit to unlit side. Also the possible modulation of temperature versus azimuth due to the distribution of particle spin rate and orientation or due to self-gravity wakes was looked for.

The naming convention for these is similar to most of the main mission campaigns in that the designator 'VERT' is followed by a 'U' (or 'UL') or 'L' to indicate whether of the unlit or lit side, then an indicator of 'LP', 'MP', or 'HP' to describe the phase regime it was taken at.

Almost all of these are azimuthal scans, although there are a few lit side observations and one unlit one (rev 67) where large swaths of ring were covered with quasi-radial scans in order to gain insight into the rings' behavior at a large number of radii instead of just the designated radii at which azimuthal scans were usually done. Additionally, the very first lit-side VERT (rev 7) contains a large

number of footprints aimed at building a temperature map of both the shadow and noon side regions of the rings.

The VENC and VCAS observations were designed in XM, at times when Cassini was close enough to Saturn that the FP1 footprints fit inside the Cassini or trans-Encke regions of the rings.

Pointing: These were all FP1 to rings, mostly azimuthal scans.

Instrument Parameters: Spectral resolution of 15cm^{-1} .

List of observations:

Observation	Start Time	Duration
CIRS_007RB_VERTLMP001_PRIME	2005-119T06:00:00	000T11:30:00
CIRS_007RB_VERTLMP003_PRIME	2005-120T16:30:00	000T09:30:00
CIRS_009RA_VERTLMP001_PRIME	2005-156T06:00:00	000T07:00:00
CIRS_009RI_VERTLMP001_PRIME	2005-156T13:00:00	000T08:00:00
CIRS_009RA_VERTLLP001_PRIME	2005-158T02:00:00	000T11:00:00
CIRS_010RB_VERTLMP001_PRIME	2005-175T04:45:00	000T03:00:00
CIRS_010RC_VERTLLP001_PRIME	2005-176T01:00:00	000T04:00:00
CIRS_013RB_VERTLMP001_PRIME	2005-229T18:30:00	000T03:00:00
CIRS_033RI_VERTLMP001_PRIME	2006-324T09:45:00	000T03:15:00
CIRS_034RI_VERTLMP001_PRIME	2006-336T09:00:00	000T03:00:00
CIRS_034RI_VERTLLP001_PRIME	2006-336T14:50:00	000T04:40:00
CIRS_036RI_VERTLMP001_PRIME	2006-363T23:30:00	000T03:00:00
CIRS_037RI_VERTLMP001_PRIME	2007-015T18:00:00	000T02:00:00
CIRS_041RC_VERTLLP001_PRIME	2007-083T08:50:00	000T08:00:00
CIRS_066RI_VERTLMP001_PRIME	2008-121T15:20:00	000T11:40:00
CIRS_072RI_VERTLLP001_PRIME	2008-169T12:00:00	000T03:55:00
CIRS_008RB_VERTULHP001_PRIME	2005-141T17:36:00	000T03:09:00
CIRS_008RI_VERTULHP003_PRIME	2005-141T23:40:00	000T01:50:00
CIRS_010RC_VERTULHP001_PRIME	2005-178T07:36:00	000T03:24:00
CIRS_030RA_VERTULMP001_PRIME	2006-287T07:50:00	000T01:45:00
CIRS_030RA_VERTULMP001_PRIME	2006-287T07:50:00	000T01:45:00
CIRS_033RB_VERTULHP001_PRIME	2006-327T02:30:00	000T04:30:00

CIRS_034RI_VERTULMP001_PRIME	2006-337T04:30:00	000T05:45:00
CIRS_034RB_VERTULHP001_PRIME	2006-339T23:20:00	000T07:00:00
CIRS_041RC_VERTULHP001_PRIME	2007-079T15:15:00	000T04:25:00
CIRS_041RA_VERTULHP001_PRIME	2007-080T07:05:00	000T03:45:00
CIRS_043RB_VERTULMP001_PRIME	2007-112T17:00:00	000T03:45:00
CIRS_043RB_VERTULMP002_PRIME	2007-111T07:50:00	000T05:40:00
CIRS_043RC_VERTULHP001_PRIME	2007-114T06:45:00	000T03:00:00
CIRS_044RA_VERTULMP002_PRIME	2007-128T13:15:00	000T06:30:00
CIRS_044RA_VERTULMP001_PRIME	2007-129T16:30:00	000T03:15:00
CIRS_057RI_VERTULMP001_PRIME	2008-025T20:50:00	000T08:00:00
CIRS_058RI_VERTULMP001_PRIME	2008-036T13:06:00	000T06:30:00
CIRS_061RI_VERTULLP001_PRIME	2008-069T12:21:00	000T08:00:00
CIRS_062RB_VERTULMP001_PRIME	2008-081T09:50:00	000T13:15:00
CIRS_065RI_VERTULMP001_PRIME	2008-109T15:48:00	000T06:00:00
CIRS_067RI_VERTULMP001_PRIME	2008-130T06:00:00	000T06:00:00
CIRS_071RC_VERTULLP001_PRIME	2008-158T12:41:00	000T05:00:00
CIRS_071RC_VERTULLP002_PRIME	2008-159T04:41:00	000T05:00:00
CIRS_072RI_VERTULMP001_PRIME	2008-167T05:10:00	000T01:20:00
CIRS_073RI_VERTULMP001_PRIME	2008-174T04:39:00	000T07:31:00
CIRS_087RI_VENCUNLP001_PRIME	2008-275T17:13:00	000T07:59:00
CIRS_098RI_VENCLSHP001_PRIME	2008-361T16:27:00	000T05:32:00
CIRS_102RI_VENCUNMP001_PRIME	2009-032T14:22:00	000T06:02:00
CIRS_056RI_VERTULCAS001_PRIME	2008-015T10:00:00	000T04:30:00
CIRS_057RI_VERTULCAS001_PRIME	2008-027T06:05:00	000T05:05:00

iii. *radial structure campaign*: SUBM and TEMP scans were designed to reveal radial variation in ring structure or ice properties by scanning radially. SUBM were originally designed as low latitude scans that would use high spectral resolution at Ansa to maximize S/N and give information on whether a sub-millimeter rolloff varied radially. TEMP scans were originally designed as higher latitude scans done at a faster slew rate in order to reveal trends in temperature evolution.

1. Observation Type: SUBM[U,L]XX[LMH]

Prime Instrument: CIRS

Usual Riders:

Number of Observations:

28 SUBML (PM)
 54 SUBMU (PM)
 7 SUBMS (XM)
 1 SUBMMLP (PM)
 1 SUBMLVEN(PM)

These were originally planned as a campaign to collect radial scans slowly at high spectral resolution in order to detect any variation in the sub-millimeter wavelength region in the form of "rolloff" or spectral features. Given that the radial scans were to be slow, it was anticipated that most of these observations would only have one or maybe two scans, and during negotiations they were preferentially placed in the timeline at low spacecraft elevations, where high signal to noise could be obtained by looking at the Ansa.

Analysis showed that the S/N of FP1 is not good enough to see spectral features without averaging together many spectra, and after rev 60 the observations were conducted at lower resolution with faster radial scans, in order to supplement the TEMP campaign.

The naming convention is that 'L' or 'U' follows the 'SUBM' designation, either for 'Lit' or 'Unlit' (which map to North and South, as all of these took place in Prime Mission before the equinox). The characters after this indicate the approximate latitude (sub-spacecraft elevation) and whether it was at low, medium or high phase (LP, MP, HP).

Pointing:

Originally these were taken with FP1 to rings, and planned with R_RAD_LON adjusted to a slow scan across either Ansa. Several of them have "COMP"-like portions where they take many footprints at a particular location in the rings. After rev 60 the scans are faster

Instrument Parameters:

The initial observations were at 0.5 or 1cm⁻¹ resolution, with 15cm⁻¹ appearing late in the prime mission.

List of observations:

Observation	Start Time	Duration
CIRS_00ARI_SUBMU07LP001_PRIME	2004-301T11:10:00	000T06:05:00
CIRS_00ARI_SUBML06HP001_PRIME	2004-303T12:15:00	000T04:45:00
CIRS_006RI_SUBML07LP001_PRIME	2005-104T06:25:00	000T03:55:00
CIRS_006RI_SUBMU04HP001_PRIME	2005-105T11:25:00	000T02:30:00
CIRS_007RI_SUBMU14HP001_PRIME	2005-123T10:49:00	000T07:27:00
CIRS_008RI_SUBML20LP001_PRIME	2005-140T11:00:00	000T07:00:00
CIRS_008RI_SUBMU10HP001_PRIME	2005-142T01:30:00	000T06:30:00

CIRS_009RI_SUBML20LP001_PRIME	2005-157T03:00:00	000T06:30:00
CIRS_009RI_SUBML20LP002_PRIME	2005-158T13:00:00	000T07:00:00
CIRS_009RI_SUBMU15HP003_PRIME	2005-159T19:37:00	000T06:40:00
CIRS_026RI_SUBML07MP001_PRIME	2006-204T00:45:00	000T06:15:00
CIRS_026RI_SUBMU15HP001_PRIME	2006-206T06:00:00	000T08:00:00
CIRS_028RI_SUBMU24MP001_PRIME	2006-253T06:00:00	000T05:30:00
CIRS_029RI_SUBML16MP001_PRIME	2006-267T20:30:00	000T06:30:00
CIRS_029RI_SUBML16MP001_PRIME	2006-267T20:30:00	000T06:30:00
CIRS_029RI_SUBMU36HP001_PRIME	2006-270T03:45:00	000T07:15:00
CIRS_031RI_SUBML20MP001_PRIME	2006-299T15:15:00	000T09:15:00
CIRS_031RI_SUBMU50MP001_PRIME	2006-301T14:00:00	000T08:00:00
CIRS_032RI_SUBMU07HP001_PRIME	2006-309T18:10:00	000T08:05:00
CIRS_032RI_SUBML07HP001_PRIME	2006-311T00:00:00	000T08:00:00
CIRS_033RI_SUBML07HP001_PRIME	2006-323T03:15:00	000T04:00:00
CIRS_034RI_SUBMU07HP001_PRIME	2006-333T16:45:00	000T08:00:00
CIRS_035RI_SUBML52MP001_PRIME	2006-348T08:15:00	000T08:00:00
CIRS_035RI_SUBMU20MP001_PRIME	2006-349T17:15:00	000T08:00:00
CIRS_036RI_SUBML27HP002_PRIME	2006-363T13:00:00	000T08:00:00
CIRS_036RI_SUBML17LP001_PRIME	2006-365T15:00:00	000T05:30:00
CIRS_036RI_SUBMU35MP001_PRIME	2007-001T21:00:00	000T07:20:00
CIRS_037RI_SUBMU45MP001_PRIME	2007-019T21:20:00	000T06:00:00
CIRS_038RI_SUBMMLP001_PRIME	2007-035T14:07:00	000T05:15:00
CIRS_039RI_SUBML10HP001_PRIME	2007-047T19:50:00	000T05:30:00
CIRS_039RI_SUBML59MP001_PRIME	2007-050T12:00:00	000T08:40:00
CIRS_039RI_SUBML40LP001_PRIME	2007-051T11:00:00	000T09:30:00
CIRS_041RI_SUBMU25HP001_PRIME	2007-080T23:00:00	000T07:55:00
CIRS_041RI_SUBMU10HP001_PRIME	2007-081T08:55:00	000T04:00:00
CIRS_042RI_SUBMU40HP001_PRIME	2007-097T07:48:00	000T06:19:00
CIRS_042RI_SUBMU10HP001_PRIME	2007-098T00:20:00	000T03:40:00
CIRS_043RI_SUBMU45MP001_PRIME	2007-113T04:45:00	000T05:00:00
CIRS_050RI_SUBMU04LP001_PRIME	2007-273T23:20:00	000T04:00:00
CIRS_053RI_SUBMU10MP001_PRIME	2007-335T23:30:00	000T07:45:00
CIRS_053RI_SUBML07LP001_PRIME	2007-337T18:40:00	000T06:33:00
CIRS_054RI_SUBML08LP001_PRIME	2007-353T20:16:00	000T05:30:00
CIRS_056RI_SUBMU05LP001_PRIME	2008-018T18:50:00	000T06:30:00

CIRS_057RI_SUBML20LP001_PRIME	2008-028T13:45:00	000T06:20:00
CIRS_058RI_SUBMU35LP001_PRIME	2008-037T18:36:00	000T08:00:00
CIRS_060RI_SUBMU30LP001_PRIME	2008-058T11:31:00	000T08:35:00
CIRS_060RI_SUBMU45MP001_PRIME	2008-059T19:20:00	000T08:00:00
CIRS_060RI_SUBMU47MP001_PRIME	2008-060T11:20:00	000T04:40:00
CIRS_060RI_SUBMU50MP001_PRIME	2008-060T21:00:00	000T03:20:00
CIRS_060RI_SUBML10LP001_PRIME	2008-063T11:15:00	000T03:30:00
CIRS_060RI_SUBML10LP101_PRIME	2008-063T17:45:00	000T01:45:00
CIRS_060RI_SUBML10LP102_PRIME	2008-063T20:00:00	000T05:00:00
CIRS_061RI_SUBMU45MP001_PRIME	2008-070T11:06:00	000T08:00:00
CIRS_061RI_SUBMU50MP001_PRIME	2008-071T10:35:00	000T07:00:00
CIRS_062RI_SUBMU30MP001_PRIME	2008-079T10:05:00	000T08:00:00
CIRS_062RI_SUBMU39MP001_PRIME	2008-080T14:20:00	000T08:00:00
CIRS_063RI_SUBMU28LP001_PRIME	2008-088T14:35:00	000T08:00:00
CIRS_063RI_SUBMU55MP001_PRIME	2008-091T09:05:00	000T08:00:00
CIRS_063RI_SUBMLVENC001_PRIME	2008-092T23:07:00	000T06:58:00
CIRS_065RI_SUBMU55MP001_PRIME	2008-110T07:50:00	000T01:50:00
CIRS_065RI_SUBMU55MP002_PRIME	2008-110T14:50:00	000T04:40:00
CIRS_065RI_SUBMU60MP001_PRIME	2008-111T07:32:00	000T04:48:00
CIRS_065RI_SUBML39LP001_PRIME	2008-112T14:30:00	000T07:00:00
CIRS_065RI_SUBMU10LP001_PRIME	2008-115T08:02:00	000T08:00:00
CIRS_066RI_SUBMU40MP001_PRIME	2008-118T14:17:00	000T07:00:00
CIRS_066RI_SUBMU40MP001_PRIME	2008-118T14:17:00	000T07:00:00
CIRS_066RI_SUBMU50MP001_PRIME	2008-119T07:16:00	000T08:54:00
CIRS_067RI_SUBMU35LP001_PRIME	2008-127T07:15:00	000T08:15:00
CIRS_067RI_SUBMU35LP001_PRIME	2008-127T07:15:00	000T08:15:00
CIRS_068RI_SUBMU20LP001_PRIME	2008-135T06:44:00	000T08:00:00
CIRS_068RI_SUBMU33LP001_PRIME	2008-136T05:59:00	000T06:00:00
CIRS_068RI_SUBMU33LP001_PRIME	2008-136T05:59:00	000T06:00:00
CIRS_070RI_SUBMU35LP001_PRIME	2008-152T09:00:00	000T08:00:00
CIRS_070RI_SUBML32LP001_PRIME	2008-154T22:27:00	000T08:00:00
CIRS_070RI_SUBMU08LP001_PRIME	2008-157T04:41:00	000T07:00:00
CIRS_071RI_SUBMU17LP001_PRIME	2008-158T04:41:00	000T08:00:00
CIRS_072RI_SUBMU12LP001_PRIME	2008-164T21:10:00	000T07:00:00
CIRS_073RI_SUBMU25LP001_PRIME	2008-173T05:19:00	000T02:30:00

CIRS_073RI_SUBMU17LP001_PRIME	2008-172T10:09:00	000T07:00:00
CIRS_073RI_SUBMU25LP002_PRIME	2008-173T09:29:00	000T02:30:00
CIRS_073RI_SUBML25LP001_PRIME	2008-176T03:39:00	000T09:00:00
CIRS_074RI_SUBML25LP002_PRIME	2008-183T00:00:00	000T08:38:00
CIRS_075RI_SUBMU14LP001_PRIME	2008-186T02:55:00	000T08:00:00
CIRS_075RI_SUBMU40MP001_PRIME	2008-188T02:23:00	000T07:29:00
CIRS_076RI_SUBMU45MP001_PRIME	2008-195T12:22:00	000T03:00:00
CIRS_077RI_SUBML24MP001_PRIME	2008-204T11:50:00	000T04:00:00
CIRS_078RI_SUBMU27LP001_PRIME	2008-208T07:36:00	000T09:00:00
CIRS_084RI_SUBMS10LP001_PRIME	2008-256T15:29:00	000T05:16:00
CIRS_086RI_SUBMS45LP001_PRIME	2008-269T23:20:00	000T08:45:00
CIRS_089RI_SUBMS45LP001_PRIME	2008-291T18:00:00	000T07:00:00
CIRS_090RI_SUBMS10LP001_PRIME	2008-300T13:45:00	000T09:00:00
CIRS_093RI_SUBMS30LP001_PRIME	2008-322T19:04:00	000T08:40:00
CIRS_096RI_SUBMS10LP001_PRIME	2008-347T18:52:00	000T08:00:00
CIRS_100RI_SUBMS20LP001_PRIME	2009-017T16:00:00	000T12:02:00
CIRS_100RI_SUBMS20LP001_PRIME	2009-017T16:00:00	000T12:02:00

2. Observation Type: TEMPL*, TEMPU*, TEMPN, TEMPS

Prime Instrument: CIRS

Usual Riders:

Number of Observations

31 TEMPL pm

45 TEMPU pm

4 TEMPN xm

4 TEMPS xm

This campaign was aimed at observing radial variation in ring temperature to constrain differences in structure across the rings. While both the 'SUBM' campaigns and 'TEMP' campaigns used radial scans, the 'TEMP' campaign was designed to use faster scans and obtain a larger variety of observation geometries. Approximately mid-way through the prime mission the TEMPs started to be placed in the timeline during negotiations at phases and latitudes that had not been previously observed.

The naming convention is that 'L' or 'U' following 'TEMP' indicates whether it observed the lit or unlit side of the rings (corresponding to South or North, as these were all taken during the prime mission prior to Saturn equinox). Following

that is an approximate sub-spacecraft latitude and 'LP', 'MP', or 'HP' to indicate whether it was at low, medium or high phase angle.

Toward the end of prime mission the 'L' and 'U' were replaced with 'S' and 'N', for observing the South or North side of the rings, in anticipation of directions reversing after Saturn Equinox. There are 8 such observations.

There are more TEMP observations of the unlit side of the rings than the lit side simply because observing time on the unlit side was not as heavily subscribed as on the lit side.

Pointing: These use FP1 to rings, and were nearly all performed with radial scans programmed via the R_RAD_LON module. The initial observations had at most a couple of radial scans, but toward the end of main mission, after approximately rev 60, more scans were used, when possible, and at faster rates.

Instrument Parameters: These were all taken at 15cm⁻¹ resolution and primarily with FP1; FP3 and FP4 were always included, but were omitted when data volume constraints required it.

List of observations:

Observation	Start Time	Duration
CIRS_00BRI_TEMPL06MP001_PRIME	2004-350T19:30:00	000T04:00:00
CIRS_00BRI_TEMPL06MP001_PRIME	2004-350T19:30:00	000T04:00:00
CIRS_007RI_TEMPL20LP001_PRIME	2005-122T03:35:00	000T02:00:00
CIRS_009RI_TEMPL20LP001_PRIME	2005-156T22:00:00	000T05:00:00
CIRS_014RI_TEMPL15LP001_PRIME	2005-247T04:00:00	000T06:00:00
CIRS_028RI_TEMPL10MP001_PRIME	2006-252T00:30:00	000T02:00:00
CIRS_029RI_TEMPL10HP001_PRIME	2006-267T07:30:00	000T02:40:00
CIRS_029RI_TEMPL10HP001_PRIME	2006-267T07:30:00	000T02:40:00
CIRS_033RI_TEMPL20HP001_PRIME	2006-323T17:15:00	000T02:00:00
CIRS_035RI_TEMPL25LP001_PRIME	2006-349T03:30:00	000T02:00:00
CIRS_036RI_TEMPL57LP001_PRIME	2006-364T18:30:00	000T01:00:00
CIRS_037RI_TEMPL35LP001_PRIME	2007-016T22:30:00	000T02:00:00
CIRS_040RI_TEMPL55MP001_PRIME	2007-066T21:51:00	000T02:00:00
CIRS_040RI_TEMPL40LP001_PRIME	2007-067T09:41:00	000T02:40:00
CIRS_042RI_TEMPL43LP001_PRIME	2007-099T10:15:00	000T02:00:00
CIRS_043RI_TEMPL25MP001_PRIME	2007-115T16:30:00	000T02:00:00
CIRS_055RI_TEMPL37MP001_PRIME	2008-004T04:45:00	000T02:03:00
CIRS_056RI_TEMPL05MP001_PRIME	2008-017T11:20:00	000T03:00:00
CIRS_057RI_TEMPL10LP001_PRIME	2008-029T06:05:00	000T02:00:00
CIRS_058RI_TEMPL16LP001_PRIME	2008-040T16:00:00	000T02:00:00

CIRS_061RI_TEMPL30MP001_PRIME	2008-073T11:50:00	000T05:01:00
CIRS_061RI_TEMPL15LP001_PRIME	2008-074T02:50:00	000T03:35:00
CIRS_065RI_TEMPL55MP001_PRIME	2008-112T02:05:00	000T05:00:00
CIRS_068RI_TEMPL48LP001_PRIME	2008-139T10:05:00	000T02:09:00
CIRS_069RI_TEMPL25LP001_PRIME	2008-148T05:19:32	000T02:25:00
CIRS_070RI_TEMPL42LP001_PRIME	2008-154T10:00:00	000T01:27:00
CIRS_071RI_TEMPL20LP001_PRIME	2008-162T03:50:00	000T03:10:00
CIRS_072RI_TEMPL53MP001_PRIME	2008-168T11:45:00	000T03:00:00
CIRS_074RI_TEMPL10LP001_PRIME	2008-184T04:00:00	000T03:00:00
CIRS_074RI_TEMPL13LP001_PRIME	2008-183T20:30:00	000T03:15:00
CIRS_075RI_TEMPL17LP001_PRIME	2008-191T02:40:00	000T01:05:00
CIRS_075RI_TEMPL17LP002_PRIME	2008-191T07:30:00	000T01:15:00
CIRS_079RI_TEMP20LP001_PRIME	2008-214T07:35:00	000T06:15:00
CIRS_079RI_TEMP45HP001_PRIME	2008-217T06:45:00	000T01:15:00
CIRS_080RI_TEMP45LP001_PRIME	2008-223T08:50:00	000T06:00:00
CIRS_079RI_TEMP60HP001_PRIME	2008-217T01:45:00	000T01:00:00
CIRS_00BRI_TEMP05LP001_PRIME	2004-349T17:52:00	000T04:00:00
CIRS_00BRI_TEMP05LP001_PRIME	2004-349T17:52:00	000T04:00:00
CIRS_007RI_TEMP011HP001_PRIME	2005-123T18:16:00	000T03:30:00
CIRS_008RI_TEMP017HP001_PRIME	2005-141T15:08:00	000T02:28:00
CIRS_009RI_TEMP012HP002_PRIME	2005-160T02:17:00	000T01:43:00
CIRS_010RI_TEMP008HP002_PRIME	2005-178T11:00:00	000T02:00:00
CIRS_012RI_TEMP005HP001_PRIME	2005-215T01:30:00	000T03:50:00
CIRS_013RI_TEMP009HP001_PRIME	2005-233T06:00:00	000T04:45:00
CIRS_026RI_TEMP015HP002_PRIME	2006-206T02:00:00	000T04:00:00
CIRS_028RI_TEMP022HP001_PRIME	2006-253T21:30:00	000T04:00:00
CIRS_029RI_TEMP030MP001_PRIME	2006-269T02:30:00	000T03:30:00
CIRS_029RI_TEMP035HP001_PRIME	2006-271T01:00:00	000T03:00:00
CIRS_030RI_TEMP020MP001_PRIME	2006-285T08:35:00	000T01:10:00
CIRS_030RI_TEMP010MP001_PRIME	2006-285T05:00:00	000T01:35:00
CIRS_030RI_TEMP040MP001_PRIME	2006-285T20:30:00	000T03:00:00
CIRS_030RI_TEMP045MP001_PRIME	2006-286T07:00:00	000T02:30:00
CIRS_032RI_TEMP005HP002_PRIME	2006-310T02:15:00	000T05:00:00

CIRS_033RI_TEMP05HP001_PRIME	2006-325T15:30:00	000T03:15:00
CIRS_034RI_TEMP05HP001_PRIME	2006-334T00:45:00	000T05:00:00
CIRS_036RI_TEMP05LP001_PRIME	2007-001T02:00:00	000T02:30:00
CIRS_037RI_TEMP028MP001_PRIME	2007-018T21:50:00	000T04:00:00
CIRS_037RI_TEMP055MP001_PRIME	2007-021T00:30:00	000T01:15:00
CIRS_041RI_TEMP045HP001_PRIME	2007-079T19:40:00	000T03:20:00
CIRS_041RI_TEMP015HP001_PRIME	2007-081T06:55:00	000T02:00:00
CIRS_055RI_TEMP033MP001_PRIME	2008-001T15:33:00	000T02:45:00
CIRS_056RI_TEMP045MP001_PRIME	2008-015T07:05:00	000T02:55:00
CIRS_057RI_TEMP005LP001_PRIME	2008-030T14:30:00	000T04:00:00
CIRS_060RI_TEMP057MP001_PRIME	2008-061T12:00:00	000T01:15:00
CIRS_060RI_TEMP020LP001_PRIME	2008-067T11:51:00	000T05:00:00
CIRS_062RI_TEMP047MP001_PRIME	2008-080T09:50:00	000T04:00:00
CIRS_062RI_TEMP028HP001_PRIME	2008-083T02:20:00	000T03:00:00
CIRS_063RI_TEMP049MP001_PRIME	2008-090T18:34:00	000T04:30:00
CIRS_063RI_TEMP016LP001_PRIME	2008-096T17:49:00	000T04:00:00
CIRS_064RI_TEMP030LP001_PRIME	2008-098T17:34:00	000T04:00:00
CIRS_064RI_TEMP015MP001_PRIME	2008-106T07:33:00	000T04:00:00
CIRS_065RI_TEMP060MP001_PRIME	2008-110T19:30:00	000T04:15:00
CIRS_065RI_TEMP026HP001_PRIME	2008-111T16:00:00	000T04:05:00
CIRS_065RI_TEMP006LP001_PRIME	2008-114T17:32:00	000T04:00:00
CIRS_065RI_TEMP015LP001_PRIME	2008-115T16:32:00	000T04:00:00
CIRS_066RI_TEMP020LP001_PRIME	2008-125T06:46:00	000T04:00:00
CIRS_067RI_TEMP058MP001_PRIME	2008-129T16:30:00	000T04:00:00
CIRS_068RI_TEMP020LP001_PRIME	2008-135T14:44:00	000T04:00:00
CIRS_068RI_TEMP035LP001_PRIME	2008-136T12:29:00	000T04:00:00
CIRS_070RI_TEMP016LP001_PRIME	2008-150T22:42:00	000T04:00:00
CIRS_074RI_TEMP016LP001_PRIME	2008-180T03:23:00	000T03:30:00
CIRS_074RI_TEMP006LP001_PRIME	2008-185T11:50:00	000T04:00:00
CIRS_079RI_TEMP060MP001_PRIME	2008-218T02:35:00	000T05:00:00
CIRS_079RI_TEMP020LP001_PRIME	2008-218T20:35:00	000T05:00:00
CIRS_080RI_TEMP010LP001_PRIME	2008-227T00:44:00	000T06:00:00
CIRS_082RI_TEMP020LP001_PRIME	2008-240T23:59:00	000T08:50:00

iv. *Spectral features campaign* (COMPs, FMONITORs, FMOVIEs, ANSASTAREs):

i. Observation Type: COMP[A/C]

Prime instrument: CIRS

Riders: ISS, UVIS, VIMS

Number of observations: 8 Prime Mission, 3 Extended Mission (see later for CSM)

Primary boresight: CIRS_FP1, CIRS_FP3, CIRS_FP4

Spectral resolution: 0.5 cm^{-1} (401 RTI) & 3 cm^{-1} (96 RTI)

Description: COMP scans were designed to take long integrations from points in the A, B, or C ring near the ansae in order to look for spectral features. The goal of these observations to 1) determine the location of the spectral "roll-off" in the far IR and the factors by which it varies (hint: grain size), 2) determine water ice type (amorphous versus crystalline, and 3) determine any observable contaminants.

Emissivity spectra are produced by dividing the observed radiance by the best fit black body. Long integrations (several hours) were necessary to gain signal-to-noise for feature determination. Thus, due to competition during the Prime and Extended Missions, distant observations were most easily observable. COMPs taken in the CSM took on a slightly different flavor to allow for specific, localized ring regions to be targeted (see later). In addition, calibrations from DSCAL4000 database is best for reducing noise levels to maximize feature determination.

ii. Observation Type: FMONITOR

Prime Instrument: CIRS

Usual Riders: ISS

Number of Observations: 73

These observations took place early in the prime mission, and were actually designed with the primary objective of facilitating ISS imagery of the F ring. The pointing was designed to return long integrations of the B and A rings by CIRS, while the ISS WAC took imagery of the F ring.

For CIRS, these function much like the COMP observations. Refer to notes on the CIRS_FMONITOR*_ISS observations for details on ISS imagery taken.

There are two types of FMONITOR: a) observations that are 6 to 10 hours long and occur in groups of 2 to 4 observations, where observations within the group are separated by 1 to 10 days; b) observations that are 30-90 minutes long, occur in groups of 5 up to 16, where observations within the group are separated by on the order of one hour.

There is no definitive way to associate groups of observations that were planned together, but there are 12 groups of type (a) observations, two of which are single observations, and there are 4 groups of type (b) observations.

Observations of type (a) typically take deep space off one Ansa, then an almost equal number of spectra are taken on the Ansa, with FP3/4 and FP1 on A and/or B ring. The observation then takes a short amount of data with FP3/4 and FP1 on the other Ansa, and this process repeats several times. The deep space are interspersed, specified by a pointing such that the projected radius in the ring plane is from 5 to 15 R_S.

Observations of type (b) proceed similarly to type (a), although they are much shorter in duration. In between the Ansaes, they swing through Saturn.

Pointing: The pointing is either FP3/4 or FP1 to rings, with specific pointing set such that the footprints of the CIRS focal planes are near the outer edge of the main rings at the Ansaes. They are taken from approximately 30R_S, with an emission angle of up to 20degrees.

Instrument Parameters: These appear to all have 0.5cm⁻¹ resolution, and FP3 takes spectra from all 10 detectors.

List of observations:

Observation	Start Time	Duration
CIRS_00ARI_FMONITOR001_PRIME	2004-311T22:48:00	000T06:30:00
CIRS_00BRI_FMONITOR001_PRIME	2004-335T10:20:00	000T06:50:00
CIRS_00CRI_FMONITOR001_PRIME	2005-020T12:30:00	000T08:00:00
CIRS_00CRI_FMONITOR002_PRIME	2005-021T12:15:00	000T04:00:00
CIRS_00CRI_FMONITOR003_PRIME	2005-024T12:00:00	000T04:00:00
CIRS_00CRI_FMONITOR004_PRIME	2005-026T12:00:00	000T04:00:00
CIRS_00CRI_FMONITOR005_PRIME	2005-027T12:00:00	000T04:00:00
CIRS_00CRI_FMONITOR006_PRIME	2005-028T12:00:00	000T04:00:00
CIRS_006RI_FMONITOR001_PRIME	2005-109T06:15:00	000T08:15:00
CIRS_006RI_FMONITOR002_PRIME	2005-111T07:28:00	000T10:00:00
CIRS_006RI_FMONITOR003_PRIME	2005-112T05:43:00	000T11:44:00
CIRS_008RI_FMONITOR001_PRIME	2005-145T03:06:00	000T08:17:00
CIRS_008RI_FMONITOR002_PRIME	2005-149T01:21:00	000T08:00:00
CIRS_009RI_FMONITOR001_PRIME	2005-153T02:13:00	000T08:00:00
CIRS_009RI_FMONITOR002_PRIME	2005-155T15:00:00	000T00:30:00
CIRS_009RI_FMONITOR003_PRIME	2005-163T02:35:00	000T00:30:00
CIRS_009RI_FMONITOR004_PRIME	2005-163T03:59:00	000T00:30:00
CIRS_009RI_FMONITOR005_PRIME	2005-163T05:55:00	000T00:30:00
CIRS_009RI_FMONITOR006_PRIME	2005-163T07:59:00	000T00:30:00
CIRS_009RI_FMONITOR007_PRIME	2005-166T02:47:00	000T01:28:00
CIRS_009RI_FMONITOR008_PRIME	2005-166T04:55:00	000T01:28:00
CIRS_009RI_FMONITOR009_PRIME	2005-166T07:03:00	000T01:28:00
CIRS_009RI_FMONITOR010_PRIME	2005-166T21:23:00	000T01:28:00
CIRS_009RI_FMONITOR011_PRIME	2005-166T23:31:00	000T01:28:00
CIRS_009RI_FMONITOR012_PRIME	2005-167T01:39:00	000T01:28:00
CIRS_009RI_FMONITOR013_PRIME	2005-167T03:47:00	000T01:28:00
CIRS_009RI_FMONITOR014_PRIME	2005-167T05:55:00	000T01:28:00

CIRS_009RI_FMONITOR015_PRIME	2005-168T05:24:00	000T01:28:00
CIRS_009RI_FMONITOR016_PRIME	2005-168T07:32:00	000T01:28:00
CIRS_009RI_FMONITOR017_PRIME	2005-168T09:40:00	000T01:28:00
CIRS_009RI_FMONITOR018_PRIME	2005-168T11:48:00	000T01:28:00
CIRS_010RI_FMONITOR001_PRIME	2005-181T03:37:00	000T08:00:00
CIRS_010RI_FMONITOR002_PRIME	2005-182T01:25:00	000T06:57:00
CIRS_010RI_FMONITOR003_PRIME	2005-169T02:44:00	000T01:28:00
CIRS_010RI_FMONITOR004_PRIME	2005-169T04:52:00	000T01:28:00
CIRS_010RI_FMONITOR005_PRIME	2005-169T07:00:00	000T01:28:00
CIRS_010RI_FMONITOR006_PRIME	2005-169T09:08:00	000T01:28:00
CIRS_010RI_FMONITOR007_PRIME	2005-169T11:16:00	000T01:28:00
CIRS_010RI_FMONITOR008_PRIME	2005-170T01:20:00	000T01:28:00
CIRS_010RI_FMONITOR010_PRIME	2005-170T05:36:00	000T01:28:00
CIRS_012RI_FMONITOR001_PRIME	2005-218T00:22:00	000T08:00:00
CIRS_013RI_FMONITOR001_PRIME	2005-238T00:33:00	000T08:00:00
CIRS_013RI_FMONITOR002_PRIME	2005-239T02:33:00	000T08:00:00
CIRS_014RI_FMONITOR001_PRIME	2005-242T02:18:00	000T08:00:00
CIRS_027RI_FMONITOR001_PRIME	2006-223T01:15:00	000T02:15:00
CIRS_027RI_FMONITOR002_PRIME	2006-223T04:00:00	000T00:45:00
CIRS_027RI_FMONITOR003_PRIME	2006-236T01:21:00	000T01:00:00
CIRS_027RI_FMONITOR004_PRIME	2006-236T03:21:00	000T01:00:00
CIRS_027RI_FMONITOR005_PRIME	2006-236T05:21:00	000T01:00:00
CIRS_027RI_FMONITOR006_PRIME	2006-236T07:21:00	000T01:00:00
CIRS_027RI_FMONITOR007_PRIME	2006-236T09:21:00	000T01:00:00
CIRS_027RI_FMONITOR008_PRIME	2006-236T11:21:00	000T01:00:00
CIRS_034RI_FMONITOR001_PRIME	2006-333T01:46:00	000T05:00:00
CIRS_035RI_FMONITOR001_PRIME	2006-343T22:02:00	000T08:00:00
CIRS_036RI_FMONITOR003_PRIME	2006-360T14:49:00	000T05:00:00
CIRS_038RI_FMONITOR001_PRIME	2007-025T22:51:00	000T04:00:00
CIRS_039RI_FMONITOR002_PRIME	2007-054T19:22:00	000T05:00:00
CIRS_041RI_FMONITOR001_PRIME	2007-076T19:15:00	000T04:00:00
CIRS_042RI_FMONITOR001_PRIME	2007-092T00:21:30	000T06:53:30
CIRS_042RI_FMONITOR002_PRIME	2007-105T08:17:00	000T06:30:00
CIRS_042RI_FMONITOR003_PRIME	2007-105T20:17:00	000T01:00:00
CIRS_043RI_FMONITOR001_PRIME	2007-109T08:45:00	000T11:45:00

CIRS_043RI_FMONITOR002_PRIME	2007-119T13:15:00	000T06:00:00
CIRS_049RI_FMONITOR001_PRIME	2007-249T15:00:00	000T01:20:00
CIRS_049RI_FMONITOR002_PRIME	2007-249T16:30:00	000T01:20:00
CIRS_049RI_FMONITOR003_PRIME	2007-249T18:00:00	000T01:20:00
CIRS_049RI_FMONITOR004_PRIME	2007-249T19:30:00	000T01:20:00
CIRS_049RI_FMONITOR005_PRIME	2007-249T21:00:00	000T01:20:00
CIRS_050RI_FMONITOR001_PRIME	2007-263T21:36:00	000T06:00:00
CIRS_053RI_FMONITOR002_PRIME	2007-332T17:30:00	000T08:00:00
CIRS_055RI_FMONITOR001_PRIME	2007-361T08:17:00	000T05:30:00
CIRS_055RI_FMONITOR002_PRIME	2008-008T17:15:00	000T07:00:00
CIRS_056RI_FMONITOR001_PRIME	2008-020T17:15:00	000T07:00:00

3. Observation Type: FMOVIE, ANSASTARE

Prime Instrument: CIRS

Usual Riders:

Number of Observations:

3 FMOVIEA

4 FMOVIEB

1 FMOVIEC

6 ANSASTARE

These observations were all designed to capture signal from F Ring with FP1. The FMOVIE observations were designed to find temperature signal from the rings, and to see if there was a difference in brightness from one Ansa to the other. They were taken at low emission angle in order to maximize line of sight optical depth through the F ring, and flipped back and forth between Ansa. The ANSASTARE observations were added in the Solstice mission in order to capture complete rotations of the ring in order to look for features. They are at higher emission angles because the team learned that the FMOVIE geometry was not optimal.

Pointing: The FMOVIEs place FP1 just off the main rings, typically with $144,000\text{km} < r_{\text{FP1}} < 160,000\text{km}$. They acquire data at one Ansa for a short period of time, on the order of 15 minutes, then swing through Saturn to the other Ansa. Some of them collect 15 minute segments of deep space during this cycle, whereas others acquire deep space only at the beginning and end of the observation. This strategy was designed to obtain a somewhat uniform longitudinal coverage of the F ring without observing for a full 14 hour rotational period.

The emission angle is less than 1 degree, and they are taken from approximately $10 R_s$.

The ANSASTAREs were designed to capture a complete rotation of the F ring. Because the team did not anticipate getting full 15 hour observations approved during Solstice Mission planning, they were designed in pairs of 8 hour long observations, arranged so that the two members of each pair were close together in time and captured complementary longitude ranges. There were some logistical issues scheduling these, where observations were shifted in the timeline to accommodate other teams, and also incorrect Ansaes were targeted on at least one occasion, which compromised the longitudinal coverage of some of these observations. A thorough check on longitude ranges actually collected has not been done yet.

These observations focused FP1 off one Ansa and merely took data at the same pointing for the duration of the observation. The team determined that better signal results when the F ring is viewed from a high enough elevation that its filling factor across the FP1 FOV is significant (i.e., edge-on viewing is not optimal), so these are taken at emission angles of up to 10 degrees from the ring plane.

Instrument Parameters: All of these observations were taken at 15cm^{-1} resolution, due to the expected low signal.

List of observations:

Observation	Start Time	Duration
CIRS_003RF_FMOVIEA001_PRIME	2005-047T09:20:00	000T04:35:00
CIRS_005RF_FMOVIEA001_PRIME	2005-088T04:53:00	000T07:35:00
CIRS_003RF_FMOVIEA002_PRIME	2005-047T14:35:00	000T01:14:00
CIRS_019RF_FMOVIEB003_PRIME	2005-359T08:55:00	000T10:35:00
CIRS_021RF_FMOVIEB001_PRIME	2006-055T10:12:00	000T04:53:00
CIRS_019RF_FMOVIEB002_PRIME	2005-359T04:00:00	000T04:00:00
CIRS_023RF_FMOVIEB002_PRIME	2006-119T08:44:00	000T08:30:00
CIRS_049RF_FMOVIEC001_PRIME	2007-240T22:40:00	000T05:10:00
CIRS_255RF_ANSASTARE001_PRIME	2017-004T02:09:00	000T09:51:00
CIRS_255RF_ANSASTARE002_PRIME	2017-005T06:59:00	000T09:52:00
CIRS_274RI_ANSASTARE001_PRIME	2017-137T03:09:00	000T14:00:00
CIRS_277RI_ANSASTARE001_PRIME	2017-157T18:07:00	000T18:10:00
CIRS_286RI_ANSASTARE001_PRIME	2017-215T16:55:00	000T09:44:00
CIRS_288RI_ANSASTARE001_PRIME	2017-227T19:00:00	000T06:53:00

Findings from the main mission scans influenced designs in the rest of the mission. Principally it was found that:

- CIRS did not have enough stability in the region below 440 cm⁻¹ (upwards of 22μm) to really detect a rolloff; SUBM measurements started to merge with TEMPS
- No spectral features were obvious or would likely be detectable using COMP measurements. These were phased out (to return in XXM, mostly as fillers of unused time).
- There was a much bigger dependence of temperature on geometry and radial location than had been considered before.
- The isolated particle model used to justify the VERT and SHAD observations was not so clear cut.

c. EXTENDED MISSION (XM):

During XM planning, the TWT suggested that the information return from azimuthal scans was small, as a cooling curve can be fit with only a few points instead of requiring a complete scan. It was suggested to design more observations which kept radial scans, but spaced so that the data could be used to fit cooling curves as the particles moved.

At this point, the large variation in temperature with viewing geometry and location on the rings led the team to attempt to get a fairly uniform coverage in the latitude-phase plane that Nicholson developed for VIMS scheduling.

- Azimuthal campaign:* VERT measurements turned into VCAS and VENC, specialized observations that had high enough resolution to see the Cassini division and trans-Encke division.

1. See *VERTS in the Prime Mission section for details.*

- Phase/lat AND particle properties:* The VERT, TEMP and SUBM scans became TMAP and VTMP. Originally [I THINK] the distinction between these was that the VTMPs were at higher Sub-spacecraft latitude and the TMAPs lower, but the identities of these two sets of observations seem to have merged. These were ambitious observations designed to cover what the VERT and TEMP's had done together in main mission, and scanned at fast rates across the rings with the objective of catching the cooling curve points that the TWT had suggested. It was found that these were not RBOT-friendly, and they were phased out as Equinox approached. In addition to fixing particle properties, some attention was paid to the coverage of these observations in phase-latitude space, as the rings team came to realize that the viewing geometry played an important role in the temperature returned.

1. Observation Type: TMAP*

Prime Instrument: CIRS

Usual Riders:

Number of Observations:

28 TMAPN*

16 TMAPS*

2 TMAPS

The TMAP campaign was a continuation of the TEMP campaign designed for the extended mission. During the presentation of CIRS strategies to the Rings TWT prior to XM, the TWT argued that azimuthal observations did not represent good

use of time, given the few points needed to constrain cooling curves (at this point in time, the subtle variation in azimuthal signal due to wake structures was not appreciated). Consequently the TMAP observations were updated to include a large number of radial scans, taken faster than during the TEMP observations.

These were subsequently discovered to strain the spacecraft's ability to dissipate angular momentum (they were "not RBOT friendly"), and other instrument teams, particularly VIMS, complained that they could not ride along on observations that slewed as fast as the TMAPS. They were discontinued in the solstice mission.

The naming convention is that 'N' or 'S' following 'TMAP' indicates whether it observed the North or South of the rings. Following that is an approximate sub-spacecraft latitude and 'LP', 'MP', or 'HP' to indicate whether it was at low, medium or high phase angle.

Pointing: These use FP1 to rings, and were nearly all performed with radial scans programmed via the R_RAD_LON module. The initial observations had at most a couple of radial scans, but toward the end of main mission, after approximately rev 60, more scans were added at faster rates.

Instrument Parameters: These were all taken at 15cm^{-1} resolution and primarily with FP1; FP3 and FP4 were always included, but were omitted when data volume constraints required it.

List of observations:

Observation	Start Time	Duration
CIRS_081RI_TMAPN30LP001_PRIME	2008-230T00:30:00	000T07:40:00
CIRS_085RI_TMAPN20LP001_PRIME	2008-258T22:54:00	000T03:15:00
CIRS_085RI_TMAPN30LP001_PRIME	2008-259T02:09:00	000T08:00:00
CIRS_088RI_TMAPN20LP001_PRIME	2008-281T07:10:00	000T04:05:00
CIRS_088RI_TMAPN45LP001_PRIME	2008-282T06:00:00	000T05:15:00
CIRS_089RI_TMAPN20LP001_PRIME	2008-287T23:40:00	000T09:55:00
CIRS_092RI_TMAPN20LP001_PRIME	2008-310T00:00:00	000T09:00:00
CIRS_092RI_TMAPN30LP001_PRIME	2008-310T19:48:00	000T06:10:00
CIRS_092RI_TMAPN45LP001_PRIME	2008-311T18:00:00	000T09:00:00
CIRS_092RI_TMAPN10LP001_PRIME	2008-317T06:45:00	000T08:00:00
CIRS_096RI_TMAPN20LP001_PRIME	2008-341T22:07:00	000T06:55:00
CIRS_096RI_TMAPN45LP001_PRIME	2008-342T17:52:00	000T05:20:00
CIRS_098RI_TMAPN30LP001_PRIME	2008-357T22:54:00	000T07:40:00
CIRS_098RI_TMAPN45LP001_PRIME	2008-358T18:30:00	000T04:00:00
CIRS_105RI_TMAPN45LP001_PRIME	2009-064T08:00:00	000T08:00:00
CIRS_107RI_TMAPN45MP001_PRIME	2009-091T10:15:00	000T06:20:00
CIRS_108RI_TMAPN30LP001_PRIME	2009-102T15:44:00	000T07:00:00

CIRS_109RI_TMAPN45LP001_PRIME	2009-118T22:52:00	000T04:00:00
CIRS_111RI_TMAPN45LP001_PRIME	2009-148T07:38:00	000T09:30:00
CIRS_114RI_TMAPN30MP001_PRIME	2009-186T23:33:00	000T02:25:00
CIRS_114RI_TMAPN45MP001_PRIME	2009-193T21:00:00	000T09:07:00
CIRS_114RI_TMAPN30MP002_PRIME	2009-196T07:39:00	000T09:41:00
CIRS_106RI_TMAPN20LP001_PRIME	2009-075T07:45:00	000T10:00:00
CIRS_115RI_TMAPN25MP001_PRIME	2009-212T01:55:00	000T04:25:00
CIRS_116RI_TMAPN20MP001_PRIME	2009-225T08:45:00	000T06:30:00
CIRS_116RI_TMAPN20MP002_PRIME	2009-227T19:20:00	000T12:10:00
CIRS_117RI_TMAPN10LP002_PRIME	2009-240T20:40:00	000T06:00:00
CIRS_118RI_TMAPN10LP002_PRIME	2009-264T22:55:00	000T08:00:00
CIRS_080RI_TMAPS20LP001_PRIME	2008-226T09:05:00	000T05:15:00
CIRS_085RI_TMAPS10LP001_PRIME	2008-263T15:05:00	000T04:10:00
CIRS_087RI_TMAPS10LP001_PRIME	2008-278T14:15:00	000T04:00:00
CIRS_088RI_TMAPS30LP001_PRIME	2008-285T01:40:00	000T04:00:00
CIRS_090RI_TMAPS45LP001_PRIME	2008-299T03:04:00	000T07:08:00
CIRS_092RI_TMAPS10LP001_PRIME	2008-315T20:00:00	000T08:44:00
CIRS_094RI_TMAPS45LP001_PRIME	2008-330T01:05:00	000T07:10:00
CIRS_100RI_TMAPS45LP001_PRIME	2009-016T14:35:00	000T08:00:00
CIRS_102RI_TMAPS45MP001_PRIME	2009-035T15:29:00	000T04:00:00
CIRS_103RI_TMAPS45MP001_PRIME	2009-047T17:25:00	000T09:30:00
CIRS_103RI_TMAPS30LP001_PRIME	2009-048T18:15:00	000T08:40:00
CIRS_104RI_TMAPS45MP001_PRIME	2009-059T12:30:00	000T08:30:00
CIRS_104RI_TMAPS30LP001_PRIME	2009-060T12:20:00	000T06:30:00
CIRS_108RI_TMAPS45MP001_PRIME	2009-099T10:59:00	000T08:00:00
CIRS_109RI_TMAPS20LP001_PRIME	2009-115T08:40:00	000T06:15:00
CIRS_111RI_TMAPS45MP001_PRIME	2009-145T07:54:00	000T04:00:00
CIRS_134RI_TMAPS001_PRIME	2010-183T04:29:00	000T05:00:00
CIRS_134RI_TMAPS002_PRIME	2010-184T13:29:00	000T05:00:00

1. Observation Type: VTMP

Prime Instrument: CIRS

Usual Riders:

Number of Observations

- 1 VT MPL
- 2 VT MPU
- 11 VT MPN
- 9 VT MPS

These observations were introduced late in the prime mission and the extended mission and superseded the previous VERTs, for the same reason that the TMAPs were introduced to supersede the TEMPs. That reason was that the rings team decided that azimuthal scans did not return much information compared to the time they took. It was reasoned that by using radial scans placed at a grid of local times, one could constrain heating and cooling curves at many radii instead of at a few designated radii.

The VTMP observations focus mostly on radial scans away from the shadow region, although a few of the observations do look at the shadow region-- hence also taking on the role of the previous SHAD observations.

The naming designation is similar to the prime mission campaigns, with 'VTMP' being followed by 'U' or 'L' to indicate unlit or lit side, and then an approximate latitude followed by a general indicator of whether it was at low, medium, or high phase angle ('LP', 'MP', or 'HP'). In later observations 'N' and 'S' supersede the use of 'U' and 'L' to denote the side of the rings being observed, where 'N' indicates the North side and 'S' the South side.

Pointing: The observations are FP1 to rings and are usually long blocks of time, with a series of radial spokes. If the observation was long enough, sometimes an azimuthal scan was added. Also, 6 of the observations make use of the P_SHAD_DUR module, which created quasi-radial scans but where the local hour angle varied with radius according to Keplerian rotation rate, such that all points along the scan are an equal number of minutes away from shadow ingress or egress.

Instrument Parameters: These were all designed at 15cm⁻¹ resolution for rapid, high S/N resolution of the spectrum that would yield temperature and filling factor information.

List of observations:

Observation	Start Time	Duration
CIRS_077RI_VTMPU37MP001_PRIME	2008-202T04:50:00	000T03:45:00
CIRS_078RI_VTMPU36LP001_PRIME	2008-209T01:40:00	000T05:25:00
CIRS_081RI_VTMPN60LP001_PRIME	2008-231T00:30:00	000T04:55:00
CIRS_086RI_VTMPN60LP001_PRIME	2008-267T15:34:00	000T09:56:00
CIRS_089RI_VTMPN60LP001_PRIME	2008-289T20:55:00	000T05:50:00
CIRS_090RI_VTMPN60LP001_PRIME	2008-296T20:31:00	000T09:30:00
CIRS_098RI_VTMPN60MP001_PRIME	2008-359T23:24:00	000T06:12:00

CIRS_104RI_VTMPN60MP001_PRIME	2009-054T15:00:00	000T11:00:00
CIRS_106RI_VTMPN60MP001_PRIME	2009-077T16:20:00	000T08:00:00
CIRS_113RI_VTMPN60MP001_PRIME	2009-178T17:35:00	000T07:00:00
CIRS_103RI_VTMPN60MP002_PRIME	2009-042T16:14:00	000T10:41:00
CIRS_107RI_VTMPN60MP002_PRIME	2009-090T16:45:00	000T06:40:00
CIRS_109RI_VTMPN60MP002_PRIME	2009-121T06:22:00	000T08:00:00
CIRS_062RI_VTMPLLP002_PRIME	2008-084T09:50:00	000T07:00:00
CIRS_086RI_VTMPS70MP001_PRIME	2008-269T08:00:00	000T04:00:00
CIRS_087RI_VTMPS60MP001_PRIME	2008-277T01:20:00	000T02:35:00
CIRS_090RI_VTMPS60MP001_PRIME	2008-298T19:04:00	000T08:00:00
CIRS_102RI_VTMPS60MP001_PRIME	2009-034T14:14:00	000T08:00:00
CIRS_104RI_VTMPS60MP001_PRIME	2009-058T05:10:00	000T04:30:00
CIRS_104RI_VTMPS60MP002_PRIME	2009-058T18:30:00	000T06:50:00
CIRS_108RI_VTMPS60MP002_PRIME	2009-098T10:59:00	000T08:00:00
CIRS_109RI_VTMPS60MP001_PRIME	2009-113T08:40:00	000T09:15:00
CIRS_110RI_VTMPS60MP001_PRIME	2009-128T11:51:00	000T08:00:00

iii. *Vertical structure campaign:* The TDIF were introduced to cover opposite sides of the rings at similar geometry, as a radial analogue to what the VERTs had been intended to do in main mission.

See TDIF section under SOLSTICE MISSION (below).

iv. *Equinox planning:* The orbital plan for the end of extended mission offered very little opportunity for getting observations of the rings right before and after the equinox event. This fact was not appreciated until late in the planning, and CIRS was the only ORS instrument to suffer from this deficiency. Namely, by this time in the mission we had found that the seasonal variation of ring temperatures was important, and we expected that the cooling of the lit side right before equinox and subsequent heating of the previously unlit side would help to nail down thermal properties of the ring particles and the ring structure itself.

The campaign of EQLB (long baseline) and EQSB (short baseline) observations was organized to try to get at least some temperature data at semi-regular intervals during the 100 or so days prior to and after Equinox event. The long baseline were designed to allow observation of cooling on the lit side as the Solar emission angle decreased, and heating on the previously unlit (North) side after the event. The latter required a baseline of observations on the unlit side before the event as well. In the end, the observations were highly limited by the fact that Cassini spent most of its time in the

ring plane. Observations were placed by opportunity only, and only one opportunity for "short baseline" was found.

1. Observation Type: EQLBN/EQLBS/EQSB

Prime Instrument: CIRS

Usual Riders: VIMS

Number of Observations: 28

All observations prefaced with "EQ" were designed to sample the changes in temperature of the rings as a function of radius, just before and after the Equinox event of August, 11, 2009.

The orbital plan for the end of extended mission offered very little opportunity for getting observations of the rings right before and after the equinox event. This fact was not appreciated until late in the planning. By this time in the mission the team had found that the seasonal variation of ring temperatures was important, and it was expected that the cooling of the lit side right before equinox and subsequent heating of the previously unlit side would help to constrain thermal properties of the ring particles and their vertical distribution.

The campaign of EQLB (long baseline) and EQSB (short baseline) observations was organized to try to get at least some temperature data at semi-regular intervals during the 100 or so days prior to and after Equinox event. The long baseline were designed to allow observation of cooling on the lit side as the Solar emission angle decreased, and heating on the previously unlit (North) side after the event. The latter required a baseline of observations on the unlit side before the event as well. In the end, the observations were highly limited by the fact that Cassini spent most of its time in the ring plane. Observations were placed by opportunity only, and only one opportunity for a short baseline observation was found.

Pointing: FP1 to rings. These were all conducted as radial scans.

Instrument Parameters: FP1 was the principle focal plane, FP3 and FP4 were used as data volume permitted.

List of observations:

Observation	Start Time	Duration
CIRS_112RI_EQLBN001_PRIME	2009-162T11:40:00	000T06:05:00
CIRS_113RI_EQLBN001_PRIME	2009-177T10:40:00	000T06:00:00
CIRS_114RI_EQLBN001_PRIME	2009-192T10:23:00	000T06:00:00
CIRS_115RI_EQLBN001_PRIME	2009-208T10:12:00	000T07:08:00
CIRS_116RI_EQLBN001_PRIME	2009-225T02:15:00	000T06:00:00
CIRS_117RI_EQLBN001_PRIME	2009-240T00:45:00	000T06:00:00
CIRS_118RI_EQLBN001_PRIME	2009-264T02:00:00	000T06:00:00
CIRS_123RI_EQLBN001_PRIME	2009-360T07:35:00	000T02:00:00
CIRS_125RI_EQLBN001_PRIME	2010-027T07:00:00	000T02:00:00
CIRS_132RI_EQLBN001_PRIME	2010-151T08:15:00	000T03:30:00
CIRS_132RI_EQLBN003_PRIME	2010-152T23:15:00	000T04:15:00
CIRS_132RI_EQLBN004_PRIME	2010-153T23:59:00	000T03:16:00
CIRS_137RI_EQLBN001_PRIME	2010-246T13:20:00	000T01:30:00

CIRS_137RI_EQLBN002_PRIME	2010-246T17:10:00	000T01:30:00
CIRS_112RI_EQLBS001_PRIME	2009-159T07:35:00	000T07:00:00
CIRS_113RI_EQLBS001_PRIME	2009-175T06:20:00	000T06:00:00
CIRS_114RI_EQLBS001_PRIME	2009-191T05:35:00	000T06:00:00
CIRS_115RI_EQLBS001_PRIME	2009-206T17:20:00	000T06:00:00
CIRS_116RI_EQLBS001_PRIME	2009-223T01:35:00	000T05:00:00
CIRS_123RI_EQLBS002_PRIME	2010-001T09:52:00	000T04:00:00
CIRS_123RI_EQLBS003_PRIME	2010-002T13:38:00	000T04:00:00
CIRS_124RI_EQLBS001_PRIME	2010-007T01:55:00	000T05:00:00
CIRS_124RI_EQLBS004_PRIME	2010-009T23:29:00	000T04:01:00
CIRS_124RI_EQLBS002_PRIME	2010-008T08:05:00	000T05:00:00
CIRS_133RI_EQLBS001_PRIME	2010-175T18:56:00	000T04:15:00
CIRS_133RI_EQLBS002_PRIME	2010-176T23:20:00	000T04:30:00
CIRS_137RI_EQLBS001_PRIME	2010-245T06:52:00	000T03:00:00
CIRS_116RI_EQSBS001_PRIME	2009-224T03:00:00	000T03:00:00

d. SOLSTICE MISSION (XXM):

After the equinox mission, the primary focus of the rings observations became TDIF and phase/lat coverage. The previous TMAP and VTMP campaign, which had been found to be RBOT-unfriendly, were changed to NP and SP observations.

iv. Phase-Latitude Scans: During the planning process, the phase-latitude space was divided into several latitude and phase bins in each hemisphere (3 and 5, resp?), and observations were named with a shorthand that completely specified their geometry placement within these bins. NPxxLyyy would be an observation of the North side (lit, in this epoch) of the rings with a phase angle of approximately xx degrees and latitude of approximately yyy degrees. An SPxxLyyy would be of the South side (unlit, in this epoch). During the planning process, it was considered important to obtain observations at low, medium and high solar elevation angles as the Sun rose from 15 to 25 degrees above the ring plane (most of the mission right after Equinox remained in the ring plane, so observations below 15 degrees are not found). Consequently, during planning, these observations also had an additional field appended to the end of the name: S15, S17, S19, S21, or S23. E.g., NPxxLyyySzz. This label for solar angle was too long for the name fields in CIMS, and subsequently dropped. However, a residual 'S' along with a digit or two of solar elevation appears by mistake in several of the observations. It has no significance. There is also at least one observation, added during TWT discussions, that has an incorrect name made up on the spot during a telecon. One obvious example is P50L30S15, which has no north or south delegation (it should be "NP").

1. Observation Type: NP*, SP*

Prime Instrument: CIRS

Usual Riders:

Number of Observations

32 NP + 1 P50 (rev134) during the XXM

14 SP during the XXM

These observations were a solstice mission campaign designed to provide coverage in the parameter space of phase and latitude. During the main mission and extended mission, respectively, the TEMPS and TMAPS had been increasingly organized at trying to ensure that radial temperature scans were taken at a broad range of viewing geometries.

In planning the solstice mission observations, that objective was prioritized to the point where the radial scan observations were named according to the viewing geometry they were taken with. During the planning of the solstice mission, three bins in emission angle (latitude) were used, and five bins in phase angle were used. Further, the solar inclination angle was binned roughly into epochs in which the Sun was 18-20 degrees elevation, 20-24 degrees, and 25-27 degrees. CIRS attempted to negotiate to get at least one observation in each bin at each of the solar epochs.

It was impossible to meet those requirements because (1) the orbital structure, plotted in the phase-latitude plane, was such that some bins were almost never or never sampled, and (2) competition for observing time was intense, and these were not considered as high priority as various other observations.

The name of the observation specifies which bin it was in. The leading 'N' or 'S' according to whether the observation was of the North or South side of the rings (always lit and unlit, respectively, in this portion of the mission); the 'P' and numbers after it label the approximate phase (in degrees) of the observation, and the 'L' and numbers after it label the approximate latitude (emission angle).

During negotiations, there were originally an 'S' plus two numbers labeling the solar elevation (e.g., 19, 23, 25), but these were [mostly] dropped when observations were finalized and entered into CIMS, due to the 10 character constraint on observation name length. Some of these observations retained a vestigial 'S', sometimes followed by the solar elevation, sometimes not. This was an oversight in the naming process. The solar elevation can be easily figured out according to which rev the observation occurred in, so it was not thought necessary to keep it.

The P50L30S15 in rev 134 was naming accident. It should be 'NP50L30S15'.

Pointing: All of these observations are FP1 to rings, most use the R_RAD_LON module for pointing, but some used the P_SHAD_DUR module which built radial scans in which the points at all radii were the same number of minutes before or after shadow ingress or shadow egress.

As with the TEMPS and TMAPS but to a lesser degree, the radial scans were planned primarily for local times near one or both Ansaes. But observations that

were longer and/or at higher elevation often have additional scans not directly related to the phase/lat requirements.

Instrument Parameters: These observations were all taken at 15cm⁻¹ resolution, and FP3 and FP4 were used only as data volume permitted.

List of observations:

Observation	Start Time	Duration
CIRS_169RI_NP140L30001_PRIME	2012-204T19:25:00	000T00:55:00
CIRS_170RI_NP50L30S001_PRIME	2012-226T09:45:00	000T04:30:00
CIRS_172RI_NP20L30S001_PRIME	2012-269T06:06:00	000T03:00:00
CIRS_173RI_NP50L30N001_PRIME	2012-292T15:05:00	000T03:00:00
CIRS_174RI_NP50L30006_PIE	2012-316T21:30:00	000T05:00:00
CIRS_176RI_NP50L70004_PIE	2012-345T15:30:00	000T04:00:00
CIRS_176RI_NP20L70001_PIE	2012-346T02:30:00	000T04:00:00
CIRS_179RI_NP20L30S001_PRIME	2013-020T00:00:00	000T06:00:00
CIRS_179RI_NP10L30N001_PRIME	2013-020T15:50:00	000T07:00:00
CIRS_180RI_NP50L70S001_PRIME	2013-032T19:00:00	000T07:09:00
CIRS_181RI_NP20L70S001_PRIME	2013-046T13:28:00	000T03:52:00
CIRS_181RI_NP20L30S001_PRIME	2013-046T17:20:00	000T03:56:00
CIRS_185RI_NP20L70001_PRIME	2013-094T03:20:00	000T04:00:00
CIRS_185RI_NP10L30001_PRIME	2013-094T14:20:00	000T03:00:00
CIRS_186RI_NP20L70001_PRIME	2013-103T14:11:00	000T05:25:00
CIRS_189RI_NP10L30001_PRIME	2013-132T16:06:00	000T04:47:00
CIRS_180RI_NP10L30012_PIE	2013-033T17:19:00	000T05:00:00
CIRS_183RI_NP20L30029_PIE	2013-070T12:35:00	000T04:00:00
CIRS_191RI_NP50L70001_PRIME	2013-153T13:49:00	000T06:00:00
CIRS_194RI_NP20L70019_PIE	2013-189T22:00:00	000T04:00:00
CIRS_194RI_NP20L30019_PRIME	2013-190T02:00:00	000T06:00:00
CIRS_196RI_NP50L70024_PIE	2013-228T21:30:00	000T04:00:00
CIRS_196RI_NP10L30028_PIE	2013-239T10:11:00	000T04:00:00
CIRS_198RI_NP20L30054_PIE	2013-285T15:00:00	000T04:05:00
CIRS_234RI_NP20L10001_PRIME	2016-093T08:46:00	000T03:00:00
CIRS_237RI_NP20L30S2006_PRIME	2016-178T23:34:00	000T05:00:00
CIRS_239RI_NP50L30S2010_PRIME	2016-219T18:36:00	000T04:00:00
CIRS_243RI_NP50L30S2001_PRIME	2016-265T18:34:00	000T04:00:00
CIRS_243RI_NP50L30S2002_PRIME	2016-267T23:15:00	000T03:41:00
CIRS_243RI_NP20L30S2001_PRIME	2016-267T19:15:00	000T04:00:00

CIRS_246RI_NP50L30S2001_PRIME	2016-295T05:00:00	000T05:00:00
CIRS_265RI_NP140L50S001_PRIME	2017-073T01:20:00	000T03:00:00
CIRS_201RI_SP90L70S022_PRIME	2014-035T18:02:00	000T04:00:00
CIRS_202RI_SP90L30S022_PRIME	2014-066T22:21:00	000T04:00:00
CIRS_202RI_SP140L70S022_PRIME	2014-068T00:02:00	000T04:00:00
CIRS_202RI_SP140L30S023_PRIME	2014-069T01:32:00	000T04:00:00
CIRS_206RI_SP160L70001_PRIME	2014-199T21:16:00	000T04:00:00
CIRS_208RI_SP50L30001_PRIME	2014-261T08:58:00	000T06:00:00
CIRS_208RI_SP90L70001_PRIME	2014-262T13:21:00	000T04:00:00
CIRS_208RI_SP140L70001_PRIME	2014-263T09:13:00	000T04:00:00
CIRS_211RI_SP50L30001_PRIME	2015-009T09:07:00	000T03:00:00
CIRS_211RI_SP90L30001_PRIME	2015-009T12:07:00	000T04:00:00
CIRS_211RI_SP140L30001_PRIME	2015-010T07:40:00	000T04:00:00
CIRS_234RI_SP140L20001_PRIME	2016-094T01:46:00	000T02:00:00
CIRS_241RI_SP140L70S006_PRIME	2016-244T21:00:00	000T03:00:00
CIRS_245RI_SP140L30S001_PRIME	2016-289T08:56:00	000T02:31:00

ii. *Thermal Difference Campaign*: The TDIF campaign remained here, with a name change to TDIF[NORTH,SOUTH].

1. observation type: lit/unlit thermal differential observations
observation descriptor: TDIF[NIS][##][LHP] (pre-2013);
TDIF[(NORTH)|(SOUTH)] (2013 and later)
prime instrument: CIRS
riders: ISS (pre-2013 only), UVIS, VIMS (pre-2013 only)
number of observations: 30 - 15 south, 15 north
primary boresight: CIRS_FP1
spectral resolution: 15 cm⁻¹ (39 RTI)
MIR observation mode: centers

Among the thermal sources heating Saturn's rings, the Sun is by far the most dominant (with the exception of periods at or very near equinox). The ability of the Sun's radiation to penetrate the rings -- particularly in the more optically thick regions of the rings -- creates a temperature asymmetry between the side of the rings directly exposed to the Sun (the lit side) and the opposite face of the rings (the unlit side). Measuring the temperature differences between the lit and unlit sides has the potential to reveal how energy is exchanged normal to the ring plane. However, attempts to discern this information from any two scans is complicated by the fact that retrieved ring temperatures are dependent on observation geometry and would require the incorporation of a model that describes how ring temperature and observation geometry are correlated. This

goal of this campaign was to produce paired sets of scans of the rings taken at similar solar hour, phase and elevation angles and with inclination angles distinguished only by their sign. In other words, the scans on one side of the ring plane have an observation geometry that is similar to that of corresponding scans flipped about the ring plane. Such scans can be directly compared with minimal impact from differences in viewing geometry and without the need to resort to models.

Lit/unlit thermal differential observations (TDIFs) typically contain one or more radial scans along a constant solar hour angle. Paired opportunities to view opposite sides of the rings were identified by looking for periods that were not too widely separated in time where the spacecraft could view the same phase, emission and local solar hour angles on the lit and unlit sides of the rings. A circular, polar orbit would be the ideal trajectory to implement such an observing campaign. Because Cassini was not in a circular or polar orbit, there are differences between paired sets of scans. The spacecraft's range to the rings was the observing parameter that differed most significantly between pairs of scans. And while efforts were made to achieve identical phase and emission angles, operational practicalities often meant that these parameters could not be made precisely the same. Often more time was given to one observation in a paired set. In such cases, the additional time was used to obtain other scans. For instance, CIRS_089RI_TDIFN45HP001_PRIME contains a radial scan at a local hour angle of 12, another at a local hour angle of 18 and several scans near Saturn's shadow that were typical of the CIRS egress/ingress shadow scan campaign; those two radial scans were intended to be compared with the two radial scans in CIRS_093RI_TDIFS45H001_PRIME. Temperature differences between the lit and unlit sides of the rings vary with season and location in the rings. In the B ring, such differences were minimized near equinox and at their maximum near solstice. Unlit/lit temperature differences in the C ring are never very much greater than zero between coordinated TDIF observations.

Unfortunately, it can be difficult to tell from the names of the observations in this campaign which observations were intended to be compared to which. They must simply be reviewed. However, clues exist in their names which allows one to narrow down the possibilities. TDIFs prior to 2013 contain either an 'N' or an 'S' denoting 'north' or 'south', respectively, after the 'TDIF' string in the observation descriptor. The two-digit number that follows suggests the subspacecraft latitude on Saturn, which roughly proxies as the spacecraft elevation angle (less so the closer the spacecraft was to Saturn). Observations taken from above Saturn's northern hemisphere from a particular (northern) latitude will have their complementary scans in a southern TDIF from a similar (southern) latitude not more than a few orbits removed. In practice, the subspacecraft latitude coded into the TDIF observation names was either '20' or '45'. And although the final two characters in the observation descriptor were intended to discern between low (LP) and high (HP) phase angle observations, all TDIF observations in this phase of the mission were taken at phase angles greater than 90 degrees, owing to geometrical constraints and integration scheduling.

Complementary TDIF pairs are far easier to discern starting in rev 186 (April 2013). Although the naming convention was simplified (subspacecraft latitude and phase are not included), paired observations are easier to spot. These complementary sets of TDIFs typically fall in the same rev and have complementary names ('TDIFNORTH' versus 'TDIFSOUTH'); the sole violation of this is the pair in which the NORTH TDIF was taken on rev 191 and the SOUTH TDIF was acquired in rev 194. Observation strategies were refined by

this point in the mission such that observation pairs were more closely coordinated. Finally, it is important to recall that the sense of 'lit' and 'unlit' changed over the course of this observation campaign. Prior to August 2009, 'lit' TDIF scans were taken from over the planet's southern hemisphere; 'unlit' scans were obtained while Cassini was flying over the northern hemisphere. Following equinox, this flipped. South TDIFs contain the unlit observations after August 2009; north TDIFs are lit during this portion of Cassini's tour.

TDIFs were typically implemented as radial scans across the main rings with scan rates ranging between 1000 and 2000 km/minute, with most scans being in the lower end of that range. Early on in the TDIF campaign, a few scans were implemented as shadow scans. Observations prior to equinox were taken at ranges as close 5 Saturnian radii and as distant as 20 Saturnian radii. After 2013, most TDIFs were taken at phase angles of ~90 degrees, with one observation being at close range to Saturn (~5-8 Saturnian radii) and the other being at more distant ranges (~17-22 Saturnian radii). Scan rates were also modified in the latter set of TDIFs. TDIFs at farther distances from Saturn incorporated slower scan rates to make up for the reduced resolution of the larger CIRS footprint on the rings. CIRS was set to record spectra at 15 wavenumbers during these observations. And they were typically accompanied by ISS support imaging requests.

iii. *Shadow Region Mapping*: Detailed maps of the shadow region were brought back here under the "SHAD" moniker, which mostly used the PSHAD_DUR routine in CIMS that allowed scans to be taken at a fixed Keplerian orbital time from either the shadow entry ("ING" for ingress) or exit ("EGR" for egress).

1. observation type: egress/ingress shadow scan observations
observation descriptor: SHAD[(EGR)|(ING)][LIU]
prime instrument: CIRS
riders: UVIS (2), VIMS (3)
number of observations: 23 - 10 egress, 13 ingress; 16 unlit, 7 lit
primary boresight: CIRS_FP1
spectral resolution: 15 cm^{-1} (39 RTI)
MIR observation mode: centers

As ring particles enter Saturn's shadow, they are abruptly cut off from the most significant heat source: the Sun. They are exposed to this heat source again just as abruptly when they exit Saturn's shadow on the morning ansa.

Egress/ingress shadow scans are observations that measure the temperatures of Saturn's rings in the vicinity of Saturn's shadow to record their response to this abrupt change in their thermal forcing.

Over the course of a typical CIRS egress/ingress shadow scan, multiple radial scans across Saturn's rings were performed. For these observations the PSHAD_DUR pointing module within PDT was used to generate pointing profiles for each scan that were roughly radial but with a longitudinal offset from the edge of Saturn's egress or ingress shadow boundary. This offset was chosen to be a set fraction of the local orbital period, which is a function of radius. More simply put, the PSHAD_DUR module was used to generate radial scans that accounted for the rings differential Keplerian rotation. Ingress shadow observations would typically start with a scan that was some number of minutes from the ingress shadow boundary outside of the shadow; subsequent scans were

taken deeper and deeper into Saturn's shadow. Egress shadow observations would start with a scan just inside the egress shadow boundary, followed by multiple scans at increasing distances from this boundary. The result was a set of observations that map out the cooling and heating curves across the entirety of Saturn's main rings, sampled at discrete longitudes in each observation. Typically, C ring temperatures drop and rebound by about ~10 degrees K as its ring particles traverse the shadow. While there is little to no response on the unlit side of the most optically thick portions of the B ring, there is a subtle variation in lit B ring temperatures.

Scans were done on both the egress (morning) and ingress (dusk) ansae. Some observations were taken on the lit side of the rings; others were taken on the unlit side of Saturn's rings. This is reflected in the naming convention for (most of) these observations. 'ING' in the request name indicates that it was a scan on the ingress side of the shadow; likewise, 'EGR' was included in the request name when the rings were observed along the egress side of the shadow. Lit side scans have an 'L' in their name; unlit side scans are denoted with a 'U'. The one egress/ingress shadow scan that does not conform to this naming convention is CIRS_243RI_SHADUNL001_PRIME, which was an observation late in the mission; as the projection of Saturn's shadow onto the rings no longer extended out to the A ring owing to the solar elevation angle above the rings, ring temperatures were only measure in the C and B rings during this observation.

Egress/ingress shadow scans tended to fall at moderate phase angles and relatively high elevation angles, insuring that Saturn's shadow was visible from Cassini. Observations were typically scheduled when Cassini was somewhere between 15 and 25 Saturnian radii from the planet, particularly observations of the unlit side of the rings. Egress/ingress shadow scans at closer ranges were, with one exception, lit side observations. Observations were typically between six and eight hours in duration, with some as short as four hours and one with a fifteen-hour duration. Scan durations were generally about an hour in duration with scan rates ranging between 700 km/minute and 1500 km/minute. Because the goal of these observations was to retrieve temperature information, the instrument recorded spectra at resolution of 15 wavenumbers, which is the fastest operating mode and generates the most spectra.

The dedicated egress/ingress shadow scan campaign was implemented during the XXM mission phase, starting November 2012 and ending in October 2014. As mentioned above, one additional egress/ingress shadow scan was implemented later in the mission, in October 2016. However, some other observations included similar scans in the shadow region when they could be accommodated. Support imaging observations were included with almost every egress/ingress shadow scan.

A final note is the acquisition of a unique observation -- CIRS_196RI_SHADFP3L001_PRIME -- that was meant to address the same science goals as the rest of the egress/ingress shadow scan campaign. The chief difference is that FP3 boresight, with its higher spatial resolution, was the primary boresight for this observation. It was placed at a local hour just outside the ingress (dusk) shadow boundary and oriented so that the long axis of the detector was aligned with the local radial direction the ring plane as projected onto the sky, as was done for the A ring halo stare and C ring plateau mapping campaigns. FP3 was targeted to the mid A-ring (at a ring radius of 130515 km) and at local hour angles of 335, 345, 355, 0, and 10 degrees and stared at each location for ~90, 100, 110, 120 and 130, respectively. The increasing duration of each scan was meant to offset the fact that the ring gets progressively colder at each subsequent

local hour angle; collecting more spectra where the ring is colder helps with the decreasing signal-to-noise. This observation was not repeated.

- v. *Composition Sit & Stares*: Finally, a number of COMP scans were brought back in the guise of "COMPUNL" and "COMPLIT", as well as a number of occultation observations.

- i. observation type: regional compositional ring stares
 - observation descriptor: COMP[(LIT)|(UNL)][(A(1|2|3)) | (CD) | (B(1|2|3|4)) | (C(1|2|3))]
 - prime instrument: CIRS
 - riders: ISS, UVIS, VIMS
 - number of observations: 76
 - primary boresight: CIRS_FP1
 - spectral resolution: 3 cm⁻¹ (39 RTI)
 - MIR observation mode: centers

The CIRS instrument has a broad spectral range through the far infrared out to wavelengths of 1 millimeter. The CIRS regional compositional ring stare campaign was revived in the latter half of the Cassini mission to take a more systematic approach to the same goals that motivated such compositional stare observations in the first half of the mission: 1) determining the location of the spectral “roll-off” in the far IR and the factors that drive it, 2) providing spectral evidence for the type of water ice that dominates the far IR signal from Saturn's rings and 3) searching for the existence of observable contaminants. One of the main differences between the COMP observations taken during the latter portion of the mission was the targeting of specific regions of the rings, not just the rings themselves (the main exception being the Cassini Division, which is too narrow for CIRS to distinguish between different regions in that ring for any significant observation duration).

The design of a typical COMP observation was very simple in scope: point the CIRS FP1 boresight towards the ansa of the ring region of interest as long as possible during the observation, while also accumulating a number of deep space calibration stares (typically twenty minutes' worth) once or twice over the course of the observation. The definition for these different ring regions:

74000-79000	inner C ring (C1)
79000-84000	middle C ring (C2)
84000-89000	outer C ring (C3)
93000-99000	B1 region (begins at 92000, according to Colwell et al., 2009)
99000-104000	B2 region (ends at 104500, according to Colwell et al., 2009)
105000-110000	B3 region (begins at 104500, according to Colwell et al., 2009)
110000-115000	B4 region (ends at 116500, according to Colwell et al., 2009)
116500-117500	B5 region
118000-122000	Cassini Division

122500-127500	inner A ring (A1)
128000-133000	Middle A ring (A2)
134000-136000	trans-Encke region (A3)

are based upon and generally agree with those defined in Chapter 13 of the Saturn from Cassini-Huygens book (Colwell et al., 2009), edited by M. K. Dougherty et al. Observations of each of these ring regions was made over the course of the mission's final five years, with the sole exception of the B5 ring region, which is too narrow to have been isolated from the surrounding regions in the FP1 field of view. For observations longer than 6 hours or so, roughly five minutes' worth of closed shutter spectra were typically acquired during the middle of the observation. The intent of this campaign was to generate large numbers of spectra in the far infrared (on the order of several thousand) over the course of multiple observations that could be averaged together to provide insight that was not possible from any one single observation. Three wavenumbers was chosen as the spectral resolution for this campaign, as it is fine enough to record spectral details that might be missed in 15 wavenumber observations, yet recorded quickly enough (once every ~fifteen seconds) that a sufficiently large number of spectra might be acquired. Finally, we note that during the final year of the Cassini mission some time (typically 15-20 minutes) was sometimes used during these observations for collaboration with ISS to search for small objects at the edge of the A ring and between the A ring and the F ring.

The naming convention for these observations changed over the course of the final five years of the mission. From revs 176 through 201, all COMP observation names use the generic 'RI' target code following the rev number. The only distinction in the naming being whether the observation was of the lit (LIT) or unlit (UNL) side of the rings. Starting in rev 203, a more specific target code -- RA, RB and RC -- was used for the A, B and C rings, respectively (Cassini Division observations use the generic 'RI' code for rings). While this does not allow one to discern the specific ring region targeted during the observation, it does provide an indication as to which ring was observed. The final modification to the naming convention came in rev 227, when the two character code identifying the ring region was appended to the name, allowing one to determine the target of the observation from the observation name alone, without having to inspect the data itself.

The only geometric criterion that constrained the COMP observations (other than spacecraft flight rule constraints based on instrument health and safety) was that the range be sufficient to cleanly isolate ring regions from one another. The goal was to obtain COMPs at each ring region at a variety of observation geometries, although competition for observing time made it unfeasible to sample all geometries for each of the regions specified above. In addition, no COMP observations of the unlit side of the B ring were made. The unlit side of the B ring features the coldest temperatures in the rings, which reduces the signal-to-noise ratio of the acquired spectra.

Generally speaking, the spectra obtained from these observations are remarkably flat. A decrease in emissivity is observed at the longest wavelengths, which is not surprising, as the emissivity of water ice is known to decrease as one moves towards millimeter wavelengths. There appears to be some variation in emissivity around 200 wavenumbers (~50 microns), but this is likely an instrumental artifact. Discerning any composition information from these spectra will likely require careful modeling and data analysis, particularly at the longest wavelengths.

2. observation type: low-resolution compositional ring stares
 observation descriptor: COMP[LIU]LRES
 prime instrument: CIRS
 riders: UVIS, VIMS
 number of observations: 34
 primary boresight: CIRS_FP1
 spectral resolution: 3 cm^{-1} (39 RTI)
 MIR observation mode: centers

The goals and the implementation of the low-resolution compositional ring stare campaign is very similar to that of the regional compositional ring stare campaign. The chief difference between them is that the low-resolution compositional ring stares were taken when the spacecraft was further from the planet and no individual ring region could be distinguished (see the discussion of the extended mission compositional ring stare campaign for a description of the individual ring regions). Thus, these observations are simply stares at the A, B or C rings (these observations were made when the Cassini Division could not be isolated in the FP1 field of view) and are similar to the compositional stares implemented during the prime mission. Because these observations were taken far from the planet and competition for observing time was relatively low, these were typically very long observations. While no one observation was longer than ten hours, occasionally two nine- or ten-hour observations were scheduled subsequent to one another. The target of the observation can be discerned by the target code which follows the rev number in the observation name. And although observations of the unlit side were allowed for, none were actually scheduled, owing to the particularities of the tour; by the time these observations were implemented, the trajectory was such that long observing opportunities typically came on the lit side of the rings. The decision to schedule a low-resolution compositional ring stare versus a regular compositional ring stare hinged upon range to the target. While the spacecraft was within ~ 25 Saturnian radii from the planet, normal compositional ring stares were implemented, as this is the maximum distance at which the B1 region, the broadest of the ring regions considered for that campaign, could be resolved. Beyond a range of 25 Saturnian radii, low-resolution compositional scans were carried out. The first COMPLLRES occurred on rev 205; the final one was obtained on rev 237, after which point the range to Saturn was typically better suited to regionally-targeted compositional ring stares.

e. F-RING/PROXIMAL ORBITS:

During planning for these orbits, the RTWT solicited requests for observations that had not been done before, and that were only now possible because of the enhanced resolution that the close-up orbits provided. The CIRS rings team placed 7 observation types:

- i. RSCAN: High resolution scans of the rings. The team debated whether radial scan was important, and decided it was.
 - 1. observation type: high-resolution radial scan observations

observation descriptor: RSCAN[(LIT)|(DRK)]
prime instrument: CIRS
riders: UVIS (5), VIMS (3)
number of observations: 5 - 2 dark, 3 lit
primary boresight: CIRS_FP1
spectral resolution: 15 cm^{-1} (39 RTI)
MIR observation mode: centers

Among CIRS' three focal planes, FP1 was best suited for obtaining retrieving temperature information for Saturn's rings, as the Wien peak for blackbody radiation at temperatures typical of Saturn's main rings falls within its spectral range. Unfortunately, FP1 also has the lowest spatial resolution of the three focal planes. And spatial resolution from ISS images, UVIS occultations and VIMS observations generally far exceeded thermal scans with FP1. For this reason, the geometries in Cassini's ring grazing and grand finale orbits proved particularly beneficial for CIRS thermal ring scans. In addition to flying very close to the rings, Cassini also flew high above (and below) them, traveling in an orbit with an inclination over 60 degrees. The resulting low emission angles possible when observing near periapsis in this phase of the mission minimized foreshortening of the field of view on the rings, effectively reducing the spatial resolution and further sharpening the view of the rings from CIRS. The high-resolution radial scan campaign was designed to obtain full radial scans of the main rings at some of the highest spatial resolutions during the entire Cassini mission.

RSCANs were short observations -- typically some 3-4 hours in duration -- during which one slow scan across the main rings along a constant solar hour angle was obtained. Scans tended to follow the direction of motion of the spacecraft. During inbound scans of the lit side of the rings, FP1 was scanned radially inward; FP1 was scanned radially outward on outbound scans of the unlit side of Saturn's rings. At least one brief period of deep space calibration spectra acquisition was incorporated into the design of each RSCAN. The brief duration of these observations and the rapidly changing, close range geometry made it difficult to acquire more than one deep space calibration block during the grand finale orbits.

High-resolution radial scans implemented on the inbound portion of the end-of-mission orbits were on the lit side of the rings. They were consequently named RSCANLIT. Outbound observations of the unlit rings were labeled RSCANDRK. Unfortunately, one of the two planned unlit side of observations -- CIRS_277RI_RSCANDRK001_PRIME -- was lost because of downlink problems. The loss was significant, as the unlit side scans show an unanticipated and intriguing amount of radial structure.

Lit side RSCANs tended to fall at moderate phase angles. The one dark side RSCAN was at slightly higher phase angles. RSCANs were obtained close to Saturn, with a spacecraft range to the planet center falling between 2.5 and 6 Saturnian radii, yielding spatial resolutions as low as 600 km. The elevation angles of these observations were high, exceeding 65 degrees and approaching 90 degrees. Scan rates ranged between 400 and 700 km/min, with 400 km/min being more typical. Observations were made at 15 wavenumbers (39 RTI), yielding oversampled radial scans optimized to derive temperature information.

Because of the geometry demands on this observations campaigns, RSCANS were implemented strictly in the final year of the mission, though many other CIRS observations consist of similar radial scans at faster scan rates and farther ranges from the rings.

ii. HALO: Observations of the outer A ring, designed to look for enhancements of signal in density wave locations

1. observation type: A ring halo stare observations

observation descriptor: HALO[(LIT)|(DRK)]

prime instrument: CIRS

riders: none

number of observations: 4 - 3 dark, 1 lit

primary boresight: CIRS_FP3

spectral resolution: 15 cm^{-1} (39 RTI)

MIR observation mode: centers

Saturn's A ring is perturbed by density waves raised by its retinue of satellites. Large and small moons alike generate these waves at resonance locations that happen to fall within the A ring. VIMS, UVIS and ISS all reported photometric properties in the vicinities of the strongest of these waves that were different from that of the surrounding regions. These photometrically distinct regions were dubbed 'halos' by Cassini rings scientists. However, CIRS, with its relatively coarse spatial resolution, was not typically able to distinguish the halos from the surrounding A ring material. There is reason to suspect some signal near the halos in the thermal infrared, as the density waves might be expected to enhance particle spins and vertical motions, modifying the ring material's response to the local thermal environment. This campaign is an attempt to resolve the A ring's halos with FP3 and to generate a radial map of different halo zones.

HALO observations included multiple ~40-minute integrations at a constant solar hour angle at various halo locations. The implementation was similar to the plateau mapping observations in the C ring. The spacecraft secondary was oriented to align the FP3 array with the radial direction in the ring plane as projected onto the sky. FP3 was targeted to a radius just beyond or inside the density wave to be mapped and subsequently moved inward or outward at the beginning of a new integration to cover the entire region. The Mimas 5:3 and Janus 4:3 waves were each mapped once from the unlit side of the rings on the dusk ansa. The Janus 5:4 wave was observed from the lit and unlit sides of the rings at identical solar hour angles on the morning ansa. These features, as observed by VIMS, are described in Hedman et al. (2013). Spatial resolutions of 100-200 km in each FP3 pixel were required to resolve the halos, requiring close proximity to the A ring. These observations were all scheduled on the ring-grazing orbits, typically when the spacecraft range to Saturn was 5.5-7.5 Saturn radii. The local hour angle providing the highest spatial resolution was targeted.

Both the lit and unlit sides of the halos were mapped. Lit side stares were named HALOLIT; HALODRK denotes unlit side observations. But because there was much competition for time on the lit side of the rings when the spacecraft was close enough for this observation campaign, only one HALOLIT was incorporated into the timelines. It was easier to schedule HALO observations on the unlit side of the rings, as there was not as much competition from the other instruments for this time. These

observations were all scheduled at the end of 2016 and beginning of 2017, on revs 253 through 256.

iii. CASDIV: Azimuthal scans of the Cassini division, similar to the VCAS from extended mission, but where the field of view fit more completely into the Cassini division.

1. observation type: Cassini Division azimuthal scans

observation descriptor: CASDIV[(LIT)|(UNL)]

prime instrument: CIRS

riders: ISS (2), UVIS (3), VIMS (4)

number of observations: 5 - 2 unlit, 3 lit

primary boresight: CIRS_FP1

spectral resolution: 15 cm^{-1} (39 RTI)

MIR observation mode: centers

The Cassini Division, spanning just some 4,000 kilometers in radial extent, is relatively narrow when compared to the other main rings of Saturn. Owing to the broad angular extent of CIRS' FP1 detector, most attempts to observe the Cassini Division prior to the ring-grazing and grand finale orbits were contaminated by the A and B rings at the edges of the FP1 field of view. And although the region is often compared to the C ring, the Cassini Division appears to be very different from the C ring. It appears to have much lower thermal inertia, and it does not show the characteristic signature of small grains. These observations are an attempt to follow up on those observations with azimuthal scans that are devoid of any contamination from the neighboring rings.

CASDIV observations consist of slow azimuthal scans of the Cassini Division with FP1 trained on the center of the ring. The three ring-grazing orbit CASDIV observations were relatively long observations -- between five and seven hours each -- at ranges between 5.5 and 10 Saturn radii from the planet. Phase angles on the unlit side observations were relatively high for these observations, while it was significantly lower in the one lit side CASDIV observation in the ring-grazing orbits. The spacecraft was typically at higher elevation angles above (below) the rings to reduce the impact of foreshortening and to make it easier to resolve the Cassini Division.

The grand finale CASDIV observations were two shorter observations of four hours apiece. These were taken from greater range (14.7 to 16.3 Saturnian radii), which constrained these observations to focus on the ansae of the Cassini Division. Each was taken on the lit side of the rings. Phase angles were slightly lower than the unlit side ring-grazing CASDIVs, and the elevation angle was modest; owing to foreshortening, the Cassini Division could no longer be cleanly separated from the A and B rings with FP1 farther from the ansae. The longitudinal scan rate was a modest 0.3 degrees per minute, with the exception of the rev 255 CASDIV observation, which used a scan rate of 0.475 degrees per minute.

iv. UNSHAD: Azimuthal scans of the unshaded A ring

1. observation type: Unshaded A ring azimuthal scans

observation descriptor: UNSHAD[(LIT)|(DRK)]
prime instrument: CIRS
riders: ISS (2), UVIS (3), VIMS (4)
number of observations: 2 - 1 dark, 1 lit
primary boresight: CIRS_FP1
spectral resolution: 15 cm^{-1} (39 RTI)
MIR observation mode: centers

The 'unshadowed' in the unshadowed A ring azimuthal scan campaign refers to the fact that by early 2017 the entirety of Saturn's A ring was in sunlight around the whole of its circumference, as the outer edge of Saturn's shadow on the rings ended in the Cassini Division. This observation campaign, which consists of just two observations, was intended to facilitate studies of the subtle role of Saturn-shine in the rings' thermal balance. While the contribution to a ring particle's thermal balance due to thermal emission from Saturn is constant as one goes around the planet, that contribution due to light reflected by the disk of Saturn changes as Saturn's apparent solar illumination varies as seen from a given particle. This campaign serves as a counterpart to the equinox observations during which the Sun's role was minimized.

The UNSHAD observations were both implemented at spacecraft ranges of 6 to 11 Saturn radii from the center of Saturn, with the lit side observation on rev 270 coming at a slightly greater distance from Saturn and the rings. Both were at high elevation angles above the rings, but the unlit side (DRK) observation was made at higher phase angles than the lit side observations. In each instance, FP1 was targeted to a ring radius of 130,500 km, in the middle of the central A ring. And while the longer duration unlit side observation has a greater longitude coverage, both observations cover the same longitudes on the morning side of the rings. The scan on the unlit side was started at a solar longitude of 285 degrees and advanced at 0.4 degrees per minute; the lit side scan began at a solar longitude of 330 degrees with an azimuthal rate of 0.36 degrees per minute.

v. AZSHADSCN:

1. observation type: azimuthal shadow mapping observations
observation descriptor: AZSHADSCN
prime instrument: CIRS
riders: UVIS (1)
number of observations: 2
primary boresight: CIRS_FP3
spectral resolution: 15 cm^{-1} (39 RTI)
MIR observation mode: blinking, centers

When ring particles enter Saturn's shadow, they are abruptly cut off from the Sun, the source of the rings' most significant thermal input. The result is an abrupt cooling of the rings. However, the detailed response of the ring temperature as measured by CIRS generated by this sudden change in the thermal environment is likely to depend on the overall structure of the rings themselves and the interactions between ring particles. In the most optically thick portions of the rings, the thermal response may be like that of a static slab, as the high density of ring particles likely inhibits much motion, locking the ring particles into structures that are generally

unchanging. The least optically thick sections of the rings may also have a simple thermal response, as there may be minimal interaction between the particles; the response is more likely to be determined by individual particle properties. But regions of intermediate optical depth, where particles move across the ring plane and interact thermally are likely to show a response more complicated than that of a slab. This observation campaign is intended to provide a more detailed characterization of the rings' thermal response to the transition into Saturn's shadow.

The two observations in the azimuthal shadow mapping observation campaign consist of stares at multiple solar hour angles in the vicinity of the egress edge of Saturn's shadow. Each observation spanned about nine degrees of ring longitude, with at least one stare just outside the shadow region to establish a set of baseline temperatures. The FP3 array of pixels was aligned tangentially to the local radial direction as projected into the ring plane to target very nearly the same ring radius in each of the FP3 pixels. In addition to twenty-minute deep space stares, FP1 was scanned slowly across the region mapped with FP3. As FP1 spectra are better determinants of ring temperature -- at the expense of spatial resolution, -- the intent of this FP1 azimuthal slew was to help resolve any ambiguities in the determination of the temperature fields mapped with FP3.

Azimuthal shadow mapping observations were performed when the spacecraft was roughly 10 - 11 Saturnian radii from the planet. Phase angles were between 110 and 120 degrees, with moderate elevation angles above the ring plane of 30 to 40 degrees. Each FP3 stare had a duration of roughly ten minutes before the next solar hour angle was targeted. FP1 scans were implemented at a rate of roughly one degree of solar hour angle per minute. Overall observation times were short, at just three hours each.

One of the last CIRS observation campaigns to be implemented during the Cassini mission, only two were ever executed. Both were observations of the B ring. The AZSHADSCN implemented in rev 282 targeted the center of the optically thick B3 region, at a ring radius of 107,500 km, and used FP3's blinking mode. The rev 283 AZSHADSCN targeted the center of the less optically thick B1 region, at a ring radius of 96,000 km from Saturn, and used FP3's centers mode. The inconsistency is likely an oversight. Had these observations been conceived earlier in the mission, more ring radii would have been targeted. Each of the AZSHADSCNs included supprt imaging from ISS.

vi. PLAT: High resolution scans of the plateau regions in the C ring.

1. observation type: C ring plateau mapping observations

observation descriptor: PLAT[(LIT)(DRK)]

prime instrument: CIRS

riders: ISS (2), UVIS (2), VIMS (1)

number of observations: 2 - 1 dark, 1 lit

primary boresight: CIRS_FP3

spectral resolution: 15 cm⁻¹ (39 RTI)

MIR observation mode: centers, blinking

The inner and outer C ring contains several bright bands with a radial extent between 40 and 250 kilometers. The origin and evolution of these structures, known as plateaus, is not well understood. With visibly sharp inner and outer edges,

plateaus are unique to the C ring. They tend to have enhanced optical depth at their inner and outer edges. With their relatively narrow extent, these mysterious structures were not very accessible to CIRS for most of Cassini's tour at Saturn. This changed during Cassini's grand finale's orbits, as Cassini's trajectory at periapse made Cassini an excellent platform from which to observe the C ring. This campaign is an attempt to resolve the C ring's plateaus using FP3 to generate radial maps across these features.

PLAT observations featured multiple extended integrations across different plateaus. The implementation was similar to the halo stare observations in the A ring. The spacecraft secondary was oriented to align the FP3 array with the radial direction in the ring plane as projected onto the sky. FP3 was targeted to a radius just beyond or inside the plateau to be mapped and subsequently moved inward or outward at the beginning of a new integration to cover the plateau being targeted. The observation in rev 270 targeted just two plateaus: P8 and P11 (see Colwell et al., 2009, for plateau details). Each one was observed at three different solar hour angles in Saturn's shadow to map out their response to entry into the shadow. The duration of each stare was increased with increasing distance from the ingress shadow edge to account for lower temperatures and increase signal-to-noise. FP3 was operated in centers mode; this sacrifices spatial coverage in exchange for more spectra per pixel used, which was an important consideration observing the rings in the thermal infrared within the relatively cold shadow of Saturn. The observation in rev 283 mapped out multiple plateaus: P5, P7, P8 and P11. The Maxwell Gap was imaged as well with FP3. The plateaus were observed at the same solar hour angle on the dawn ansa for a duration of ~20 minutes apiece. Blinking mode was used during this observation, as this allowed for data to be taken with all ten FP3 pixels, extending the spatial coverage of this observation.

Both the lit (rev 283) and unlit (rev 270) sides of the plateaus were mapped. Lit side stares were named PLATLIT; PLATDRK denotes unlit side observations. The unlit observation was scheduled when Cassini was between 6 and 9 Saturnian radii from the planet. The lit observation was shorter but from closer range; Cassini was between 5.5 and 3.5 Saturn radii when this observation was made.

- vii. ANSASTARE: F ring observations were brought back as ANSASTARE observations, under the hopes that as we got close to the rings we would get more signal than had been available from the FMOVIE and FMONITOR that occurred early in the mission. These observations were not taken from close in, but during the Apoapse part of the orbit.

f. ODDS & ENDS:

i. Polarization Integrations

Observation Type: Polarization Integrations

observation descriptor: POL[RU/ARIZ]

prime instrument: CIRS

riders: TBD

number of observations: 9

primary boresight: CIRS_FP1

spectral resolution: 15 cm⁻¹ (39 RTI)

Description: The goal of these observations are to determine whether or not the rings exhibit a non-zero polarization in the thermal IR. The FP1 channel is a Martin-Puplett interferometer and allows only one linear polarization through the instrument (see Appendix ?). This along with the fact that FP1 is also a circular aperture, one can, in principal, use the instrument to detect the linear polarization of an observed target with a minimum of 3 rotations about the FP1 aperture (3 orientations are required to determine I, Q, & U and 4 orientations are required to determine I, Q, U, & V). With a body mounted instrument, this requires three distinct orientations of the spacecraft without violating flight rule constraints.

Observations were conducted by picking distances where changes in the spatial territory covered by FP1 at the three orientations are minimized (observations near apoapse satisfies this). Three distance orientations (separated by 60°) were chosen such that flight rules were avoided.

Note that it is important to also avoid geometries where the phase angle changes rapidly during the observations. Since polarization in the thermal IR is likely small, it is important to draw from a calibration set which minimizes errors from a lack of deep space observations (e.g. the DS4000 database).

ii. Stellar Occultations

Observation Type: Stellar Occultations

observation descriptor: [CWLEO/ETACAR]OCC

prime instrument: CIRS

riders: TBD

number of observations: 6 CWLeo, 5 Eta Carinae

primary boresight: CIRS_FP3

spectral resolution: 15 cm⁻¹ (39 RTI)

Description: CIRS has the ability to detect stars which exhibit strong signatures in the thermal IR. As a result, it is theoretically possible to determine the optical depth of the rings at these wavelengths. FP3 was chosen as the best boresight to use for detection of the candidate star due to peak stellar signal and good NESR. The caveat is that when one tracks a star with a CIRS boresight, the pixel containing the star contains signal from both the star and the rings. To alleviate this issue, it is important orient the FP3 boresight along the track of the star. Thus, the secondary spacecraft axis was chosen to be perpendicular to the local orbital plane of the spacecraft trajectory.

The lowest spectral resolution was chosen to allow for the maximal detection the stellar signal, in addition to allowing the most data points along the stars path.

Note that accuracy of pointing is key to correlating the radial position being probed by the star.

Note also that it is important to use a large number of DSCALs in order to minimize the noise and allow the detection of the target star.

iii. Rings On Saturn (OnSats):

Observation descriptor: ONSAT

Prime instrument: CIRS

Riders: ISS, UVIS, VIMS

Number of observations: 3

Primary boresight: CIRS_FP1, CIRS_FP3, CIRS_FP4

Spectral resolution: 15 cm⁻¹ (39 RTI)

Description: The goal of this observation is was to observe the rings with Saturn in the background source. The detected signal would be comprised of thermal radiation from the rings themselves and Saturn's thermal signature as filtered by the rings. Thus, one would have to rely on thermal spectra acquired at other times of the latitudes covered by the FOV. Filtering of Saturn signature would be dependent on several parameters (e.g. optical depth, filling factor, porosity, grain size, composition, etc.)

Scott G. Edgington 11/30/2018 10:37 AM

Comment [1]: [Check this.](#)

iv. Ring Saturn Reflections (SatRefl):

Observation descriptor: SATREFL

Prime instrument: CIRS

Riders: UVIS

Number of observations: 6

Primary boresight: CIRS_FP1, CIRS_FP3, CIRS_FP4

Spectral resolution: 3 cm⁻¹ (96 RTI)

Description: The science goal was to determine how much of Saturn's own thermal radiation is reflected from the rings for energy balance determination. The ideal geometries was where Saturn irradiation of the rings is dominant over solar effects. Thus, observations of territory in Saturn's shadow and near zero-Saturn phase angle are preferred. Several factors would influence this measurement (e.g. optical depth, ring albedo, porosity).

5. Observation Lists

Below is a table (Table 1) of the 694 CIRS prime observations for which data exist and has been pulled back from Goddard. The observations are grouped by name, and the number of each is shown, along with what revs and portion of the mission they appear in.

Following that is a table (Table 2) of the same observations, but parsed into groups representative of the purpose of the observations.

Accompanying this report is a set of thumbnail plots of the footprint size and locations acquired during each observation. Those plots are grouped according to the names given in the second table. Note that for quick rendering purposes, the (R,HA) location of each footprint is plotted onto a rendering of Saturn that is what the spacecraft would have seen at the beginning of the observation. For a number of observations, the sub-spacecraft elevation and azimuth changed significantly during the observation and rings opened or closed. That is not displayed in these renderings.

Also accompanying this report is a spreadsheet listing all the CIRS prime observations. There are currently errors in it:

- a. the number of phase/lat data files (NPxxx) is significantly different from the number of observations in the spreadsheet. either observations were lost, or were not pulled back from goddard, or errors were made while trimming duplicate observations from the list;
- b. note that CIMS sometimes lists an observation twice, for no apparent reason, even when "public only" etc. are selected. there was an episode around rev 080 when Scott mistakenly loaded some observations twice using the wrong mode, so that both copies appeared (our usual method for design was to build the timing, sasf, and XML's for the observations for a whole segment, and then load the XML's into CIMS all at once). It looks like I did the same thing with some of the phase/lat observations a couple years later.
- c. There may be a PIE or two missed because they are not listed as PRIME
- d. other?

Table 1:
Observations

NAME	number	Revs Occuring	PM	XM	EQ	XXM	FProx
SHADL[LMH]P	18	000-077	X				
SHADU[LMH]P	7	010-064	X				
SHADA	1	00A	X				
SHADCAS	1	44	X				
SHADLCAS	2	42	X				
SHADULCAS	1	66	X				
SHADC[IN,OUT]	2	00A	X				
--	--	--					
SHADEGR[U,L]	9	179-209			X		
SHADING[U,L]	12	176-200			X		
--	--	--					
SHADFP3	1	196			X		
SHADUNL	1	243				X	

--	--	--					
COMP	8	00A-102	X				
COMPA	1	00A	X				
COMPC	1	00A	X				
COMPLIT	10	183-213				X	
COMPUNL	6	176-200				X	
COMPLITA	10	227-283				X	X
COMPLITB	18	232-287				X	X
COMPLITC	4	231-288				X	X
COMPLITCD	5	234-292				X	X
COMPUNLA	12	237-282				X	X
COMPUNLC	10	233-274				X	X
COMPLRES	33	205-237				X	
--	--	--					
SUBMLXX[LMH]	27(28)	00A-074	X				
SUBMUXX[LMH]	53(54)	00A-078	X				
SUBMSXX[LMH]	7	084-093		X			
SUBMMLP	1	38	X				
SUBMLVEN	1	63	X				
--	--	--					
VERTL[L,M,H]P	16	007-072	X				
VERTU[L,M,H]P	24	008-073	X				
VERTULCAS	2	56,057	X				

VCAS[LS,US][L,HP]	3	085-104		X			
VENC[UN,L][L,M,H]P	3	087-102		X			
--	--	--					
TEMPL	31	7-75	X				
TEMPU	45	00B-079	X				
TEMPN	5	079-080	X				
TEMPS	4	079-082	X				
TMAPNXX[L,M]P	28	088-118		X			
TMAPSXX[L,M]P	16	085-111		X			
TMAPS	2	134				X	
--	--	--					
NPXXXLXXX	32	176-265				X	
P50L30S15	1	134				X	
SPXXXLXXX	14	202-241				X	
--	--	--					
TDIFNXX[L,M,J]P	10	089-107		X			
TDIFSXX[L,M,J]P	10	093-106		X			
TDIFNORTH	4	186-246				X	
TDIFSOUTH	2	194,245				X	
--	--	--					
VTMPL	1	62	X				
VTMPU	2	77,078	X				
VTMPN	11	081-113		X			

VTMPS	9	087-110		X			
--	--	--					
FMONITOR	73	00A-055	X				
FMOVIEA	3	003-005	X				
FMOVIEB	4	019-023	X				
FMOVIEC	1	49		X			
ANSASTARE	6	255-286					X
--	--	--					
EQLBN	14	112-137			X		
EQLBS	13	112-133			X		
EQSB	1	116			X		
--	--	--					
CWLEOCC	5	031-089	X	X			
ETACAR	1	78		X			
ETACAROCC	5	183-269				X	X
RDOROCC	1	186				X	
URTHECAR	1	186				X	
--	--	--					
RSCAN[LIT,DRK]	5	253-277					X
HALO[DARK,LIT]	4	253-256					X
CASDIV[UNL,LIT]	5	255-292					X
UNSHAD[DRK,LIT]	2	269,270					X
AZSHADSCN	2	282,283					X

PLAT[LIT,DRK]	2	270,283					X
--	--	--					
FP34INTEG	2	008-032	X				
ONSATULM	3	026-046	X				
SPLITVIMS	1	33	X				
SPLITISS	1	34	X				
SUBRADAR[U,L]	4	051-058	X				
ZEROPHASE	1	26	X				
SATREFL	4	107-236		X		X	
POLARIZ	8	114-125		X	X		

Table 2: Observations by Purpose

Number	Generic name	Includes
25	SHAD_PM	SHADL, SHADU
7	SHAD_PM2	SHADLCAS, SHADULCAS, SHADUNL
22	SHADOW	SHADEGR, SHADING
26	COMP_PMXM	COMP, COMPA, COMPC, COMPLIT, COMPUNL
37	COMPL_XXM	COMPLITA, COMPLITB, COMPLITC, COMPLITCD
22	COMPU_XXM	COMPUNLA, COMPUNLC
33	COMFLOWRES	COMPLL
27	SUBML_PM	SUBML

53	SUNMU_PM	SUBMU
9	SUBM_MISC	SUBMS, SUBMMLP, SUBMLVENC
16	VERTL_PM	VERTL
26	VERTU_PM	VERTU
8	VERT_MISC	VERTULCAS, VCAS, VENC
35	TEMPL_PM	TEMPL, TEMPS
50	TEMPU_PM	TEMPU, TEMPN
46	TMAP	TMAP
33	PHASLATL_XXM	NP, P50
14	PHASLATU_XXM	SP
26	TDIF	TDIF
85	FRING	FMOVIE, FMONITOR, ANSASTARE
23	VTMP	VTMPL, VTMPU, VTMPN, VTMPs
28	EQOBS	EQLBN, EQLBS, EQSB
13	OCCS	CWLEO, ETACAR, RDOR, URTHE
20	FPROX	RSCAN, HALO, CASDIV, UNSHAD, AZSHAD, PLAT

24	MISC	FP34INT, ONSAT, SPLIT, SUBR, ZEROPH, SATREFL, POLARIZ

4. Rider Observations

Philosophy: When data volume allowed for it, CIRS riders were placed on other Prime Ring observations. This allowed for CIRS observations at times when CIRS could not obtain a Prime observation. These riders allow CIRS to obtain data at a random regions of the available geometric phase space that it might have missed if no observations were conducted to begin with. Some riders may also have been part of campaigns conducted by the Rings Working Group.

5. Support Imaging Observations

Philosophy: When data volume allowed Support Images were taken during every Prime CIRS Ring observation. Occasionally, Support Images were taken when CIRS was a rider and the observation warranted it.

6. CIRS Ring Data Volume Cut Guidelines (or Why Not Collect Data 24-7?)

The following is the order of precedence of any cuts in data volume to CIRS Rings observations (and associated calibrations). They are only to be made if the need arises where data volume issues cannot be resolved without CIRS participation. Note that in 1 hour, CIRS collects 14.4 Mb at its full rate of 4000 bps.

a. Priority (Least Painful):

- i. *Cut FP4 on Ring Riders.*
 1. Keeping only FP1 and FP3.
 2. Results in a 45% (~5/11) cut in data volume.
- ii. *Cut FP4 on Ring Primes (keeping only FP1 and FP3). A 45% cut in data volume.*
 1. Keeping only FP1 and FP3.
 2. Results in a 45% (~5/11) cut in data volume.

b. Priority (Painful):

- i. *Reduce the number of hours DSCALs by an amount up to 50% –sge (12/13/11)*
 1. Due to the sensitivity of DSCALs to RWA rates, try to spread the cuts across several DSCALs. –sge (12/13/11)
- ii. *Cut FP3 and FP4 on Ring Riders.*
 1. Keeping only FP1.
- iii. Results in a 90% (~10/11) cut in data volume.

c. Priority (Extremely Painful):

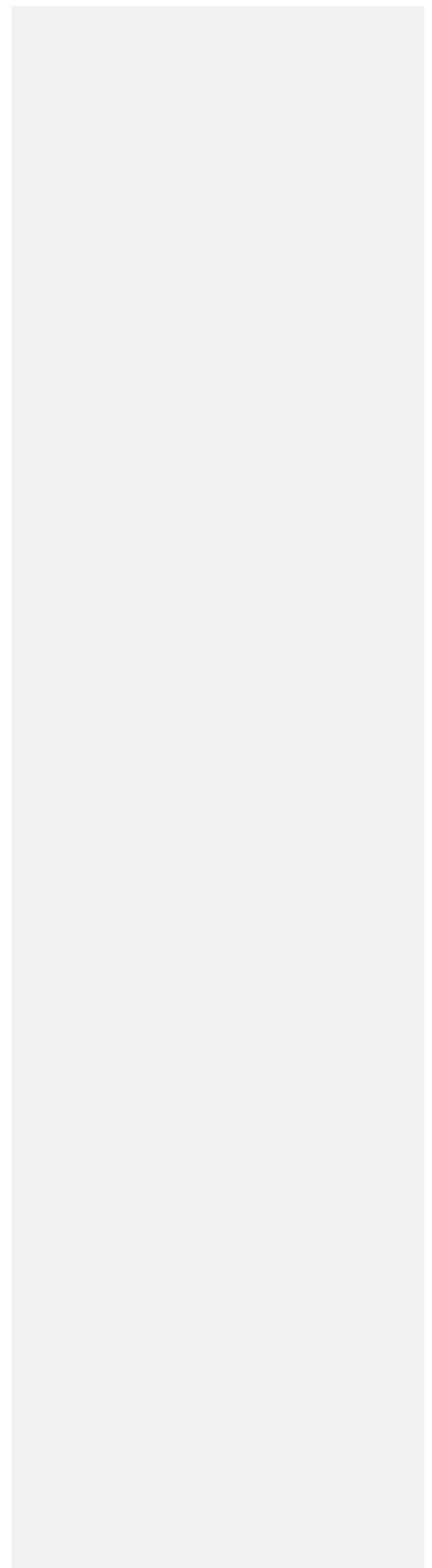
- i. *Reduce the number of hours DSCALs by an amount up to 90% (leaving a minimum of 1 hour). –sge (12/13/11)*

1. Due to the sensitivity of DSCALs to RWA rates, try to spread the cuts across several DSCALs.. –sge (12/13/11)
- ii. *Cut FP3 on Ring Primes (keeping only FP1).*
 1. Keeping only FP1.
 2. Results in a 90% (~10/11) cut in data volume.
- iii. *Cut Ring Riders.*
 1. Very last resort!
- iv. *Cut DSCAL.*
 1. Avoid this option!!! [*Note that it is better to cut two adjacent DSCALs in half, rather than cut one completely.* Reason: bracketing observations and SAP bits. –sge (01/17/08)] [Additional reasoning: Hits due to CIRS unfriendly RWA rates are quite random and makes the complete cutting of a DSCAL a bad choice. Even leaving a placeholder would help to mitigate this effect downstream. –sge (11/11/11)]
- v. *Cut Ring Primes.*
 1. Avoid this option!!!

Note also that CIRS also consistently collects between 70-80% of its specified data volume (see Shawn Boll's Data Utilization study). [Please note that DSCALs should have already been tweaked to reflect this fact. –sge (11/11/11)]

7. Rings Database
 - a. Summary
 - b. Functionality
8. Time Ordered Listing of All CIRS Rings Observations
 - a. Primes (By type? Time Ordered?)
 - b. Riders (Time Ordered?)
 - c. Support Images (Time Ordered?)
9. Useful References
 - a. 2004 SSR Paper
 - b. 2017 Review Paper
 - c. Estelle's and Mark's PDS Document
10. Appendices
 - a. Finding Temperature and Filling Factors
 - i. (algorithm used by Stu?)
 - b. Error Propagation
 - c. Occultation Analysis
 - d. Using CIRS as a Polarizer
 - e. CIRS and VIMS Heating Model

- i. Probably not here, but in a broader CIRS document



1.1. SATURN'S RINGS

The four-year Cassini tour has three distinct intervals of inclined orbits which are of primary interest for ring science (Cuzzi *et al.*, 2002; Matson *et al.*, 2002; Wolf, 2002). The early inclined sequence, which begins about 9 months into the tour, catches the rings close to their maximum opening angle, and near their warmest. These orbits reach a maximum inclination of about 20° . This sequence is followed by almost a year with the spacecraft orbiting in Saturn's equatorial plane. This time is good for edge-on ring measurements, primarily of the faint rings. The Titan 180° transfer sequence begins about two years into the tour. This sequence has two stages, an "up-leg" where the orbit inclination is increasing, and a "down-leg", where the orbit inclination is decreasing. The maximum inclination in this sequence is about 50° . A few months later the final, high inclination sequence begins. The spacecraft ends the 4-year tour in a high-inclination orbit (about 75°) with periapse on the lit side of the rings. This time provides a unique, high-inclination view of the rings.

SOI. The short period of time immediately following the Saturn Orbit insertion burn is of key interest for CIRS ring science. The spacecraft soars over the unilluminated side of the main rings and is nearly an order of magnitude closer to the rings than it will be at any other time in the mission. A single scan of a portion of the main rings will be obtained at 15.5 cm^{-1} resolution. CIRS FP1 resolution will range from 40 to 100 km, and FP3/4 resolution will range from 3 to 8 km, with the highest resolution over the A ring.

The main types of CIRS ring observations are listed below, in order of increasing spacecraft elevation. A schematic of these observations is shown in Fig. 1. Typical ring radial resolution for focal planes FP1 and FP3/4 as a function of distance from the rings is shown in Fig. 2.

- *Faint Ring Long Integrations.* The low optical depths of the faint D, E, F and G rings will pose particular observing challenges for CIRS. These rings are best viewed edge-on because this geometry enhances the instrument fill factor. Low spectral resolution of 15.5 cm^{-1} with FP1 provides the best signal-to-noise and should be sufficient for detecting the variations of emissivity with wavelength, which is our primary measurement goal. From close range ($\sim 10 R_s$) and small opening angle, the FP1 filling factor will approach 1% when pointed at the F ring's ansa. Integrations of ~ 10 minutes should yield usable signals. However, because the F ring is so clumpy, it needs to be sampled at many longitudes before a truly representative spectrum can be obtained. Observations will consist of alternating between both ring ansae every ~ 30 minutes to achieve the most complete rotational coverage of this ring. The E ring will be observed by pointing FP1 near the orbit of Enceladus, where the long edge-on line of sight through the ring maximizes the fill factor. However, this fill factor will still remain quite low, $\sim 10^{-4}$, so, detecting the E ring will require many, perhaps 100 or more, hours of integration. On the

other hand, because the ring is so thick vertically, the observing range can be quite large (30–40 R_s). More observing time is available then during these apoapse periods of the tour. The VIMS and UVIS instruments will also require substantial integration on this ring, so E ring observations will be cooperative activities between all of Cassini's optical remote sensing instruments. Unfortunately, the best possible fill factors for the remaining rings, D and G, are still lower than for Ring E. It is unlikely that either will be detected with CIRS.

- *Composition Integrations.* CIRS will determine with unique accuracy the ring spectrum between 50 and 1000 μm . As intimately mixed contaminants significantly influence this part of the spectrum, mixtures derived from the visible and near-infrared spectra will be tested against this new spectrum. Spectra of the three main rings over the full CIRS wavelength range will be obtained to determine possible radial variations in the bulk composition. Two types of observations will be made: high spectral resolution (0.5 cm^{-1}) FP3 emission measurements of the A, B and C rings, and high spectral resolution transmission measurements of the rings with the rings against Saturn. The former can be obtained from large ranges 20–40 R , because of FP3's fine spatial resolution; long integrations of 10–20 hours will be obtained on representative locations in each ring. The transmission measurements will be made from 20 R , at relatively low ring opening angles. This will allow a search for absorption features in the A and C rings, and the Cassini division. The same region of Saturn will be observed in at a similar spatial resolution when the rings are not present, to establish the background. The transmission spectra will be obtained over a series of emission angles.
- *Stellar Occultations.* A handful of stellar occultations are observed by CIRS to directly obtain the ring opacity in the infrared. Only a limited number targets are observable by CIRS, including CW Leo and Eta Carinae. Eta Carinae occultations are only observable during the final month of the tour. Occultations are observed in one FP3 pixel (CW Leo) or one FP4 pixel (Eta Carinae) at 15.5 cm^{-1} spectral resolution.
- *Radial scans.* These scans are typically executed between 5 and 20 R , over a range of spacecraft inclinations, from low (5°) to highest possible inclination (75°). Radial mapping (FP1, FP3) of the rings, on both lit and unlit sides, over a range of spacecraft elevations, local times and phase angles, is performed to obtain broadband radiometric measurements of the total flux and spectral shape in the CIRS wavelength range. Sets of observations are obtained in each of the inclined orbit intervals to map the temperature variation in the rings with changing solar illumination. Two types of scans are planned. Temperature scans will consist of spectra taken at 15.5 cm^{-1} spectral resolution of the lit and unlit sides of the rings at many incidence and emission angles and provide prime information on the ring thermal gradient as a function of radial distance to Saturn. Submillimeter scans will be made of spectra at 1 cm^{-1} spectral resolution of the lit and unlit sides of the rings to map the thermal characteristics and composition of the ring particles out to 1 mm.

- *Azimuthal scans.* These observations are executed between 5 and 20 Rs at spacecraft inclinations greater than 20°. They will be used to study the surface properties, the vertical dynamics and the spin of ring particles. Observations of the cooling and heating of the ring particles entering and emerging from the planetary shadow are planned to derive particle thermal inertias for all three main rings. It will make measurements at moderate radial resolution (typically 1000 km) across the shadow boundaries at low spectral resolution (15.5 cm⁻¹) with the FPI field of view. To constrain the vertical dynamics of ring particles, the temperatures of the main rings will be measured by CIRS along the azimuth of the main rings, from the exit of the shadow (morning) to the evening ansa, both on the unlit and unlit faces. This unique experiment will be realized with spectra at low spectral resolution (15.5 cm⁻¹). Spins create both an azimuthal asymmetry in the ring temperature and a dependence of the temperature with the emission angle, due to day/night contrast. Circumferential scans at a variety of phase and emission angles will be executed to detect azimuthal asymmetries and the anisotropy in the ring particle emission function which are both function of particles spin and thermal inertia. Occasionally, when observing time is highly disputed, long azimuthal scans (8-to-20 hours long depending on geometry and face) will be replaced by a series of radial scans at different azimuths.

There are other types of joint observations as well. Combined data from CIRS and VIMS, over a wide range of geometric and illumination conditions, will define the interior thermal distribution, from which a density distribution within the particles can be estimated. The thermal inertia and the infrared optical depth will be derived, which will provide information on regolith density, and possibly on collisional processes. The determination of the interior thermal distribution relies on the opportunities afforded by the orbiter and the semi-transparency of the ring particles at submillimeter wavelengths. Information about the particle interiors will be obtained by long spectral averages at various locations in the rings with spatial resolutions from a few hundred to several thousand km. These observations will be taken at many incidence and emission angles over the mission.

References

- Abbas, M. M., LeClair, A., Owen, T., Conrath, B. J., Flasar, F. M., Kunde, V. G., Nixon, C. A., Achterberg, R. D., Bjoraker, G., Jennings, D. J., Orton, G., and Romani, P. N.: 2003, Nitrogen isotopic ration in Jupiter's atmosphere from observations by Composite Infrared Spectrometer (CIRS) on the Cassini spacecraft, *Astrophys. J.*, in press.
- Achterberg, R. K., Conrath, B. J., Gierasch, P. J., and Flasar, F. M.: 2003, Cassini CIRS observations of ammonia in Jupiter's upper troposphere, *Bull. Amer. Astron. Soc.*, in press.
- Achterberg, R. K., and Flasar, F. M.: 1996, Planetary-scale in Saturn's upper troposphere, *Icarus* **119**, 350-369.
- Allen M., Yung, Y. L., and Gladstone, G. R.: 1992, The relative abundance of ethane to acetylene in the jovian atmosphere, *Icarus* **100**, 527-533.
- Allison, M., Godfrey, D. A., and Beebe, R. F.: 1990, A wave dynamical interpretation of Saturn's polar hexagon, *Science* **247**, 1061-1063.
- Andrews, D. G., Holton, J. R. and Leovy, C. B.: 1987, *Middle Atmosphere Dynamics*, Academic Press, Orlando, USA, 489 pp.
- Araki, S.: 1991, The dynamics of particle disks III. Dense and spinning particle disks, *Icarus* **90**, 139-171.
- Atkinson, D. H., Pollack, J. B. and Seiff, A.: 1996, Galileo doppler measurements of the deep zonal winds at Jupiter, *Science* **272**, 842-843.
- Atkinson, D. H., Ingersoll, A. P., and Seiff, A.: 1997, Deep zonal winds on Jupiter: update of doppler tracking the Galileo probe from the orbiter, *Nature* **388**, 649-650.
- Atreya, S. K., Donahue, T. M., and Kuhn, W. R.: 1978, Evolution of a nitrogen atmosphere on Titan, *Science* **201**, 611-613.
- Atreya, S. K., Edgington, S. G., Trafton, L. M., Caldwell, J. J., Noll, K. S., and Weaver, H. A.: 1995, Abundances of ammonia and carbon disulfide in the Jovian stratosphere following the impact of comet Shoemaker-Levy 9, *Geophys. Res. Lett.* **22**, 1625-1628.
- Atreya, S. K., Mahaffy, P. R., Niemann, H. B., Wong, M. H., and Owen, T. C.: 2003, Composition and origin of the atmosphere of Jupiter—an update, and implications for the extrasolar giant planets, *Planet. Space Sci.*, **51**, 105-112.
- Atreya, S. K., Wong, M. H., Owen, T. C., Mahaffy, P. R., Niemann, H. B., dePater, I., Drossart, P., Encrenaz, Th.: 1999, A comparison of the atmospheres of Jupiter and Saturn: deep atmospheric composition, cloud structure, vertical mixing, and origin, *Planet. Space Sci.*, **47**, 1243-1262.
- Aumann, H.H. and Kieffer, H.H. 1973, Determination of particles sizes in Saturn's rings from their eclipse cooling and heating curves, *Astrophys. J.* **186**, 305-311.
- Awal, M., and Lunine, J. I.: 1994, Moist convective clouds in Titan's atmosphere. *Geophys. Res. Lett.* **21**, 2491-2494.
- De Avillez Pereira, R., Baulch, D. L., Pilling, M. J., Robertson, S. H., and Zeng, G. 1997: Temperature and pressure dependence of the multichannel rate coefficients for the CH₃ + OH system, *J. Phys. Chem A.* **101**, 9681-9693.

- Baines, K. H., and Bergstralh, J. T.: 1986, The spectrum of the uranian atmosphere: constraints from the geometric albedo spectrum and H₂ and CH₄ line profiles, *Icarus* **109**, 20-39.
- Baines, K. H., Michelson, M. E., Larson, L. E., and Ferguson, D. W.: 1995, The abundance of methane and ortho/para hydrogen in Uranus and Neptune: implications for new laboratory 4-0 H₂ quadrupole line parameters, *Icarus* **114**, 328-340.
- Bandfield, J.L.: 2002, Global mineral distributions on Mars, *J. Geophys. Res. (Planets)*, **107**, pp. 9-1, CiteID 5042.
- Barnet, C. D., Westphal, J. A., Beebe, R. F., and Huber, L. F.: 1992, Hubble Space Telescope observations of the 1990 equatorial disturbance on Saturn -- zonal winds and central meridian albedos, *Icarus* **100**, 499-511.
- Beebe, R. F., Barnet, C., Sada, P. V., and Murrell, A. S.: 1992, The onset and growth of the 1990 equatorial disturbance on Saturn, *Icarus* **95**, 163-172.
- Bell, J.F., Cruikshank, D.P., and Gaffey, M.J.: 1985, The composition and origin of the Iapetus dark material, *Icarus* **61**, 192-207.
- de Bergh, C., Schmitt, B., Binzel, r. P., and Bus, S. J.: 2003, Spectroscopy of Phoebe in the 0.8-2.5 micron range, *Bull. Amer. Astron. Soc.* **35**, 940.
- Bézard, B., Coustenis, A. and McKay, C. P.: 1995, Titan's stratospheric temperature asymmetry: a radiative origin?, *Icarus* **113**, 267-276.
- Bézard, B., Drossart, P., Lellouch, E., Tarrago, G., and Maillard, J. P.: 1989, Detection of arsine in Saturn, *Astrophys. J.* **346**, 509-513.
- Bézard, B., Feuchtgruber, H., Moses, J. I., and Encrenaz, T.: 1998, Detection of methyl radicals (CH₃) on Saturn, *Astron. Astroph.* **334**, L41-L44.
- Bézard, B., Gautier, D., and Conrath, B.: 1984, A seasonal model of the saturnian upper troposphere—comparison with Voyager infrared measurements, *Icarus* **60**, 274-288.
- Bézard, B., Gautier, D., and Marten, A.: 1986, Detectability of HD and nonequilibrium species in the upper atmospheres of the giant planets from their submillimeter spectrum, *Astron. Astrophys.* **161**, 387-402.
- Bézard, B., Marten, A., and Paubert, G.: 1993, Detection of acetonitrile on Titan, *Bull. Amer. Astron. Soc.* **25**, 1100.
- Bézard, B., Moses, J. I., Lacy, J., Greathouse, T., Richter, M., and Griffith, C.: 2001a, Detection of ethylene (C₂H₄) on Jupiter and Saturn in non-auroral regions, *Bull. Amer. Astron. Soc.* **33**, 1079-1080.
- Bézard, B., Drossart, P., Encrenaz, T. and Feuchtbruber, H.: 2001b, Benzene on the giant planets, *Icarus* **155**, 492-500.
- Bird, M. K., Dutta-Roy, R., Heyl, M., Allison, M., Asmar, S. W., Folkner, W. M., Preston, R. A., Atkinson, D. H., Edenhoffer, P., Plettemeier, D., Wohlmuth, R., Iess, L., and Tyler, G. L.: 2002, The Huygens Doppler Wind Experiment, *Space Sci. Rev.* **104**, 613-640.
- Bossard, A., Kamga, R., and Raulin, F.: 1986, Gas phase synthesis of organo-phosphorous compounds and the atmosphere of the giant planets, *Icarus* **67**, 305-324.
- Brasunas, J. C.: 2002, Phase anomalies in Fourier-transform spectrometers: an absorbing beam splitter is neither sufficient nor necessary, *Appl. Optics* **41**, 2481-2487.
- Brasunas, J. C., and Lakew, B : 2003, Long-term stability of the Cassini Fourier transform spectrometer en route to Saturn, in *Recent Research Developments in Optics, Research Signpost (Kerala, India)*, in press.

- Bregman, J. D., Lester, D. F., Rank, D. M.: 1975, Observation of the ν_2 band of PH_3 in the atmosphere of Saturn, *Astrophys. J. (Lett.)* **202**, L55-L56.
- Briggs, F.H., and Sacket, P. D.: 1989, Radio observations of Saturn as a probe of its atmosphere and cloud structure, *Icarus* **80**, 77-103.
- Broadfoot, A. L., Sandel, B. R., Shemansky, D. E., Holberg, J. B., Smith, G. R., Strobel, D. F., McConnell, J., C., Kumar, S., Hunten, D. M., Atreya, S. K., Donahue, T. M., Moos, H. W., Bertaux, J. L., Blaont, J. E., Pomphrey, R. B., and Linick, S.: 1981 Extreme ultra-violet observations from Voyager 1 encounter with Saturn, *Science* **204**, 979-983.
- Brown, M. E.: 2000, Near-infrared spectroscopy of Centaurs and irregular satellites, *Astron. J.* **119**, 977-983.
- Brown, M. E., Bouchez, A. H., Griffith, C. A.: 2002, Direct detection of variable tropospheric clouds near Titan's south pole, *Nature* **420**, 797-797.
- Brown, R. H.: 1983, The Uranian satellites and Hyperion—new spectrophotometry and compositional implications, *Icarus* **56**, 414-425.
- Brown, R. H., and Matson, D. L.: 1987, Thermal effects of insolation propagation into the regoliths of airless bodies, *Icarus* **72**, 84-94.
- Brown, R. H. *et al.*: 2003, Cassini Visible and Infrared Mapping Spectrometer experiment, *Space Sci. Rev.*, this issue.
- Buratti, B.J.: 1985, Application of a radiative transfer model to bright icy satellites. *Icarus* **61**, 208-217.
- Buratti, B.J., Hicks, M.D., Tryka, K.A., Sittig, M.S., Newburn, R.L.: 2002. High-Resolution 0.33-0.92 μm Spectra of Iapetus, Hyperion, Phoebe, Rhea, Dione, and D-Type Asteroids: How Are They Related? *Icarus* **155**, 375-381.
- Buratti, B.J., Mosher, J.A., and Johnson, T.V.: 1990, Albedo and color maps of the saturnian satellites, *Icarus* **87**, 339-357.
- Burns, J. A., Hamilton, D. P., and Showalter, M. R.: 2001. Dusty rings and circumplanetary dust: observations and simple physics. In *Interplanetary Dust* (E. Grün, B. A. S. Gustafson, S. F. Dermott, and H. Fechtig, Eds.), Springer-Verlag, Berlin, pp. 641-725.
- Cabane, M., Chassefière, E. and Israel, G.: 1992, Formation and growth of photochemical aerosols in Titan's atmosphere, *Icarus* **96**, 176-189.
- Calcutt, S. B., Taylor, F. W., Ade, P., Kunde, V. G., and Jennings, D.: 1992, The composite infra-red spectrometer, *J. Brit. Interplanetary Soc.* **45**, 811-816.
- Caldwell, J., Hua, X.-M., Turgeon, B., Westphal, J. A., and Barnet, C. D.: 1993, The drift of Saturn's north polar spot observed by the Hubble Space Telescope, *Science* **260**, 326-329.
- Carlson, B. E., W. B. Rossow, and G. S. Orton: 1988, Cloud microphysics of the giant planets, *J. Atmos. Sci.* **45**, 2066-2081.
- Carlson, B. E., Lacin, A. A., and Rossow, W. B.: 1992, Ortho-para hydrogen equilibration on Jupiter, *Astrophys. J.* **393**, 357-372.
- Cerceau, F., Raulin, F., Courtin, R., and Gautier, D.: 1985, Infrared spectra of gaseous mononitriles: application to the atmosphere of Titan, *Icarus* **62**, 207-220.
- Charney, J. G., and Drazin, P. G.: 1961, Propagation of planetary-scale disturbances from the lower into the upper atmosphere, *J. Geophys. Res.* **66**, 83-109.

- Christensen, P.R., Bandfield, J.L., Bell, J.F., Gorelick, N., Hamilton, V.E., Ivanov, A., Jakosky, B.M., Kieffer, H.H., Lane, M.D., Malin, M.C., McConnochie, T., McEwen, A.S., McSween, H.Y., Mehall, G.L., Moersch, J.E., Neelson, K.H., Rice, J.W., Richardson, M.I., Ruff, S.W., Smith, M.D., Titus, T.N. and Wyatt, M.B.: 2003, Morphology and composition of the surface of Mars: Mars Odyssey THEMIS results, *Science* **300**, 2056-2061.
- Christensen, P. R., Bandfield, J.L., Smith, M. D., Hamilton, V. E., and Clark, R. N.: 2000a, Identification of a basaltic component on the Martian surface from Thermal Emission Spectrometer data, *J. Geophys. Res.* **105**, 9609-9621.
- Christensen, P. R., Bandfield, J. L., Clark, R. N., Edgett, K. S., Hamilton, V. E., Hoefen, T., Kieffer, H. H., Kuzmin, R. O., Lane, M. D., Malin, M. C., Morris, R. V., Pearl, J. C., Pearson, R., Roush, T. L., Ruff, S. W., and Smith, M. D.: 2000b, Detection of crystalline hematite mineralization on Mars by the Thermal Emission Spectrometer: Evidence for near-surface water, *J. Geophys. Res.* **105**, 9623-9642.
- Clark, R. N. and McCord, T. B.: 1980, The rings of Saturn: new near-infrared measurements and a 0.326-4.08 μm summary, *Icarus* **43**, 161-168.
- Clarke, D.W. and Ferris, J.P.: 1997, Chemical evolution on Titan : comparisons to the prebiotic Earth, *Origins of life and Evol. Biosphere* **27**, 225-248.
- Coll, P., Bernard, J.-M., Navarro-González, R. and Raulin, F.: 2003, Oxirane: An exotic oxygenated organic compound in Titan? *Astrophys. J.* in press.
- Coll, P., Coscia, D., Gazeau, M.-C., and Raulin, F.: 1997, New planetary atmosphere simulations: application to the organic aerosols of Titan, *Adv. Space Res.*, **19** (7), 1113-1119.
- Collins, S.A., Cook, A.F. II, Cuzzi, J.N., Danielson, G.E., Hunt, G.E., Johnson, T.V., Morrison, D., Owen, T., Pollack, J.B., Smith, B.A., and Terrile, R.J.: 1980, First Voyager view of the rings of Saturn, *Nature* **288**, 439-443.
- Colthup, N. B., Daley, L. H., and Wiberley, S. E.: 1975, *Introduction to Infrared and Raman Spectroscopy* (Academic Press, New York), 523 pp.
- Comas Sola, J.: 1908, Observations des satellites principaux de Jupiter et de Titan, *Astron. Nachr.* **179**, 289-290.
- Combes, M., Vapillon, L., Bendron, E., Coustenis, A., Lai, O., Wittenberg, R., and Sirdy, R.: 1997, Spatially resolved images of Titan by means of adaptive optics, *Icarus* **129**, 482-497.
- Connerney, J. E. C., and Waite, J. H.: 1984, New model of Saturn's ionosphere with an influx of water from the rings, *Nature* **312**, 136-138.
- Conrath, B. J., Flasar, F. M., Pirraglia, J. A., Gierasch, P. J., and Hunt, G. E.: 1981, Thermal structure and dynamics of the jovian atmosphere. 2. Visible cloud features, *J. Geophys. Res.* **86**, 8679-8775.
- Conrath, B. J., and Gierasch, P. J.: 1983 Evidence for disequilibrium of ortho and para hydrogen on Jupiter from *Voyager* IRIS measurements, *Nature* **306**, 571-572.
- Conrath, B. J., and Gierasch, P. J.: 1984, Global variation of the para fraction in Jupiter's atmosphere and implications for dynamics on the outer planets, *Icarus* **57**, 184-204.
- Conrath, B. J., and Giersach, P. J.: 1986. Retrieval of ammonia abundances and cloud opacities on Jupiter from *Voyager* IRIS spectra, *Icarus* **67**, 444-455.
- Conrath, B. J., and Pirraglia, J. A.: 1983, Thermal structure of Saturn from *Voyager* infrared measurements: implications for atmospheric dynamics, *Icarus* **53**, 286-291.

- Conrath, B. J., and Gautier, D.: 2000, Saturn helium abundance: a reanalysis of Voyager measurements, *Icarus* **144**, 124-134.
- Conrath, B. J., Gautier, D., Hanel, R. A. and Hornstein, J. S.: 1984, The helium abundance of Saturn from Voyager measurements, *Astrophys. J.* **282**, 807-815.
- Conrath, B. J., Gierasch, and Ustinov, E. A.: 1998, Thermal structure and para hydrogen fraction on the outer planets from Voyager IRIS measurements, *Icarus* **135**, 501-517.
- Cooke, Maren 1991. *Saturn's Rings: Photometric studies of the C ring and radial variation in the Keeler gap*. PhD Thesis, Cornell University, 65.
- Courtin, R., Lena, P., De Muizon, M. Rouan, D., Nicollier, C. and Wijnbergen, J. 1979. Far-infrared photometry of planets—Saturn and Venus, *Icarus* **38**, 411-419.
- Courtin, R., Gautier, D., Marten, A., and Kunde, V.: 1983, The $^{13}\text{C}/^{12}\text{C}$ ratio in Jupiter from the Voyager infrared investigation, *Icarus* **53**, 121-132.
- Courtin, R., Gautier, D., Marten, A., Bézard, B., and Hanel, R.: 1984, The composition of Saturn's atmosphere at northern temperate latitudes from Voyager IRIS spectra: NH_3 , PH_3 , C_2H_2 , C_2H_4 , CH_4 , CH_3D , CH_3 , and the Saturnian D/H isotopic ratio, *Astrophys. J.* **287**, 899-916.
- Courtin, R., Gautier, D., and McKay, C. P.: 1995, Titan's thermal emission spectrum: re-analysis of the Voyager infrared measurements, *Icarus* **114**, 144-162.
- Coustenis, A., and Bézard, B.: 1995, Titan's atmosphere from Voyager infrared observations. IV. Latitudinal variations of temperature and composition, *Icarus* **115**, 126-140.
- Coustenis, A., Bézard, B. and Gautier, D.: 1989a, Titan's atmosphere from Voyager infrared observations. I. The gas composition of Titan's equatorial region, *Icarus* **113**, 267-276.
- Coustenis, A., Bézard, B. and Gautier, D.: 1989b, Titan's atmosphere from Voyager infrared observations. II. The CH_3D abundance and D/H ratio from the 900-1200 cm^{-1} spectral region, *Icarus* **82**, 67-80.
- Coustenis, A., Bézard, B., Gautier, D., Marten, A., and Samuelson R.: 1991. Titan's atmosphere from Voyager infrared observations. III. Vertical distributions of hydrocarbons and nitriles near Titan's north polar hood, *Icarus* **89**, 152-167.
- Coustenis, A., Encrenaz, Th., Bézard, B., Bjoraker, G., Graner, G., Dang-Nhu, M., and Arié, E.: 1993, Modeling Titan's thermal infrared spectrum for high-resolution space observations, *Icarus* **102**, 240-260.
- Coustenis, A., Gendron, E., Lai, O., Veran., J.-P. Woillez, J., Combes, M., Vapillon, L., Fusco, Th., Mugnier, L., Rannou, P.: 2001, Images of Titan at 1.3 and 1.6 microns with adaptive optics at the CFHT, *Icarus* **154**, 501-515.
- Coustenis, A., Salma, A., Lellouch, E., Encrenaz, Th., Bjoraker, G. L., Samuelson, R. E., de Graauw, Th., Feuchtgruber, H., and Kessler, M. F.: 1998, Evidence for water vapor in Titan's atmosphere from ISO/SWS data, *Astron. Astrophys.* **336**, L85-L89.
- Coustenis, A., Salma, A., Schulz, B., Ott, S., Lellouch, E., Encrenaz, Th., Gautier, D., and Feuchtgruber, H.: 2003, Titan's atmosphere from ISO mid-infrared spectroscopy, *Icarus* **161**, 383-403.
- Coustenis, A., Schmitt, B., Khanna, R. K., and Trotta, F.: 1999, Plausible condensates in Titan's stratosphere from Voyager infrared data, *Planet. Space Sci.* **47**, 1305-1329.
- Craig, I. J. D., and Brown, J. C.: 1986, *Inverse Problems in Astronomy*, Boston: Adam Hilger Ltd.
- Cruikshank, D.P.: 1979, The radius and albedo of Hyperion, *Icarus* **37**, 307-309.

- Cruikshank, D.P., and Brown, R.H.: 1982, Surface composition and radius of Hyperion, *Icarus* **50**, 82-87.
- Cruikshank, D. P., Brown, R. H., Calvin, W. M., Roush, T. L., and Bartholomew, M. J.: 1998, Ices on the satellites of Jupiter, Saturn, and Uranus, in *Solar System Ices*, Kluwer Academic Publishers (B. Schmitt, C. de Bergh, and M. Festou, eds.), Kluwer, Dordrecht, pp. 579-606.
- Cruikshank, D.P., Veverka, J., and Lebofsky, L.A.: 1984, Satellites of Saturn: Optical properties, in *Saturn*, eds T. Gehrels and M.S. Matthews, University of Arizona Press, Tucson, pp. 640-667.
- Cunningham, C.T., Ade, P.A.R., Robson, E.I., Nolt, I.G., and Radostitz, J.V.: 1981, The submillimeter spectra of the planets: narrow-band photometry, *Icarus* **48**, 127-139.
- Cuzzi, J.N., Lissauer, J.J., Esposito, L.W., Holberg, J.B., Marouf, E.A., Tyler, G.L., and Boischoy, A.: 1984, Saturn's rings: properties and processes, in *Planetary Rings*, eds. R. Greenberg and A. Brahic (Tucson: Univ. of Arizona Press), pp 72-198.
- Cuzzi, J. N., Colwell, J. E., Esposito, L. W., Porco, C. C., Murray, C. D., Nicholson, P. D., Spilker, L. J., Marouf, E. A., French, R. C., Rappaport, N., and Muhleman, D.: 2002, Saturn's rings: pre-Cassini status and mission, *Space Sci. Rev.* **118**, 209-251.
- Cuzzi, J. N. and Estrada, P. R.: 1998, Compositional evolution of Saturn's rings due to meteoroid bombardment, *Icarus* **132**, 1-35.
- Danielson, R. E., J. J. Caldwell, and D. R. Larch 1973, An inversion in the atmosphere of Titan, *Icarus* **20**, 437-443.
- Delitsky, M.L., and Lane, A.L.: 1998, Ice chemistry on the Galilean satellites, *J. Geophys. Res.* **103**, 31,391-31,403.
- Delitsky, M.L., and Lane, A.L.: 2002, Saturn's inner satellites: Ice chemistry and magnetospheric effects, *J. Geophys. Res.* **107**, 3.1-3.17.
- Delitsky, M.L., Lane, A.L., Henry-Riyad, H., and Tidwell, T.T.: 2003, Saturn's satellites: Potential for organic chemistry, *Bull. Amer. Astron. Soc.* **35**, 914.
- Delpech, C., Guillemin, J.-C., Paillous, P., Khelifi, M., Bruston, P., and Raulin, F.: 1994, Infrared spectra of triacetylene in the 4000-220 cm⁻¹ region: absolute band intensity and implications for the atmosphere of Titan, *Spectrochimica Acta* **50A**, 1095-1100.
- Desch, M. D. and Kaiser, M. L.: 1981, Voyager measurement of the rotation period of Saturn's magnetic field, *Geophys. Res. Lett.* **8**, 253-256.
- De Pater, I. and Dickel, J.R. 1991, Multifrequency radio observations of Saturn at ring inclination angles between 5 and 26 degrees, *Icarus* **94**, 474-492.
- Dermott, S. F., and Sagan, C.: 1995, Tidal effects of disconnected hydrocarbon seas on Titan, *Nature* **374**, 238-240.
- Dones, L., Cuzzi, J.N., and Showalter, M.R.: 1993, Voyager photometry of Saturn's A ring, *Icarus* **105**, 184-215.
- Doyle, L. R., Dones, L., and Cuzzi, J. N.: 1989, Radiative transfer modeling of Saturn's outer B ring, *Icarus* **80**, 104-135.
- Drossart, P., Lellouch, E., Bézard, B., Maillard, J. P., and Tarrago, G.: 1990, Jupiter—evidence for a phosphine enhancement at high northern latitudes, *Icarus* **83**, 248-253.
- Dubouloz, N., Raulin, F., Lellouch, E., and Gautier, D.: 1989, Titan's hypothesized ocean properties: the influence of surface temperature and atmospheric composition uncertainties. *Icarus* **82**, 81-96.

- Dunkerton, T.: 1978, On the mean meridional mass motions of the stratosphere and mesosphere, *J. Atmos. Sci.* **35**, 2325-2333.
- Eliassen, A., and Palm, E.: 1961, On the transfer of energy in stationary mountain waves, *Geophys. Publ.* **22**(3), 1-23
- Ellsworth, K., and Schubert, G.: 1983, Saturn's icy satellites: Thermal and structural models, *Icarus* **54**, 490-510.
- Epstein, E. E., Janssen, M. A., Cuzzi, J. N.: 1984, Saturn's rings – 3mm low-inclination observations and derived properties, *Icarus* **58**, 403-411.
- Esposito, L.W., Cuzzi, J.N., Holberg, J.H., Marouf, E.A., Tyler, G.L., and Porco, C.C.: 1984, Saturn's rings: structure, dynamics, and particle properties, in *Saturn*, eds. T. Gehrels and M.S. Matthews (Tucson: Univ. of Arizona Press), pp 463-545.
- Esposito, L. W., *et al.*: 2003, Cassini Ultraviolet Imaging Spectrometer experiment, *Space Sci. Rev.*, this issue.
- Estrada, P. R. and Cuzzi, J. N.: 1996, Voyager observations of the color of Saturn's rings, *Icarus* **122**, 251-272.
- Ferrari, C., Galdemard, P., Lagage, P.O., Pantin, E., and Quoirin, C.: 2003, Imaging Saturn's rings with CAMIRAS: thermal inertia of B and C rings. *Astron. Astroph.*, in press.
- Feuchtgruber, H., Lellouch, E., De Graauw, T., Bézard, B., Encrenaz, and Griffin, M.: 1997, External supply of oxygen to the atmospheres of the giant planets, *Nature* **389**, 159-162.
- Flasar, F. M.: 1983, Oceans on Titan?, *Science* **221**, 55-57.
- Flasar, F. M.: 1998a, The composition of Titan's atmosphere: a meteorological perspective. *Planet. Space Sci.* **46**, 1109-1124.
- Flasar, F. M.: 1998b, The dynamic meteorology of Titan, *Planet. Space Sci.* **46**, 1125-1147.
- Flasar, F. M., and Conrath, B. J.: 1990, Titan's stratospheric temperature: a case for dynamical inertia?, *Icarus* **85**, 346-354.
- Flasar, F. M., and Conrath, B. J.: 1992, The meteorology of Titan, in *Proceedings Symposium on Titan*, European Space Agency SP-338, 89-99.
- Flasar, F. M., Conrath, B. J., Pirraglia, J. A., Clark, P. C., French, R. G., and Gierasch, P. J.: 1981b, Thermal structure and dynamics of the jovian atmosphere. 1. The great red spot, *J. Geophys. Res.* **86**, 8759-8767.
- Flasar, F. M., Kunde, V. G., Achterberg, R. K., Conrath, B. J., Simon-Miller, A. A., Nixon, C. A., Gierasch, P. J., Romani, P. N., Bézard, B., Irwin, P., Bjoraker, G. L., Brasunas, J. C., Jennings, D. E., Pearl, J. C., Smith, M. D., Orton, G. S., Spilker, L. J., Carlson, R., Calcutt, S. B., Read, P. L., Taylor, F. W., Fouchet, T., Parrish, P., Barucci, A., Courtin, R., Coustenis, A., Gautier D., Lellouch, E., Marten, A., Prangé, R., Biraud, Y., Ferrari, C., Owen, T. C., Abbas, M. M., Samuelson, R. E, Raulin, F., Ade, P., Césarsky, C. J., Grossman, K. U., and Coradini, A.: 2004, An intense stratospheric jet on Jupiter, *Nature* **427**, 132-135.
- Flasar, F. M. Samuelson, R. E., and Conrath, B. J.: 1981, Titan's atmosphere: temperature and dynamics, *Nature* **292**, 693-698.
- Fortney, J.I., and Hubbard, W.B.: 2003, Phase separation in giant planets: inhomogeneous evolution of Saturn, *Icarus* **164**, 228-243.
- Fouchet, T., Orton, G. S., Irwin, P. G. J., and Calcutt, S. B.: 2003, Upper limits on hydrogen halides in Jupiter from Cassini/CIRS observations, *Icarus*, submitted.

- Fouchet, T., Irwin, P. G. J., Parrish, P., Calcutt, S. B., Taylor, F. W., Nixon, C., and Owen, T.: 2003, Search for spatial variation in the jovian $^{14}\text{N}/^{15}\text{N}$ ratio from Cassini/CIRS observations, *Icarus*, in press.
- Fouchet, T., Prangé, R., Connerney, J.E.C., Courtin, R., Ben Jaffel, L, Noll, K., and McConnell, J.C.: 1996, HST spectro-imaging of Saturn and search for water from the rings, *Bull. Amer. Astron. Soc.* **28**, 1129.
- Friedson, A. J., West, R. A., Hronek, A. K., Larsen, N. A., and Dalal, N.: 1999, Transport and mixing in Jupiter's stratosphere inferred from Comet SL-9 dust migration, *Icarus* **138**, 141-156.
- Froidevaux, L.: 1981, Saturn's rings: infrared brightness variation with solar elevation, *Icarus*, **46**, 4-17.
- Froidevaux, L., and Ingersoll, A.P.: 1980, Temperatures and optical depths of Saturn's rings and a brightness temperature of Titan, *J. Geophys. Res.* **85**, 5929-5936.
- Froidevaux, L., Matthews, K., and Neugebauer, G. : 1981, Thermal response of Saturn's ring particles during and after eclipse, *Icarus* **46**, 18-26.
- Gautier, D., Conrath, B., Flasar, M., Hanel, R., Kunde, V., Chedin, A., and Scott, N.: 1981., The helium abundance of Jupiter from Voyager, *J. Geophys. Res.* **86**, 8713-8720.
- Gautier, D., and Grossman, K.: 1972, New method for determination of the mixing ratio hydrogen to helium in the giant planets, *J. Atmos. Sci.* **29**, 788-792.
- Gautier, D. and Owen, T.: 1983, Cosmogonical implications of elemental and isotopic abundances in atmospheres of the giant planets, *Nature* **304**, 691-694.
- Gautier, D., and Owen, T. :1989, The composition of the outer planets' atmospheres, in *Origins and Evolution of Planetary and Satellite Atmospheres*, ed S. K. Atreya, J. B. Pollack, & M. S. Matthews, Tucson: The University of Arizona Press, pp. 487-512.
- Gautier, D. and Owen, T.: 1983, Cosmogonical implications of elemental and isotopic abundances in atmospheres of the giant planets, *Nature* **304**, 691-694.
- Gendron, E., Coustenis, A., Drossart, P., Combes, M., Hirtzig, M., Lacombe, F., Rouan, D., Collin, C., Pau, S., Lagrange, A.-M.: 2003, VLT/NACO adaptive optics imaging of Titan, *Astron. Astroph.*, in press.
- Gierasch, P. J. and Conrath, B. J.: 1987, Vertical temperature gradients on Uranus—implications for layered convection, *J. Geophys. Res.* **92**, 15019-15029.
- Gierasch, P. J. and Conrath, B. J.: 1993, Dynamics of the atmospheres of the outer planets: post-Voyager measurement objectives, *J. Geophys. Res.* **98**, 5459-5469.
- Gierasch, P. J., Conrath, B. J., and Magalhães, J. A.: 1986, Zonal mean properties of Jupiter's upper troposphere from Voyager infrared observations, *Icarus* **67**, 456-483.
- Gierasch, P. J., Conrath, B. J., and Read, P. L.: 2003. Non-conservation of Ertel potential vorticity in hydrogen atmospheres, submitted to *Icarus*.
- Gierasch, P. J., and Goody, R. M.: 1969, Radiative time constants in the atmosphere of Jupiter, *J. Atmos. Sci.* **26**, 979-980.
- Gille, J. C., and House, F. B.: 1971, Inversion of limb radiance measurements. 1. Temperature and thickness, *J. Atmos. Sci.* **28**, 1427-1442.
- Gillett, F. C., Forrest, W. J. and Merrill, K. M.: 1973, 8-13 micron observations of Titan, *Astrophys. J.* **184**, L93-L95.

- Gillett F. C.:1975, Further observations of the 8-13 micron spectrum of Titan, *Astrophys. J.* **201**, L41-L43.
- Gladman, B., Kavelaars, J. J., Holman, M., Nicholson, P. D., Burns, J. A., Hergenrother, C. W., Petit, J.-M., Marsden, B. G., Jacobson, R., Gray, W., Grav, T.: 2001. Discovery of 12 satellites of Saturn exhibiting orbital clustering, *Nature* **412**, 163-166
- Gladstone, G. D., Allen, M., Yung, Y. L.: 1996, Hydrocarbon photochemistry in the upper atmosphere of Jupiter, *Icarus* **119**, 1-52.
- Godfrey, D. A.: 1986, The rotation period of Saturn's polar hexagon, *Science* **247**, 1206-1208.
- Godfrey, D. A.: 1988, A hexagonal feature around Saturn's north pole, *Icarus* **76**, 335-356.
- Goody, R. M., and Yung, Y. L.: 1989, *Atmospheric Radiation: Theoretical Basis*, Oxford: Clarendon Press (2nd ed.).
- de Graauw, T., Feuchtgruber, H., Bézard, B., Drossart, P., Encrenaz, T., Beintema, D. A., Griffin, M., Heras, A., Kessler, M., Leech, K., Lellouch, E., Morris, P., Roelfsema, P. R., RoosSerote, M., Salama, A., Vandenbussche, B., Valentijn, E. A., Davis, G. R., Naylor, D. A.: 1997, First results of ISO-SWS observations of Saturn: detection of CO₂, CH₃C₂H, C₂H₂ and tropospheric H₂O, *Astron. Astrophys.* **321**, L13-16.
- Greathouse, T., Moses, J., Bézard, B., Griffith, C., Lacy, J., Knez, C., and Richter, M.: 2003, Latitudinal variations of temperature, C₂H₂ and C₂H₄ in Saturn's stratosphere along with the detection of propane, *Bull. Amer. Astron. Soc.* **35**, 1019
- Griffin, M. J., Naylor, D. A., Davis, G. R., Ade, P. A. R., Oldman, P. G., Swinyard, B. M., Gautier, D., Lellouch, E., Orton, G. S., Encrenaz, Th., de Graauw, T., Furniss, I., Smith, H., Armand, C., Burgdorf, M., Di Giorgio, A., Ewart, D., Gry, C., King, K. J., Lim, T., Molinari, S., Price, M., Sidher, S., Smith, A., Texier, D., Trams, N., Unger, S. J., and Salama, A.: 1996, First detection of the 56 μ m rotational line of HD in Saturn's atmosphere, *Astron. Astrophys.* **315**, L389-L392.
- Griffith, C. A., Owen, T., Geballe, T. R., Rayner, J., Rannou, P. : 2003, Evidence for the exposure of water ice on Titan's surface, *Science*, **300**, 628-630.
- Griffith, C. A., Owen, T., Miller, G. A., and Geballe, T.: 1998, Transient clouds in Titan's lower atmosphere, *Nature* **395**, 575-578.
- Griffith, C. A., Hall, J. L., and Geballe, T. R.: 2000, Detection of daily clouds on Titan, *Science* **290**, 509-513.
- Grossman, A.W., Muhleman, D.O., and Berge, G.L., 1989, High-resolution microwave images of Saturn, *Science* **245**, 1211-1215.
- Grundy, W.M., Buie, M.W., Stansberry, J.A. and Spencer, J.R.: 1999, Near-infrared spectra of icy outer solar system surfaces: remote determination of H₂O ice temperatures, *Icarus* **142**, 536-549.
- Guillot, T.: 1999, A comparison of the interiors of Jupiter and Saturn, *Planet. Space Sci.* **47**, 1183-1200.
- Gurwell, M. A., and Muhleman, D. O.; 1995. CO on Titan: Evidence for a well-mixed vertical profile, *Icarus* **117**, 375-382.
- Haff, P. K.; Siscoe, G. L.; Eviatar, A.: 1983, Ring and plasma - The enigmas of Enceladus, *Icarus* **56**, 426-438.
- Hamilton, D. P., and Burns, J. A.: 1994, Origin of Saturn's E ring: self-sustained, naturally, *Science* **264**, 550-553.

- Hanel, R., Conrath, B., Flasar, M., Kunde, V., Lowman, P., Maguire, W., Pearl, J., Pirraglia, J., and Samuelson, R.: 1979, Infrared observations of the Jovian system from Voyager 1, *Science* **204**, 972-976.
- Hanel, R., Crosby, D., Herath, L., Vanous, D., Collins, D., Creswick, H., Harris, C., and Rhodes, M.: 1980, Infrared spectrometer from Voyager, *Applied Optics* **19**, 1391-1400.
- Hanel, R., Conrath, B., Flasar, F. M., Kunde, V., Maguire, W., Pearl, J. C., Pirraglia, J. A., Samuelson, R., Herath, L., Allison, M., Cruikshank, D., Gautier, D., Gierasch, P., Horn, L., Koppány, R., and Ponnaperuma, C.: 1981, Infrared observations of the Saturnian system from Voyager 1, *Science* **212**, 192-200.
- Hanel, R. A., Conrath, B. J., Flasar, F. M., Kunde, V. G., Maguire, W., Pearl, J. C., Pirraglia, J. A., Samuelson, R., Cruikshank, D. P., Gautier, D., Gierasch, P., Horn, L., and Ponnaperuma, C.: 1982, Infrared observations of the Saturnian system from Voyager 2, *Science* **215**, 544-548.
- Hanel, R. A., Conrath, B. J., Jennings, D. E., and Samuelson, R. E.: 2003, *Exploration of the Solar System by Infrared Remote Sensing*, 2nd ed., Cambridge University Press
- Hanel, R. A., Conrath, B. J., Kunde, V. G., Pearl, J. C., and Pirraglia, J. A.: 1983, Albedo, internal heat flux, and energy balance of Saturn, *Icarus*, **53**, 262-285.
- Hanel, R. A., Schlachman, B., Clark, f. D., Prokesh, C. H., Taylor, J. B., Wilson, W. M., and Chaney, L.: 1970, The Nimbus III Michelson Interferometer, *Appl. Optics* **9**, 1767-1774.
- Hapke, B.: 1996a, Applications of an energy transfer model to three problems in planetary regoliths: The solid-state greenhouse, thermal beaming, and emittance spectra, *J. Geophys. Res.* **101**, 16,833-16,840.
- Hapke, B.: 1996b, A model of radiative and conductive energy transport in planetary regoliths. *J. Geophys. Res.* **101**, 16,817-16,832.
- Hansen G.B.: 1997, The infrared absorption spectrum of carbon dioxide ice from 1.8 to 333 μm , *J. Geophys. Res.* **102**, 21,569-21,587.
- Held, I. M., and Hou, A. Y.: 1980, Nonlinear axially symmetric circulations in a nearly inviscid atmosphere, *J. Atmos. Sci.* **37**, 515-533.
- Herzberg, G.: 1945, *Infrared and raman spectra of polyatomic molecules*, D. van Nostrand, New York, pp. 194 ff.
- Hidayat, T., Marten, A., Bézard, B., Gautier, D., Owen, T., Matthews, H. E., and Paubert, G.: 1997, Millimeter and submillimeter heterodyne observations of Titan: retrieval of the vertical profile of HCN and the $^{13}\text{C}/^{12}\text{C}$ ratio, *Icarus* **126**, 170-182.
- Hidayat, T., Marten, A., Bézard, B., and Gautier, D.: 1998, Millimeter and submillimeter heterodyne observations of Titan: the vertical profile of carbon monoxide in its stratosphere, *Icarus* **133**, 109-133.
- Hinson, D. P., and Tyler, G. L.: 1983, internal gravity in Titan's atmosphere observed by Voyager radio occultation, *Icarus* **54**, 337-352.
- Hoefen, T.M., Clark, R.N., Bandfield, J.L., Smith, J.C., and Christensen, P.R.: 2003, Discovery of olivine in the Nili Fossae region of Mars, *Science (in the press)*
- Holton, J. R.: 1979, *An Introduction to Dynamic Meteorology*, Academic Press, New York, 2nd ed.
- Horanyi, M., Burns, J. A., and Hamilton, D. P.: 1992, Dynamics of Saturn's E Ring particles, *Icarus* **97**, 248-259.

- Hoskins, B. J., McIntyre, M. E., and Robertson, A. W. : 1985, On the use and significance of isentropic potential vorticity maps, *Quart. J. Royal Met. Soc.* **111**, 877-904.
- Hourdin, F., Talagrand, O., Sadourny, R., Courtin, R., Gautier, D., and McKay, C. P.: 1995, Numerical simulation of the general circulation of the atmosphere of Titan, *Icarus* **117**, 358-374.
- Hubbard, W. B.: 1980, Intrinsic luminosities of the jovian planets, *Rev. Geophys. Space Phys.* **18**, 1-9.
- Hubbard, W. B., Sicardy, B., Miles, R., Hollis, A. J., Forrest, R. W., Nicolson, I. K. M., Appleby, G., Beisker, W., Bittner, C., Bode, H.-J., Bruns, M., Denzau, H., Nezel, M., Riedel, E., Struckmann, H., Arlot, J. E., Roques, F., Sevre, F., Thuillot, W., Hoffmann, M., Geyer, E. H., Buil, C., Colas, F., Lecacheux, J., Klots, A., Thouvenot, E., Vidal, J. L., Carreira, E., Rossi, F., Blanco, C., Cristaldi, S., Nevo, Y., Reitsema, H. J., Brosch, N., Cernis, K., Zdanavicius, K., Wasserman, L. H., Hunter, D. M., Gautier, D., Lellouch, E., Yelle, R. V., Rizk, B., Flasar, F. M., Porco, C. C., Toubanc, D. and Corugedo, G.: 1993, The occultation of 28 Sgr by Titan, *Astron. Astrophys.* **269**, 541-563.
- Hubbard, W. B., Hunten, D. M., Reitsema, D. M., Brosch, N., Nevo, Y., Carreira, E., Rossi, F., and Wasserman, L. H.: 1990, Results for Titan's atmosphere from its occultation of 28 Sagittarii, *Nature* **343**, 353-355.
- Hudgins, D.M., Sandford, S.A., Allamandola, L.J. and Tielens, A.G. 1993, Mid-and far-infrared spectroscopy of ices: constants and integrated absorbance, *Astrophys J. Suppl.* **86**, 713-870.
- Hudson, B.L. and Moore, M.H.: 1993, Far-infrared investigations of a methanol clathrate hydrate: implications for astronomical observations, *Astrophys. J.* **404**, L29-L32.
- Hunten, D. M., Tomasko, M. G., Flasar, F. M., Samuelson, R. E., Strobel, D. F., and Stevenson, D. J.: 1984, Titan, in *Saturn*, ed. T. Gehrels and M. Matthews, University of Arizona Press, pp. 671-759.
- Ingersoll, A. P., Beebe, R. F., Conrath, B. J., and Hunt, G. E.: 1984, Structure and dynamics of Saturn's atmosphere, in *Saturn*, ed. T. Gehrels and M. Matthews, University of Arizona Press, pp. 195-238.
- Ingersoll, A., Orton, G. S., Münch, G., Neugebauer, G., and Chase, S. C.: 1980, Pioneer Saturn infrared radiometer: preliminary results, *Science* **207**, 439-443.
- Ingersoll, A. P., and Porco, C. C.: 1978, Solar heating and internal heat flow on Jupiter, *Icarus* **35**, 27-43.
- Irwin, P. G. J., Parrish, P., Fouchet, T., Calcutt, S. B., Taylor, F. W., Simon-Miller, A. A., and Nixon, C. A.: 2003, Retrievals of jovian tropospheric phosphine from Cassini/CIRS, *Icarus*, in press.
- Kargel, J. S., Pozio, S.: 1996, The Volcanic and tectonic history of Enceladus, *Icarus* **119**, 385-404.
- Karkoschka, E., and Tomasko, M.G.: 1992, Saturn's upper troposphere 1986-1989, *Icarus* **97**, 161-181.
- Kaye, J. A., and Strobel, D. F.: 1984. Phosphine photochemistry in the atmosphere of Saturn, *Icarus* **59**, 314-335.
- Kawata, Y.: 1983, Infrared brightness temperature of Saturn's rings based on the inhomogeneous multilayer assumption, *Icarus* **56**, 453-464.
- Kawata, Y., and Irvine, W.M.: 1975, Thermal emission from a multiple scattering model of Saturn's rings, *Icarus* **24**, 472-482.

- Khanna, R. K., Perera-Jarmer, M. A., and Ospina M. J.: 1987, Vibration infrared and Raman spectra of dicyanoacetylene, *Spectrochim. Acta* **43A**, 421-425.
- Khare, B. N., Sagan, C., Thompson, W. R., Arakawa, E. T., Meissen, C., and Tuminello, P. S.: 1994, Optical properties of poly-HCN and their astronomical applications, *Canad. J. Chem.* **72**, 678-694.
- Khelifi M., Nollet, M., Paillous, P., Bruston, P., Raulin, F., Benilan, Y., and Khanna, R.: 1999, Absolute intensities of the infrared bands of gaseous acrylonitrile, *J. Mol. Spectrosc.*, **194**, 206-210).
- Khelifi, M., Paillous, P., Bruston, P., Raulin, F., and Guillemain, J.-C.: 1996, Absolute IR band intensities of CH₃N, CH₂N, and CH₃CN in the 250-4300 cm⁻¹ region and upper limits of abundance in Titan's stratosphere, *Icarus*, **124**, 318-328.
- Khelifi, M., Paillous, P., Bruston, P., Guillemain, J.-C., Bénilan, Y., Daoudi, A., and Raulin, F.: 1997, Gas infrared spectra, assignments, and absolute IR band intensities of C₂N₂ in the 250-3500 cm⁻¹ region: implications for Titan's atmosphere, *Spectrochimica Acta*, **53A**, 707-712.
- Khelifi, M., and Raulin, F.: 1991, Infrared intensities and frequencies of 2-butyne nitrile: application to the atmosphere of Titan, *Spectrochim. Acta* **47A**, 171-176.
- Khelifi M., Raulin, F., and Dang-Nhu, M.: 1992, Benzene n₄-band integrated intensity versus temperature, *J. Mol. Spectrosc.* **154**, 235-239.
- Kliore, A. J., Anderson, J. D., Armstrong, J. W., Asmar, S. W., Hamilton, C. L., Rappaport, N. J., Wahlquist, H. D., Ambrosini, R., Bertotti, B., Flasar, F. M., French, R. G., Iess, L., Marouf, E. A., and Nagy, A. F.: 2003, Cassini radio science, *Space Sci. Rev.*, this issue.
- Kliore, A., Patel, I., R., Lindal, G. F., Sweetnam, D. N., Hotz, H. B., Waite, J. H., and McDonough, T. R.: 1980, Structure of the ionosphere and atmosphere of Saturn from Pioneer-11 Saturn radio occultation, *J. Geophys. Res.* **85**, 5857-5870.
- Kuiper, G.: 1944, Titan: a satellite with an atmosphere, *Astrophys. J.* **100**, 378-383.
- Kunde, V. G., Aikin, A. C., Hanel, R. A., Jennings, D. E., Maguire, W. C., and Samuelson, R. E.: 1981. C₂H₂, HC₃N, and C₄N₂ in Titan's atmosphere. *Nature* **292**, 686-688.
- Kunde, V. G., Ade, P., Barney, R., Bergman, D., Borelli, R., Boyd, D., Brasunas, J., Calcutt, S., Courtin, R., Cretolle, J., Crooke, J., Davis, M., Edberg, S., Flasar M., Glenar, D., Hagopian, J., Hakun, C., Hayes, P., Herath, L., Horn, L., Jennings, D., Karpati, G., Kellebenz, C., Lakew, B., Lindsay, J., Lyons, J., Martineau, R., Martino, A., Matsumura, M., Melak, T., Michel, G., Morell, A., Mosier, C., Pack, L., Plants, M., Robinson, D., Rodriguez, L., Romani, P., Trujillo, C., Vellacott, T., and Wagner, K.: 1996, Cassini infrared fourier spectroscopic investigation, *SPIE* **2803**, 162-177.
- Kunde, V. G., Flasar, F. M., Jennings, D. E., Bézard, B., Nixon, C. A., Bjoraker, G. L., Romani, P. N., Achterberg, R. K., Conrath, B. J., Simon-Miller, A. A., Irwin, P., Brasunas, J. C., Pearl, J. C., Smith, M. D., Orton, G. S., Gierasch, P. J., Spilker, L. J., Carlson, R., Calcutt, S. B., Read, P. L., Taylor, F. W., Fouchet, T., Parrish, P., Barucci, A., Courtin, R., Coustenis, A., Gautier D., Lellouch, E., Marten, A., Prangé, R., Biraud, Y., Ferrari, C., Owen, T. C., Abbas, M. M., Samuelson, R. E., Raulin, F., Ade, P., Césarsky, C. J., Grossman, K. U., and Coradini, A.: 2004, Jupiter's atmospheric composition from thermal-infrared observations at high spectral and spatial resolution, *in preparation*.
- Lammer, H., and Bauer, S. J.: 2003, Isotopic fractionation by gravitational escape, *Space Sci. Rev.* **186**, 281-291.

- Lammer, H., Stumptner, W., Molina-Cuberos, G. J., Bauer, S. J., and Owen, T.: 2000, Nitrogen isotope fractionation and its consequence for Titan's atmospheric evolution, *Planet. Space Sci.* **48**, 529-543.
- Lane, A.L., Hord, C.W., West, R.A., Esposito, L.W., Coffeen, D.L., Sato, M., Simmons, K.E., Pomphrey, R.B. and Morris, R.B.: 1982, Photopolarimetry from Voyager 2: Preliminary results on Saturn, Titan, and the rings, *Science* **215**, 537-543.
- Lara, L., Lellouch, E., Lopez-Moreno, J. J., and Rodrigo, R.: 1996, Vertical distribution of Titan's atmospheric neutral constituents, *J. Geophys. Res.* **101**, 23261-23283.
- Lara, L. M., Bézard, B., Griffith, C. A., Lacy, J. H., and Owen, T.: 1998, High-resolution 10-micronmeter spectroscopy of ammonia and phosphine lines on Jupiter, *Icarus* **131**, 317-333.
- Lecluse, C., Robert, F., Gautier, D., and Guiraud, M.: 1996, Deuterium enrichment in giant planets, *Planet. Space Sci.* **44**, 1579-1592.
- Lellouch, E., Bézard, B., Fouchet, T., Feuchtgruber, H., Encrenaz, T., and de Graauw, T.: 2001, The deuterium abundance in Jupiter and Saturn from ISO-SWS observations, *Astron. Astrophys.* **370**, 610-622.
- Lellouch, E., Bézard, B., Moses, J. I., Davis, G. R., Drossart, P., Feuchtgruber, H., Bergin, E. A., Moreno, R., and Encrenaz, T.: 2002, The origin of water vapor and carbon dioxide in Jupiter's stratosphere, *Icarus* **159**, 112-131.
- Lellouch, E., Coustenis, A., Gautier, D., Raulin, F., Dubouloz, N. and Frère, C.: 1989, Titan's atmosphere and hypothesized ocean: a reanalysis of the Voyager 1 radio-occultation and IRIS 7.7 μm data, *Icarus* **79**, 328-349.
- Lellouch, E., Coustenis, A., Sebag, B., Cuby, J.-G., López-Valverde, M., Schmitt, B., Fouchet, T., and Crovisier, J.: 2003, Titan's 5- μm window: observations with the Very Large Telescope, *Icarus* **162**, 125-142.
- Lemmon, M., Karkoschka, E., and Tomasko, M.: 1993, Titan's rotation: surface feature observed, *Icarus* **103**, 329-332.
- Lemmon, M. T., Smith, P. H., Lorenz, R. D.: Methane abundance on Titan, measured by the Space Telescope Imaging Spectrograph, *Icarus* **160**, 365-375.
- Leovy, C. B., Friedson, A. J., and Orton, G. S.: 1991, The quasiquadrennial oscillation of Jupiter's equatorial stratosphere, *Nature* **354**, 380-382.
- Lewis, J. S.: 1971, Satellites of the outer planets: their physical and chemical nature, *Icarus* **15**, 174-185.
- Lewis, J.S.: 1972, Low temperature condensation from the solar nebula, *Icarus* **16**, 241-252.
- Leyrat, C., Ferrari, C., Spilker, L. and Charnoz, S.: 2003, Thermal radiation from Saturn's rings: new results on the spin of particles, *Bull. Amer.Astron.Soc.* **35**, 951.
- Lindal, G. F., Wood, G. E., Hotz, H. B., Sweetnam, D. N., Eshleman, V. and Tyler, G. L.: 1983, The atmosphere of Titan: an analysis of the Voyager 1 radio occultation measurements, *Icarus* **53**, 348-363.
- Lindal, G. F., Sweetnam, D. N., and Eshleman, V. R.: 1984, The atmosphere of Saturn: an analysis of the Voyager radio occultation measurements, *Astron. J.* **90**, 1136-1146.
- Linsky, J. L.: 1998, Deuterium abundance in the local ISM and possible spatial variations, *Space Sci. Rev.* **84**, 285-296.

- Lorenz, E. N.: 1967, *The Nature and Theory of the General Circulation of the Atmosphere*, World Meteorological Organization, 161 pp.
- Lorenz, R. D., McKay, C. P., and Lunine, J. I.: 1997, Photochemically driven collapse of Titan's atmosphere, *Science* **275**, 642-644.
- Low, F. J., and Rieke, G. H.: 1974, Infrared photometry of Titan, *Astrophys.J.*, **190**, L143-L145.
- Lumme, K., Irvine, W.M., and Esposito L.W.: 1983, Theoretical interpretation of the ground-based photometry of Saturn's B ring, *Icarus* **53**, 174-184.
- Lunine, J. I.: 1993, Does Titan have an ocean? A review of current understanding of Titan's surface, *Rev. Geophys.* **31**, 133-149.
- Lunine, J. I., and Rizk, B.: 1989, Thermal evolution of Titan's atmosphere, *Icarus* **80**, 370-389.
- Lunine, J. I., Stevenson, D. J., and Yung, Y. L.: 1983, Ethane ocean on Titan, *Science* **222**, 1229-1230.
- Lunine, J. I., Yung, Y. L., and Lorenz, R. D.: 1999, On the volatile inventory of Titan from isotopic abundances in nitrogen and methane, *Planet. Space Sci.* **47**, 1291-1303.
- Lutz, B. L., De Bergh, C. and Owen, T.: 1983, Titan: discovery of carbon monoxide in its atmosphere, *Science* **220**, 1374-1375.
- Lynch, D.K., Mazuk, A.L., Russell, R.W., and Hackwell, J.A.: 2000, 8-to13- μ m spectra of Saturn's A and B rings, *Icarus* **146**, 43-47.
- Magni, G., and Coradini, A.: 2003, Formation of Jupiter by nucleated instability, *Planet. Space Sci.*, in press.
- Maguire, W. C., Hanel, R. A., Jennings, D. E., Kunde, V. G. and Samuelson, R. E.: 1981, C₂H₂ and C₂H₄ in Titan's atmosphere, *Nature* **292**, 683-686.
- Mahaffy, P. R., Donahue, T. M., Atreya, S. K., Owen, T. C., and Niemann, H. B.: 1998, Galileo probe measurements of D/H and ³He/⁴He in Jupiter's atmosphere, *Space Science Rev.* **84**, 251-263.
- Marouf, E.A., Tyler, G.L., Zebker, H.A., Simpson, R.A., and Eschelman, V.R., 1983, Particle size distributions in Saturn's rings from Voyager 1 radio occultation, *Icarus* **54**, 189-211.
- Marten, A., Gautier, D., Tanguy, L., Lecacheux, A., Rosolen, C. and Paubert, G.: 1988, Abundance of carbon monoxide in the stratosphere of Titan from millimeter heterodyne observations, *Icarus* **76**, 558-562.
- Marten, A., Hidayat, T. Moreno, R., Paubert, G., Bézard, B., Gautier, D. Matthews, H., and Owen, T.: 1997, *IAU Circular* **6702**, July 19.
- Martin, D. H.: 1982, Polarizing (Martin-Puplett) interferometric spectrometers for the near- and submillimeter spectra, in *Infrared and Millimeter Waves, Vol. 6, Systems and Components*, ed. K. J. Button, Chapter 2, New York: Academic Press.
- Martin, D. H. and Puplett, E.: 1969, Polarized interferometric spectrometry for the millimeter and submillimeter spectrum, *Infrared Physics*, **10**, 105-109.
- Massie, S. T., and Hunten, D. M.: 1982, Conversion of para and ortho hydrogen in the jovian planets, *Icarus* **49**, 213-226.
- Matson, D. L., and Brown, R.H.: 1989, Solid state greenhouses and their implications for icy satellites, *Icarus* **77**, 67-81.
- Matson, D. L., and Nash, D.: 1983, Io's atmosphere: Pressure control by regolith cold trapping and surface venting, *J. Geophys. Res.* **88**, 4,771-4,783.

- Matson, D. L., Spilker, L. J., and Lebreton, J.-P.: 2002, the Cassini/Huygens mission to the saturnian system, *Space Sci. Rev.* **104**, 1-58.
- Matzler, C., 1998: Microwave properties of ice and snow, in *Solar System Ices*, eds. B. Schmitt, C. De Bergh and M. Festou, Kluwer, Dordrecht, pp.241-257.
- McCord, T., Carlson R. W., Smythe W. D., Hansen G. B., Clark R. N., Hibbitts C. A., Fanale F. P., Granahan J. C., Segura M., Matson D. L., Johnson T. V., Martin P. D., and the NIMS team: 1997, Organics and other molecules in the surfaces of Callisto and Ganymede, *Science* **278**, 271-275.
- McKay, C. P., Coustenis, A., Samuelson, R. E., Lemmon, M. T., Lorenz, R. D., Cabane, M., Rannou, P., and Drossart, P.: 2001, Physical properties of the organic aerosols and clouds on Titan, *Planet. Space Sci.* **49**, 79-99.
- McKay, C. P., J. B. Pollack, and R. Courtin 1989, The thermal structure of Titan's atmosphere, *Icarus* **80**, 23-53.
- Meier, R., Smith, B.~A., Owen, T.~C., Terrile, R.~J. : 2000, The surface of Titan from NICMOS observations with the Hubble Space Telescope, *Icarus*, **145**, 462-473.
- Meier, R. Owen, T., Matthews, H., and Marten, A.: 1997, JCMT observations of the HCN 4-3 transition, unpublished.
- Mellon, M.T., Jakosky, B.M., Kieffer, H.H., and Christensen: 2000, High-resolution thermal-inertia mapping from the Mars Global Surveyor Thermal Emission Spectrometer, *Icarus* **148**, 437-455.
- Mennella, V., Brucato, J.R., Colangeli, L., Palumbo, P., Rotundi, A., and Bussolletti, E.: 1998, Temperature dependence of the absorption of cosmic analog grains in the wavelength range 20 microns to 2 millimeters, *Astroph. J.* **496**, 1058-1066.
- Mischenko, M.I.: 1993, On the nature of the polarization opposition effect exhibited by Saturn's rings, *Astroph. J.* **411**, 351-361.
- Morrison, D.: 1974, Albedos and densities of the inner satellites of Saturn, *Icarus* **22**, 51-56.
- Morrison, D., Jones, T.J., Cruikshank, D.P., and Murphy, R.E.: 1975, The two faces of Iapetus, *Icarus* **24**, 157-171.
- Morrison, D., Owen, T., and Soderblom L.A.:1986, The satellites of Saturn, in *Satellites* (Burns J., and Matthews, M.S. eds.), Univ. of Arizona Press, Tucson, pp 764-801.
- Moses, J. I., Bézard, B., Lellouch, E., Gladstone, G. R., Feuchtgruber, H., and Allen, M.: 2000a, Photochemistry of Saturn's atmosphere. I. Hydrocarbon chemistry and comparisons with ISO observations, *Icarus* **143**, 244-298.
- Moses, J. I., Lellouch, E., Bézard, B., Gladstone, G. R., Feuchtgruber, H., and Allen, M.: 2000b, Photochemistry of Saturn's atmosphere. II. Effects of an influx of external oxygen, *Icarus* **145**, 166-202.
- Mousis, O., Gautier, D., and Coustenis, A.: 2002, The D/H ratio in methane in Titan: origin and history, *Icarus* **159**, 156-165.
- Muhleman, D.O., Grossman, A. W., Butler, B. J., and Slade, M. A.: 1990, Radar reflectivity of Titan, *Science* **248**, 975-980.
- Murphy, R.E., Cruikshank, D.P., and Morrison, D.: 1972, Radii, albedos, and 20-micron brightness temperatures of Iapetus and Rhea, *Astrophys. J.* **177**, L93-L96.
- Nicholson, P. D., Hamilton, D. P., Matthews, K. and Yoder, C.F. 1992: New observations of Saturn's coorbital satellites. *Icarus*, **100**, 464-484.

- Niemann, H. B., Atreya, S. K., Carignan, G. R., Donahue, T. M., Haberman, T. M., Harpold, D. N., Hartle, R. E., Hunten, D. M., Karsprzak, W. T., Mahaffy, P. R., Owen, T. C., Spencer, N. W., and Way, S. H.: 1996, The Galileo probe mass spectrometer: composition of Jupiter's atmosphere, *Science* **272**, 846-849.
- Niemann, H. B., Atreya, S. K., Carignan, G. R., Donahue, T. M., Haberman, J. A., Harpold, D. N., Hartle, R. E., Hunten, D. M., Karsprzak, W. T., Mahaffy, P. R., Owen, T. C., and Way, S. H.: 1998, The composition of the jovian atmosphere as determined by the Galileo probe mass spectrometer. *J. Geophys. Res.* **103**, 22831-22845.
- Nishio, M., Paillous, P., Khlifi, M., Bruston, P., and Raulin, F.: 1995, Infrared spectra of gaseous ethanenitrile in the 3500-250 cm⁻¹ Region: Absolute band intensity and implications for the atmosphere of Titan, *Spectrochim. Acta* **51A**, 617-622.
- Nixon, C. A., Achterberg, R. K., Conrath, B. J., Irwin, P. G. J., Fouchet, T., Parrish, P. D., Abbas, M. M., LeClaire, A., Romani, P. N., Simon-Miller, A. A., Jennings, D. J., Flasar, F. M., and Kunde, V. G.: 2003, Merisitional variations of C₂H₂ and C₂H₄ in Jupiter's atmosphere from Cassini CIRS infrared spectra, *in preparation*.
- Noll, K., Knacke, R. F., Geballe, T. R., Tokunaga, A. T.: 1986, Detection of carbon monoxide in Saturn, *Astrophys. J. (Lett.)* **309**, L91-L94.
- Noll, K. S., and Larson, H. P.: 1990, The spectrum of Saturn from 1990 to 2230 cm⁻¹— abundances of AsH, CHD, CO, GeH, NH, and PH, *Icarus* **89**, 168-189.
- Noll, K. S., Geballe, T. R., Knacke, R. F., and Pendleton, Y. J.: 1996, Titan's 5μm spectral window: carbon monoxide and the albedo of the surface, *Icarus* **124**, 625-631.
- Noll, K. S., Roush, T. L., Cruikshank, D. P., Pendleton, Y. J., and Johnson, R. E.: 1997, Detection of ozone on Saturn's satellites Rhea and Dione, *Nature* **388**, 45-47.
- Orsolini, Y. and Leovy, C. B.: 1989, Linear properties of eddies in a jovian troposphere forced by deep jets, *Geophys. Res. Lett.* **16**, 1245-1248.
- Orsolini, Y. and Leovy, C. B.: 1993a, A model of large-scale instabilities in the jovian troposphere. 1. Linear model, *Icarus* **106**, 392-405.
- Orsolini, Y. and Leovy, C. B.: 1993b, A model of large-scale instabilities in the jovian troposphere. 2. Quasi-linear model, *Icarus* **106**, 406-418.
- Orton, G. S.: 1992, Ground-based observations of Titan's thermal spectrum, in *Proceedings Symposium on Titan*, European Space Agency SP-338, 81-85.
- Orton, G. S., and Ingersoll, A.P.: 1980, Saturn's atmospheric temperature structure and heat budget, *J. Geophys. Res.* **85**, 5871-5881.
- Orton, G., Fisher, B., Yanamandra-Fisher, P., Baines, K., Ressler, M., Beach-Kimball, B., Jackson, B., Gezari, D., and Varosi, F.: 2003, Pre-Cassini infrared characterization of Saturn's atmosphere, *Bull. Amer. Astron. Soc.* **35**, 1018.
- Orton, G., Fisher, B., Yanamandra-Fisher, P., Baines, K. H., Momary, t. W., and Fox, O. D.: 2002, A cold hole at the pole of Jupiter, *Bull. Amer. Astron. Soc.* **34**, 855-856.
- Orton, G. S., Friedson, A. J., Caldwell, J., Hammel, H. B., Baines, K. H., Bergstralh, J. T., Martin, T. Z., Malcolm, M. E., West, R. A., Golisch, W. F., Griep, D. M., Kaminsky, C. D., Tokunaga, A. T., Baron, R., and Shure, M.: 1991, Thermal maps of Jupiter: spatial organization and time dependence of stratospheric temperatures, 1980 to 1990, *Science* **252**, 537-542.
- Orton, G. S., Friedson, A. J., Huie, M., Malcom, M., Anthony, D., Caldwell, J., Tokunaga, A., and Klavetter, J.: 1989, Time-dependent behavior of the atmosphere of Saturn from 1982-

- 1989: zonally averaged properties from thermal emission observations, *Bull. Amer. Astron. Soc.* **21**, 953-954.
- Orton, G. S., Friedson, A. J., Yanamandra-Fisher, P. A., Caldwell, J., Hammel, H. B., Baines, K. H., Bergstralh, J. T., Martin, T. Z., West, R. A., Veeder, G. J., Lynch, D. K., Russell, R., Malcom, M. E., Golisch, W. F., Griep, D. M., Kaminski, C. D., Tokunaga, A. T., Herbst, T., Shure, M.: 1994, Spatial organization and time dependence of Jupiter's tropospheric temperatures 1980-1993, *Science* **265**, 625-631.
- Orton, G.S., Serabyn, E., and Lee, Y.T.: 2001, Corrigendum, Volume 146, Number 1, pages 48-59 (2000), of the article "Vertical Distribution of PH₃ in Saturn from Observations of Its 1-0 and 3-2 Rotational Lines," *Icarus* **149**, 489-490.
- Owen, T.: 1982. The composition and origin of Titan's atmosphere. *Planet. Space Sci.*, **30**, 833.
- Owen, T., Biver, N., Marten, A., Matthews, H. E., and Meier, R.: 1999, *IAU Circ.* 7306, Nov. 11.
- Owen, T.C., Cruikshank, D.P., Dalle Ore, C.M., Geballe, T.R., Roush, T.L., and de Bergh, C.: 1999, Detection of water ice on Saturn's satellite Phoebe, *Icarus* **139**, 379-382.
- Owen, T.C., Cruikshank, D.P., Dalle Ore, C.M., Geballe, T.R., Roush, T.L., de Bergh, C., Meier, R., Pendleton, Y.J., and Khare, B.N.: 2001. Decoding the domino: The dark side of Iapetus, *Icarus* **149**, 160-172.
- Pang, K. D., Voge, C. C., Rhoads, J. W., Ajello, J. M.: 1984, The E ring of Saturn and satellite Enceladus, *J. Geophys. Res.* **89**, 9459-9470.
- Pappalardo, R., Collins, G., Helfenstein, P., McCord, T., Prockter, L., Schenk, P., and Spencer, J.: 2003, Ganymede. In *Jupiter* (F. Bagenal, ed.), Cambridge University Press, in press.
- Pearl, J., Hanel, R., Kunde, V., Maguire, W., Fox, K., Gupta, S., Ponnampereuma, C., and Raulin, F.: 1979: Identification of gaseous SO₂ and new upper limits for other gases on Io, *Nature* **280**, 757-758.
- Pilcher, C.B., Chapman, C., Lebofsky, L.A. and Kieffer, A.A.: 1970, Saturn's rings: identification of water ice frost, *Science* **167**, 1372-1373.
- Pirraglia, J. A.: 1984, Meridional heat balance of Jupiter, *Icarus* **59**, 169-174.
- Pirraglia, J. A.: 1989, Dissipationless decay of jovian jets, *Icarus* **79**, 196-207.
- Plescia, J. B.: 1983. The geology of Dione. *Icarus* **56**, 255-277.
- Pollack, J.B., Hubickyi, O., Bodenheimer, P., Lissauer, J.J., Podolak, M., and Greenzweig, Y.: 1966, Formation of giant planets by concurrent accretion of solids and gas, *Icarus* **124**, 62-85.
- Pollack, J.B., Summers, A., and Baldwin, B.: 1973, Estimates of the size of the particles in the rings of Saturn and their cosmogonic implications, *Icarus* **20**, 263-278.
- Poulet, F., and Cuzzi, J.N: 2002, The composition of Saturn's rings, *Icarus* **160**, 350-358.
- Poulet, F., Cuzzi, J.N., French, R.G., and Dones, L.: 2002, A study of Saturn's ring phase curves from HST observations, *Icarus* **158**, 224-248.
- Porco, C. C., *et al.*: 2003, Cassini Imaging Science experiment, *Space Sci. Rev.*, this issue.
- Prangé, R., Fouchet, T., Connerney, J. E.P., and Courtin, R.: 1999, FUV diagnostic of Saturn's stratosphere with the HST: Search for water influx from the rings, in planetary systems: The long view, Proc. IXème Conference de Blois, ed. J. Tran Than Van et L. Celnikier, Editions Frontières, Paris, pp. 309-312.

- Prinn, R. G. and Fegley, B., Jr.: 1989, Solar nebulae chemistry: origin of planetary, satellite, and cometary volatiles, in *Origins and Evolution of Planetary and Satellite Atmospheres*, ed S. K. Atreya, J. B. Pollack, & M. S. Matthews, Tucson: The University of Arizona Press.
- Prinn, R. G., H. P. Larson, J. J. Caldwell, and D. Gautier 1984, Composition and Chemistry of Saturn's Atmosphere, In Saturn (T. Gehrels and M. S. Matthews, eds.) pp. 88-149. Univ. of Arizona Press, Tucson.
- Puetter, R.C. and Russell, R.W.: 1977, The 2-4-mm spectrum of Saturn's rings, *Icarus* **32**, 37-40.
- Rannou, P., Hourdin, F., and McKay, C. P.: 2002, A wind origin for Titan's haze structure, *Nature* **418**, 853-856.
- Raulin, F.: 1987, Organic chemistry in the oceans of Titan, *Adv. Space Res.* **7**, 71-81.
- Raulin, F., Accaoui, B., Razaghi, A., Dang-Nhu, M., Coustenis, A., and Gautier, D.: 1990, Infrared spectra of gaseous organics : Application to the atmosphere of Titan. II. C4 alkanenitriles and benzene, *Spectrochim. Acta* **46A**, 671-683.
- Raulin, F., and Owen, T. C.: 2003, Organic chemistry and exobiology on Titan, *Space Sci. Rev.* **104**, 377-394.
- Revercomb, H. E., Buijs, H., Howell, H. B., LaPorte, D. D., Smith, W. L., and Sromovsky, L. A.: 1988, Radiometric calibration of IR Fourier transform spectrometers: solution to a problem with the High-Resolution Interferometer Sounder, *Applied Optics* **27**, 3210-3218.
- Richardson, D.: 1994, Tree code simulations of planetary rings, *Mon. Not. R. Astron. Soc.* **269**, 493-511.
- Rodgers, C. D.: 2000, *Inverse Methods for Atmospheric Sounding: Theory and Practice*, London, World Scientific Publishing.
- Roe, H. G., de Pater, I., Macintosh, B. A., McKay, C. P. : 2002, Titan's clouds from Gemini and Keck adaptive optics imaging, *Icarus* **157**, 254-258.
- Roellig, T.L., Werner, M.W., Becklin, E.E.: 1988, Thermal emission from Saturn's rings at 380 microns, *Icarus* **73**, 574-583.
- Romani, P. N.: 1989, Stratospheric aerosol production from methane photochemistry on Saturn. *B.A.A.S.* **21**, 953.
- Rosen, P.A.: 1989, Waves in Saturn's rings probed by radio occultation. Scientific report No D845-1989-1, Jet Propulsion Laboratory.
- Saari, J.M. and Shorthill, R.W.: 1963, Isotherms of crater regions on the illuminated and eclipsed Moon, *Icarus* **2**, 115-136.
- Sagan, C. and Thompson, W.: 1984, Production and condensation of organic gases in the atmosphere of Titan, *Icarus* **59**, 133-161.
- Salo, H.: 1995, Simulations of dense planetary rings III. Self-gravitating identical particles, *Icarus* **117**, 287-312.
- Samuelson, R. E.: 1983, Radiative equilibrium model of Titan's atmosphere, *Icarus* **53**, 364-387.
- Samuelson, R. E. : 1985. Clouds and aerosols of Titan's atmosphere, in *The Atmospheres of Saturn and Titan*, pp. 99-107, European Space Agency: SP-241.
- Samuelson, R. E., and Mayo, L. A.: 1991, Thermal infrared properties of Titan's atmosphere, *Icarus* **91**, 207-219.
- Samuelson, R. E., and Mayo, L. A.: 1997, Steady-state model for methane condensation in Titan's troposphere, *Planet. Space Sci.* **45**, 949-958.

- Samuelson, R. E., Hanel, R. A., Kunde, V. G. and Maguire, W. C.: 1981, Mean molecular weight and hydrogen abundance of Titan's atmosphere, *Nature* **292**, 688-693.
- Samuelson, R. E., Maguire, W. C., Hanel, R. A., Kunde, V. G., Jennings, D. E., Yung, Y. L. and Aikin, A. C.: 1983, CO₂ on Titan, *J. Geophys. Res.* **88**, 8709-8715.
- Samuelson, R. E., Mayo, L. A., Knuckles, M. A., and Khanna, R. J.: 1997a, C₂N₂ ice in Titan's north polar stratosphere, *Planet. Space Sci.* **45**, 941-948.
- Samuelson, R. E., Nath, N. R., and Borysow, A.: 1997b, Gaseous abundances and methane supersaturation in Titan's troposphere, *Planet. Space Sci.* **45**, 959-980.
- Sánchez-Lavega, A., Lecacheux, J., Colas, F., and Laques, P.: 1993, Ground-based observations of Saturn's north polar spot and hexagon, *Science* **260**, 329-332.
- Sánchez-Lavega, A., Pérez-Hoyos, S., Acarreta, J. R., and French, R. G.: 2002, No hexagonal wave around Saturn's southern pole, *Icarus* **160**, 216-219.
- Sánchez-Lavega, A., Pérez-Hoyos, S., Rojas, J. F., Hues, R., and French, R. G.: 2003, A strong decrease in Saturn's equatorial jet at cloud level, *Nature* **423**, 623-625.
- Sandel, B.R., Shemansky, D. E., Broadfoot, A. L., Holberg, J. B., Smith, G. R., McConnell, J. C., Strobel, D. F., Atreya, S. K., Donahue, T. M., Moos, H. W., Hunten, D. M., Pomphrey, R. B., and Linick, S.: 1982, Extreme ultraviolet observations from the Voyager 2 encounter with Saturn, *Science* **215**, 548-553.
- Schoeberl, M. R., and Hartmann, D. L.: 1991, The dynamics of the stratospheric polar vortex and its relation to springtime ozone depletions, *Science* **251**, 46-52.
- Schubert, G., Spohn, T., and Reynolds, R.T.: 1986, Thermal histories, compositions and internal structures of the moons of the solar system, in *Satellites*, eds. J.A. Burns and M.S. Matthews, University of Arizona Press, Tucson, pp. 224-292.
- Sears W. D.: 1995, Tidal dissipation in oceans on Titan, *Icarus* **113**, 39-56.
- Sicardy, B., Brahic, A., Ferrari, C., Gautier, D., Lecacheux, J., Lellouch, E., Roques, F., Ariot, J. E., Colas, F., Thuillot, W., Sevrès, F., Vidal, J. L., Blanco, C., Cristaldi, S., Buil, C., Klotz, A., and Thouvenot, E.: 1989, Probing Titan's atmosphere by stellar occultation. *Nature* **343**, 350-353.
- Shindo F. : 2002, *Spectroscopie IR et UV expérimentale de composés intéressants l'atmosphère de Titan*, Thèse de Doctorat de l'Université Paris 7, Spécialité Astrophysique et Techniques Spatiales.
- Shindo, F., Benilan, Y., Guillemin, J.-C., Chaquin, P., Jolly, A., and Raulin, F.: 2001a, Spectroscopy of two organic compounds involved in Titan's atmosphere chemistry : Tetracyclene (C₈H₂) and Vinylacetylene (CH₂CHCCH), *BAAS*. **33** (3), 1109.
- Shindo, F., Benilan, Y., Chaquin, P., Guillemin, J.-C., Jolly, A., and Raulin, F.: 2001b, IR spectrum of C₈H₂ : integrated band intensities and some observational implication, *J. Mol. Spectrosc.*, **210** (2), 191-195.
- Shindo, F., Benilan, Y., Guillemin, J.-C., Chaquin, P., Jolly, A., and Raulin, F.: 2002, Ultraviolet and Infrared spectrum of C₈H₂ revisited and vapor pressure curve in Titan's atmosphere, *Planet. Space Sci.* **51**, 9-17.
- Showman, A. P.: 2001, Hydrogen halides on Jupiter and Saturn, *Icarus* **152**, 140-150.
- Showalter, M. R.: 1996, Saturn's D ring in the Voyager images, *Icarus* **124**, 677-689.
- Showalter, M. R., Burns, J. A., Cuzzi, J. N., and Pollack, J. B.: 1987, Jupiter's ring system: new results on structure and particle properties, *Icarus* **69**, 458-498.

- Showalter, M.R. and Cuzzi, J.N.: 1993, Seeing ghosts: photometry of Saturn's G ring, *Icarus* **103**, 124-143.
- Showalter, M. R., Cuzzi, J. N., and Larson, S. M.: 1991, Structure and particle properties of Saturn's E Ring, *Icarus* **94**, 451-473.
- Showalter, M. R., Pollack, J. B., Ockert, M. E., Doyle, L., and Dalton, J. B.: 1992, A photometric study of Saturn's F ring, *Icarus* **100**, 394-411.
- Shu, F.H., J.N. Cuzzi, and J.J. Lissauer: 1982, Bending waves in Saturn's rings, *Icarus* **53**, 185-206.
- Sicardy, B., Brahic, A., Ferrari, C., Gautier, D., Lecacheux, J., Lellouch, E., Roques, F., Ariot, J. E., Colas, F., Thuillot, W., Sèvres, F., Vidal, J. L., Blanco, C., Cristaldi, S., Buil, C., Klotz, A. and Thouvenot, E.: 1990, Probing Titan's atmosphere by stellar occultation, *Nature* **343**, 350-353.
- Simonelli, D. P., Kay, J., Adinolfi, D., Veverka, J., Thomas, P. C., and Helfenstein, P., 1999: Pheobe: albedo map and photometric properties, *Icarus* **138**, 249-258.
- Smith, B. A., Soderblom, L., Beebe, R., Boyce, J., Briggs, G., Bunker, A., Collins, S. A., Hansen, C. J., Johnson, T. V., Mitchell, J. L., Terrile, Carr, M., Cook II, A. F., Cuzzi, J., Pollack, J. B., Danielson, G. E., Ingersoll, A., Davies, M. E., Hunt, Masursky, H., Morrison, D., Owen, T., Sagan, C., Veverka, J., Strom, R., and Suomi, V. E.: 1981, Encounter with Saturn: Voyager 1 imaging science results, *Science* **212**, 163-191.
- Smith, B.A., Soderblom, L., Batson, R., Bridges, P., Inge, J., Masursky, H., Shoemaker, E., Beebe, R., Boyce, J., Briggs, G., Bunker, A., Collins, S. A., Hansen, C. J., Johnson, T. V., Mitchell, J. L., Terrile, R. J., Cook II, A. F., Cuzzi, J., Pollack, J. B., Danielson, G. E., Ingersoll, A., Davies, M. E., Hunt, G. E., Morrison, D., Owen, T., Sagan, C., Veverka, J., Strom, R., and Suomi, V. E.: 1982, A new look at the Saturn system: the Voyager 2 images, *Science* **215**, 504-537.
- Smith, M. D., Conrath, B. J., and Gautier, D.: 1996, Dynamical influence on the isotopic enrichment of CH₄D in the outer planets, *Icarus* **124**, 598-607.
- Smith, M. D., and Gierasch, P. J.: 1995, Convection in the outer planet atmospheres including ortho-para hydrogen conversion, *Icarus* **116**, 159-179.
- Smith, P. H., Lemmon, M. T., Lorenz, R. D., Sromovsky, L. A., Caldwell, J. J., and Allison, M. D.: 1996, Titan's surface, revealed by HST imaging, *Icarus* **119**, 336-349.
- Smith, R.G., Robinson, G., Hyland, A. R., and Carpenter, G. L.: 1994, Molecular ices as temperature indicators for interstellar dust: the 44- μ m and 62- μ m lattice features of H₂O ice, *Month. Not. Roy. Astron. Soc.* **271**, 481-489.
- Smith, W. H., and Baines, K. H.: 1990, H S(3) and S(4) transitions in the atmospheres of Neptune and Uranus—observations and analysis, *Icarus* **85**, 109-119.
- Snyder-Hale, A. and Hapke, B.: 2002, A time-dependent model of radiative and conductive thermal energy transport in planetary regoliths with applications to the Moon and Mercury, *Icarus*, **156**, 318-334.
- Socrates, G. 1980. *Infrared characteristic group frequencies*, Wiley-Interscience, New York, pp xx-yy.
- Spencer, J.R.: 1987, The surfaces of Europa, Ganymede, and Callisto: An investigation using Voyager IRIS thermal infrared spectra. Ph.D. Thesis, University of Arizona, Tucson.
- Spencer, J.: 1990, A rough-surface thermophysical model for airless planets, *Icarus* **83**, 27-38.

- Spencer, J.R., Tamppari, L.K., Martin, T.Z., and Travis, L.D.: 1999, Temperatures on Europa from Galileo PPR: Nighttime thermal anomalies, *Science* **284**, 1514-1516.
- Spilker, L., Pilorz, S., Ferrari, C., Pearl, J. and Wallis, B.: 2003, Thermal and energy balance measurements of Saturn's C ring, *Bull. Amer. Astron. Soc.* **35**, 929.
- Sprague, A.L.: 2000, Thermal emission spectroscopy and data analysis of solar system regoliths, in *Thermal emission spectroscopy and analysis of dust, disks and regoliths*; eds. M.L. Sitko, A.L. Sprague, and D.K. Lynch, Lunar and Planetary Institute, Houston, pp 167-186.
- Sromovsky, L. A., Suomi, V. E., Pollack, J. B., Krauss, R. J., Limaye, S. S., Owen, T., Revercomb, H. E. and Sagan, C.: 1981, Implications of Titan's north-south brightness asymmetry, *Nature* **292**, 698-702.
- Sromovsky, L. A., Revercomb, H. E., Krauss, R. J., and Suomi, V. E.: 1983, Voyager 2 observations of Saturn's northern mid-latitude cloud features: morphology, motions and evolution, *J. Geophys. Res.* **88**, 8650-8666.
- Strobel, D.: 1982, Chemistry and Evolution of Titan's atmosphere, *Planet. Space Sci.* **30**, 839-848.
- Tholen, D. J., and Zellner, B.: 1983, Eight-color photometry of Hyperion, Iapetus, and Phoebe, *Icarus* **53**, 341-347.
- Thomas, P. and Veverka, J.: 1985, Hyperion - Analysis of Voyager observations, *Icarus* **64**, 414-424.
- Thompson W. R. and Sagan C.: 1984, Titan: far infrared and microwave remote sensing of methane clouds and organic haze, *Icarus* **60**, 236-259.
- Thompson, W. R., Todd, H., Schwartz, J., Khare, B.N., and Sagan, C.: 1991, Plasma discharge in N₂ + CH₄ at low pressures: experimental results and applications to Titan, *Icarus* **90**, 57- 73.
- Tokunga, A. T.: 1980, The detection of C₂H₂ on Saturn and Titan, *Bull. Amer. Astron. Soc.* **12**, 669.
- Tokunaga, A.T., Caldwell, J. and Nolt, I.G. 1980, The 20-mm brightness temperature of the unilluminated side of Saturn's rings, *Nature* **287**, 212-214.
- Tomasko, M. G., West, R. A., Orton, G. S., and Tieffell, V. G.: 1984, Clouds and aerosols in Saturn's atmosphere, in *Saturn* (T. Gehrels and M. S. Matthews, Eds.) pp. 150-194. Univ. of Arizona Press, Tucson.
- Tomasko, M. G., *et al.*: 2002, The descent imager/spectral radiometer (DISR) experiment on the Huygens entry probe of Titan, *Space Sci. Rev.* **104**, 469-551.
- Toon, O. B., McKay, C., Courtin, R., and Ackerman, T.: 1988. Methane Rain on Titan. *Icarus* **75**, 255-284.
- Tyler, G.L., Eshleman, V.R., Anderson, J.D., Levy, G.S., Lindal, G.F., Wood, G.E. and Croft, T.A.: 1981, Radio science investigations of the Saturn system with Voyager 1: Preliminary results, *Science* **212**, 201-206.
- Van Allen, J. A.: 1983, Absorption of energetic protons by Saturn's ring G, *J. Geophys. Res.* **88**, 6911-6918.
- de Vanssay, E., Gazeau, M.C., Guillemin, J.C., and Raulin, F.: 1995, Experimental simulation of Titan's organic chemistry at low temperature, *Planet. Space Sci.* **43**, 25-31.
- Warren, S.G.: 1984, Optical constants of ice from the ultraviolet to the microwave, *App. Opt.*, **23**, 1206-1225.

- Weisstein, E. W. and Serabyn, E.: 1996, Submillimeter line search in Jupiter and Saturn, *Icarus* **123**, 23-36.
- West, R. A., Strobel, D. F., and Tomasko, M. G.: 1986, Clouds, aerosols, and photochemistry in the jovian atmosphere, *Icarus* **65**, 161-217.
- Whitcomb, S.E., Hildebrand, R.H., and Keene, J. 1980, Brightness temperatures at Saturn's disk and rings at 400 and 700 micrometers, *Science* **210**, 788-789.
- Wilson, P.D., and Sagan, C.: 1995, Spectrophotometry and organic matter on Iapetus, 1. Compositional models, *J. Geophys. Res.* **100**, 7,531-7,537.
- Wilson, P.D.; Sagan, C.: 1996, Spectrophotometry and organic matter on Iapetus 2. Models of interhemispheric asymmetry, *Icarus* **122**, 92-106.
- Wolf, A. A.: 2002, Touring the saturnian system, *Space Sci. Rev.* **104**, 101-128.
- Wong, A-S., Morgan, C. G., Yang, Y. L., and Owen, T.: 2002, Evolution of CO on Titan. *Icarus* **155**, 382-397.
- Wong, M. H., BJORAKER, G. L., Smith, M. D., Flasar, F. M., and Nixon, C. A.: 2003, Identification of the 10- μ m ammonia ice feature on Jupiter, *Planet. Space Sci.*, in press.
- Yanamandra-Fisher, P. A., Orton, G. S., Fisher, B. M., and Sánchez-Lavega, A.: 2001, Saturn's 5.2- μ m cold spots: unexpected cloud variability, *Icarus* **150**, 189-193.
- Yelle, R. V.: 1991. Non-LTE models of Titan's upper atmosphere, *Astrophys. J.* **383**, 380-400.
- Yelle, R. V. and McGrath, M. A.: 1996, Ultraviolet spectroscopy of the SL9 impact sites. I. The 175-230 nm region, *Icarus* **119**, 90-111.
- Yoder, C. F.; Synnott, S. P. and Salo, H.: 1989. Orbits and masses of Saturn's co-orbiting satellites, Janus and Epimetheus. *Astron. J.* **98**, 1875-1889.
- Yung, Y. L., Allen, M., and Pinto J. P.: 1984, Photochemistry of the atmosphere of Titan: comparison between model and observations, *Astrophys. J. Supp.* **55**, 465-506.
- Yung, Y. L.: 1987, An update of nitrile photochemistry on Titan, *Icarus* **72**, 468-472.
- von Zahn, U., and Hunten, D. :1996, The helium mass fraction in Jupiter's atmosphere, *Science* **272**, 849-851.

Figure Captions

Fig. 1: CIRS observations of Saturn's rings as a function of spacecraft elevation. Typical CIRS ring observations are depicted as a function of the observed ring opening angle.

Fig. 2: CIRS FP1 and FP3/4 spatial resolution as a function of distance from the rings. The spatial resolution for FP1 and a single pixel in FP3 or FP4 are shown as a function of the distance from the rings, for normal ring viewing. The curves above also depict the ring radial resolution when viewing the rings at either ansa. For comparison, the radial extent of ring features such as the Cassini Division, B ring plateau/C ring ramp, and C ringlets are indicated.

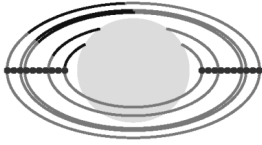
Faint Ring Long
Integration:



Composition Long
Integration:



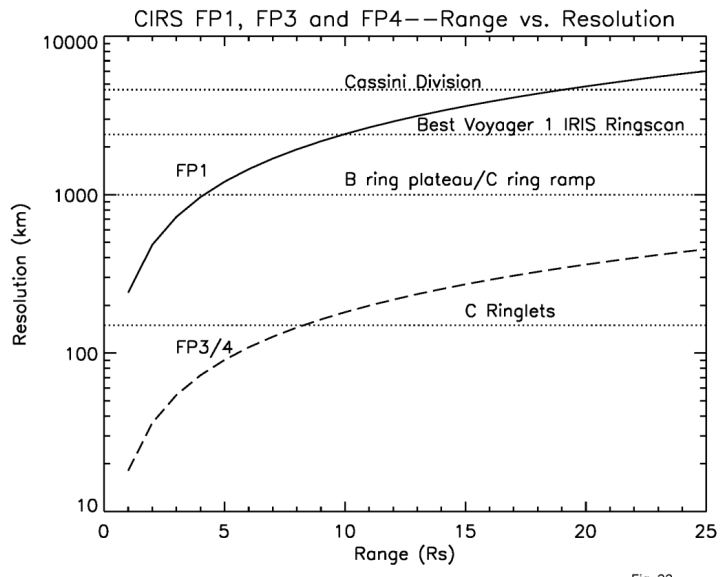
Radial Scans:



Azimuthal Scans:



Fig. 32



Planning

This section of the Rings target notebook contains a detailed view of the observation planning, design, and development as they were prepared and intended to execute on the spacecraft. It is important to note that the user MAY find small differences in pointing or timing between what was planned and what executed on board. CIRS planned 2711 observations of the Rings over the course of the Cassini mission which are in the time ordered listings included in this section

The time ordered listing contains the name, the start time, duration, and end time for each Icy satellite observation. If the observation was within a moveable block of time, there will be an entry in the Epoch column – a simplistic way to use this information is as an alert to the user that there may be a shift in the start and end time due to a change in the time of closest approach to the target (time of flight error).

The name itself gives much information about the observation. The naming convention is complex enough that a decoder ring has been provided below:

In the example of CIRS_000RB_COMP001_PRIME, CIRS (first 4 characters indicate the instrument that is collecting data); 000RB (second group of 5 characters indicate the Cassini revolution or orbit number is 000 and the target id – in this case RB stands for the B Ring); COMP001 (the third group of up to 10 characters indicates that this observation is involves composition and that it is the first in a series of similar/repeatable observations in the revolution or orbit); PRIME (the last 5 characters indicate that CIRS controlled the pointing of the spacecraft for this observation).

It is important to note that in many cases CIRS collected data while other instruments controlled the pointing – this category of observations were called “riders” or “collaborative riders”. This class of observations are easily identified by the last few characters in the observation name – ie UVIS, VIMS, ISS, SI (support imaging), and RIDER.

For each observation in the time ordered listing, there exists ancillary data that was generated during the integration and implementation process. There is a graphical image (ODD plot) that depicts the target at some point of time in the observation – this can give the user a quick look at the placement and spatial resolution of the CIRS field of views. The planned pointing and instrument commanding can be viewed in the shortform (sfof) text file. The planned c-kernels (ck) provide the highest level of detailed pointing available for the observation. Cubes exist for all the observations and are delivered with our data to the atmospheric node of PDS however we are providing those for all the CIRS rider observations as capturing all the ancillary files for each rider was very time consuming and out of the scope of our budget. These files are all accessible by hyper-link from the time-ordered listing.

In addition, rows in the TOL highlighted in orange are observations lost in execution due to instrument or spacecraft anomaly. Details are available in the Database section of this handbook.